



UNIL | Université de Lausanne

Unicentre

CH-1015 Lausanne

<http://serval.unil.ch>

---

Year : 2019

## Intestinal lamina propria fibroblasts - phenotype and function for IgA+ plasma cells

Renevey François

Renevey François, 2019, Intestinal lamina propria fibroblasts - phenotype and function  
for IgA+ plasma cells

Originally published at : Thesis, University of Lausanne

Posted at the University of Lausanne Open Archive <http://serval.unil.ch>

Document URN : urn:nbn:ch:serval-BIB\_6502810935D66

### **Droits d'auteur**

L'Université de Lausanne attire expressément l'attention des utilisateurs sur le fait que tous les documents publiés dans l'Archive SERVAL sont protégés par le droit d'auteur, conformément à la loi fédérale sur le droit d'auteur et les droits voisins (LDA). A ce titre, il est indispensable d'obtenir le consentement préalable de l'auteur et/ou de l'éditeur avant toute utilisation d'une oeuvre ou d'une partie d'une oeuvre ne relevant pas d'une utilisation à des fins personnelles au sens de la LDA (art. 19, al. 1 lettre a). A défaut, tout contrevenant s'expose aux sanctions prévues par cette loi. Nous déclinons toute responsabilité en la matière.

### **Copyright**

The University of Lausanne expressly draws the attention of users to the fact that all documents published in the SERVAL Archive are protected by copyright in accordance with federal law on copyright and similar rights (LDA). Accordingly it is indispensable to obtain prior consent from the author and/or publisher before any use of a work or part of a work for purposes other than personal use within the meaning of LDA (art. 19, para. 1 letter a). Failure to do so will expose offenders to the sanctions laid down by this law. We accept no liability in this respect.



**UNIL** | Université de Lausanne

Faculté de biologie  
et de médecine

**Département de Biochimie**

**Intestinal lamina propria fibroblasts –  
phenotype and function for IgA<sup>+</sup> plasma cells**

**Thèse de doctorat ès sciences de la vie (PhD)**

présentée à la

Faculté de biologie et de médecine  
de l'Université de Lausanne

par

**François RENEVEY**

Biologiste diplômé de l'Université de Lausanne

**Jury**

Prof. Valentin Rousson, Président  
Prof./Dr Sanjiv Luther, Directeur de thèse  
Prof./Dre Tatiana Petrova, Experte  
Prof./Dr Dominique Velin, Expert  
Prof./Dre Anja Erika Hauser, Experte externe

Lausanne 2019



# Imprimatur

Vu le rapport présenté par le jury d'examen, composé de

|                                |          |                                |
|--------------------------------|----------|--------------------------------|
| <b>Président·e</b>             | Monsieur | Prof. Valentin <b>Rousson</b>  |
| <b>Directeur·rice de thèse</b> | Monsieur | Prof. Sanjiv <b>Luther</b>     |
| <b>Experts·es</b>              | Madame   | Prof. Tatiana <b>Petrova</b>   |
|                                | Monsieur | Dr Dominique <b>Velin</b>      |
|                                | Madame   | Prof. Anja Erika <b>Hauser</b> |

le Conseil de Faculté autorise l'impression de la thèse de

**Monsieur François Renevey**

Maîtrise universitaire ès Sciences en biologie médicale Université de Lausanne

intitulée

**Intestinal lamina propria fibroblasts –  
phenotype and function for IgA<sup>+</sup> plasma cells**

Lausanne, le 15 mars 2019

pour le Doyen  
de la Faculté de biologie et de médecine

Prof. Valentin Rousson

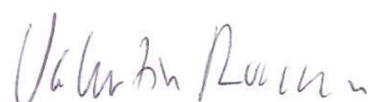




## Table of Contents

|   |           |
|---|-----------|
| <b>1 Abstract</b> .....   | <b>9</b>  |
| <b>2 Résumé</b> .....   | <b>11</b> |
| <b>3 Abbreviations</b> .....  | <b>13</b> |
| <b>4 Introduction</b> .....   | <b>17</b> |
| 4.1 The gut: a huge exchange interface in perpetual contact with microorganisms and food antigens.....  | 17        |
| 4.2 The actors of the intestinal immune system.....   | 19        |
| 4.3 Secretory IgA antibodies represent one of the major effectors ensuring mucosal homeostasis and defense .....  | 22        |
| 4.3.1 IgA function .....  | 22        |
| 4.3.2 IgA deficiency in human .....   | 24        |
| 4.3.3 IgA deficiency in mice .....  | 25        |
| 4.4 Induction of intestinal IgA responses and the migration of plasmablasts to the LP ..  | 26        |
| 4.4.1 Inductive sites .....   | 26        |
| 4.4.2 IgA response .....  | 28        |
| 4.5 Bone marrow plasma cell survival niche .....  | 31        |
| 4.6 The transient PC niche of peripheral lymph nodes .....  | 36        |
| 4.7 IgA plasma cell survival niche in the intestinal lamina propria .....   | 38        |
| 4.8 Intestinal fibroblasts .....  | 42        |
| 4.9 Aims of this thesis .....   | 46        |
| <b>5 Results</b> .....  | <b>47</b> |
| 5.1 Fibroblasts of the lamina propria form a dense network in which IgA <sup>+</sup> PC reside and represent a rich source of PC survival factors. .... | 47        |
| 5.2 iFB in the subepithelial layer are distinct from iFB in the core of the villus .....  | 51        |
| 5.3 Stromal cells in the LP of the SI are highly heterogeneous as assessed by flow cytometric and histological analysis.....                            | 53        |
| 5.4 iFB and myeloid cells promote PC survival and IgA production in a contact dependent manner. ....  | 59        |
| 5.5 The IgA PC niche is constituted of one or several PC that are showing cell-cell contacts with multiple iFB.....                                     | 67        |
| 5.6 IgA PC survival is CD44 dependent <i>in vitro</i> . ....  | 70        |
| 5.7 IgA PC homeostasis is impaired in CD44KO mice. ....   | 76        |
| <b>6 Discussion</b> .....   | <b>81</b> |
| 6.1 Intestinal fibroblasts .....  | 81        |
| 6.1.1 Intestinal fibroblast heterogeneity .....   | 81        |
| 6.1.2 Subepithelial iFB – telocytes .....   | 81        |
| 6.1.3 The lamina propria smooth muscle cells (SMC).....   | 84        |
| 6.1.4 Internal iFB.....   | 85        |
| 6.1.5 The size of the iFB population is underestimated by flow cytometric analysis...85   |           |
| 6.1.6 Conclusions.....  | 87        |
| 6.2 iFB and myeloid cells as niche cells for IgA PC survival.....   | 88        |
| 6.2.1 Synergistic PC survival effect by iFB and M $\phi$ .....  | 89        |
| 6.2.2 Role for epithelial cells in IgA <sup>+</sup> PC survival?.....   | 90        |
| 6.2.3 Role for endothelial cells in IgA <sup>+</sup> PC survival? .....   | 91        |
| 6.2.4 Role for eosinophils in IgA <sup>+</sup> PC survival? .....   | 91        |
| 6.3 Is the survival of IgA <sup>+</sup> PC really independent of IL-6, BAFF or APRIL? .....   | 93        |

## Table of contents

---

|          |  |            |
|----------|--|------------|
| 6.3.1    | Role of IL-6.....  | 93         |
| 6.3.2    | Role of APRIL.....   | 94         |
| 6.3.3    | Role of BAFF.....  | 95         |
| 6.3.4    | Is there an iFB subset functionally dedicated to PC survival?.....                         | 95         |
| 6.4      | PC survival promoted by adherent cells is mediated by CD44 interactions <i>in vitro</i> .. | 97         |
| 6.4.1    | PC survival is mediated by CD44 <i>in vitro</i> .....                                      | 97         |
| 6.4.2    | HA as the main CD44 ligand for IgA <sup>+</sup> PC survival?.....                          | 99         |
| 6.4.3    | Alternative ligands for CD44?.....   | 101        |
| 6.5      | IgA <sup>+</sup> PC homeostasis is impaired in CD44KO mice .....                           | 102        |
| 6.6      | General conclusions.....   | 105        |
| 6.7      | Contributions by others .....  | 107        |
| <b>7</b> | <b>Material and methods .....</b>  | <b>109</b> |
| <b>8</b> | <b>Annexes.....</b>  | <b>115</b> |
| <b>9</b> | <b>References .....</b>  | <b>121</b> |





# 1 Abstract

Due to the continuous pressure of an extremely diverse and numerous microbiota in the gut lumen, the majority of immune cells of the body reside in the intestinal mucosa regulating the complex and delicate balance between effective immunological control of the microbiota and pathogens, the tolerance towards food antigens and commensals, and the preservation of tissue homeostasis. Among the various immune cells populating the mucosa, plasma cells (PC) are responsible for the production of the major antibody isotype secreted, namely IgA, which is crucial for preventing the entry of the microbiota into the body and for preventing tissue inflammation. In fact, IgA deficiency in mice and humans leads to an altered microbiota composition, or dysbiosis, and higher susceptibility to certain types of infections, highlighting the need for a constantly high IgA production by PC in healthy mammals. The sustained IgA production is maintained by the continuous development of new IgA<sup>+</sup> PC, their migration into the intestinal lamina propria (LP), and the maintenance of IgA<sup>+</sup> PC in this site allowing IgA secretion and transport into the gut lumen. Regarding their survival, PC are known to be particularly prone to die when extracted from their tissue and their survival is thought to be regulated by extracellular stimuli existing in limiting amounts and provided by a specialized microenvironment, called survival niche. Currently, the cell types and factors defining and regulating this niche for IgA<sup>+</sup> PC are poorly defined. Therefore, the aim of this thesis was to explore the nature of this particularly important PC niche.

In this study, we show that intestinal collagen1 $\alpha$ 1<sup>+</sup> podoplanin<sup>+</sup> fibroblasts (iFB) form a dense and organized network throughout the LP making extensive physical contacts with all immune cells including IgA<sup>+</sup> PC and constituting the main source of known PC survival factors including *baff* and *cxcl12*, besides being one of the *april* sources. I have established a new *in vitro* culture system mimicking the complex LP microenvironment where IgA<sup>+</sup> PC reside in order to define the cells and factors that are critical for PC homeostasis. I observed that purified iFB as well as macrophages (M $\phi$ ) are the LP cell types most efficient at promoting IgA<sup>+</sup> PC survival and IgA production. Interestingly, they achieve PC survival in a synergistic and cell contact-dependent fashion. When screening for membrane-bound factors using inhibitors in our coculture system, I identified the surface protein CD44 as positive regulator of PC survival and IgA secretion. Using CD44-deficient cells CD44 was found to be important on the niche cells and even more on IgA<sup>+</sup> PC. Finally, investigation of the

## Abstract

---

CD44-deficient mouse phenotype revealed that IgA<sup>+</sup> PC are selectively reduced in number within the LP which correlated with an even greater defect in the levels of fecal IgA in comparison with wildtype mice, while IgA<sup>+</sup> PC development in inductive sites, such as Peyer's patches and mesenteric lymph nodes, seemed normal. Altogether, this study characterized the iFB network both histologically and functionally with a new level of detail and revealed that these cells are a major structural and functional component of the IgA<sup>+</sup> PC niche allowing PC maintenance in a CD44-dependent fashion and in synergy with myeloid cells. These findings improve our understanding of how intestinal homeostasis and microbiome control is achieved and regulated, and should be of relevance for the development of oral vaccines that typically aim to induce a potent IgA response at mucosal surfaces.

## 2 Résumé

Due à la pression constante du microbiome, une communauté impressionnante de cellules immunitaires colonise la muqueuse intestinale, régulant ainsi le délicat équilibre entre un contrôle immunitaire efficace du microbiome et une préservation de l'intégrité des tissus. Parmi les différents types cellulaires participant à l'homéostasie de l'intestin, les cellules plasma (PC) sont responsables de la production massive d'IgA qui régule directement la flore intestinale et participe à la défense contre les pathogènes entériques. En effet, une déficience dans la sécrétion d'IgA conduit à une altération de la composition du microbiome, appelée dysbiose, et une prédisposition à développer certaines infections entériques. La production soutenue d'IgA est maintenue grâce à la génération continue de nouvelles PC, leur migration dans la muqueuse intestinale et la survie de ces PC une fois dans leur site effecteur. Concernant leur survie, les PC sont connues pour être particulièrement sensibles à la mort cellulaire, ce qui implique qu'elles ont constamment besoin de stimulus, appelés facteurs de survie, provenant de leur environnement. Les cellules qui fournissent les facteurs de survie aux PC sont localisées dans des endroits restreints et spécialisés à cette fonction. On peut les trouver dans la moelle osseuse, la médulla des ganglions lymphatiques, et potentiellement l'intestin. Actuellement, les facteurs et les types cellulaires responsables de la survie des PC qui sécrètent les IgA dans l'intestin ne sont pas clairement identifiés.

Dans ce travail, je montre que les fibroblastes intestinaux (iFB), qui expriment le  $\text{collagen1}\alpha 1$  et la podoplanin, forment une structure complexe à travers toute la lamina propria et contactent physiquement les cellules immunitaires, les PC compris. Je montre que les iFB sont une source importante d'ARN messagers de plusieurs facteurs de survie connus pour PC, comme *baff* et *cxcl12*, et participent aussi à la production de *april*. Dans des expériences de coculture, la survie des PC était améliorée quand elles étaient placées en coculture avec des iFB ou des macrophages ( $M\phi$ ). Lorsque les iFB et les  $M\phi$  étaient associés, un effet synergétique a été mesuré sur la survie et la fonction des PC. De manière intéressante, l'effet des iFB/  $M\phi$  sur la survie des PC est dépendant du contact entre les PC et les iFB/  $M\phi$  et est en grande partie aboli après neutralisation de la protéine transmembranaire CD44. L'implication de CD44 dans ce processus a ensuite été confirmée en utilisant des PC isolées de souris déficientes pour CD44 (ou CD44KO). En effet, les PC CD44KO étaient plus sensibles à la mort cellulaire *in vitro* que les PC normales. De

plus, j'ai pu montrer que les iFB/ M $\phi$  isolés de souris CD44KO avaient un effet sur la survie des PC réduit par rapport aux iFB/ M $\phi$  normaux. Finalement, l'investigation des souris déficientes pour CD44 a révélé que le nombre de PC était significativement réduit dans la muqueuse intestinale, alors que le développement des PC dans les sites inducteurs, tels que les plaques de Peyer ou les ganglions lymphatiques mésentériques, semblait normal. Cette étude met en lumière la structure tridimensionnelle que forment les iFB *in vivo* et révèle le nouveau rôle des iFB et des M $\phi$  dans la maintenance de la population de PC dans l'intestin ainsi que le rôle important de CD44 dans ce processus.

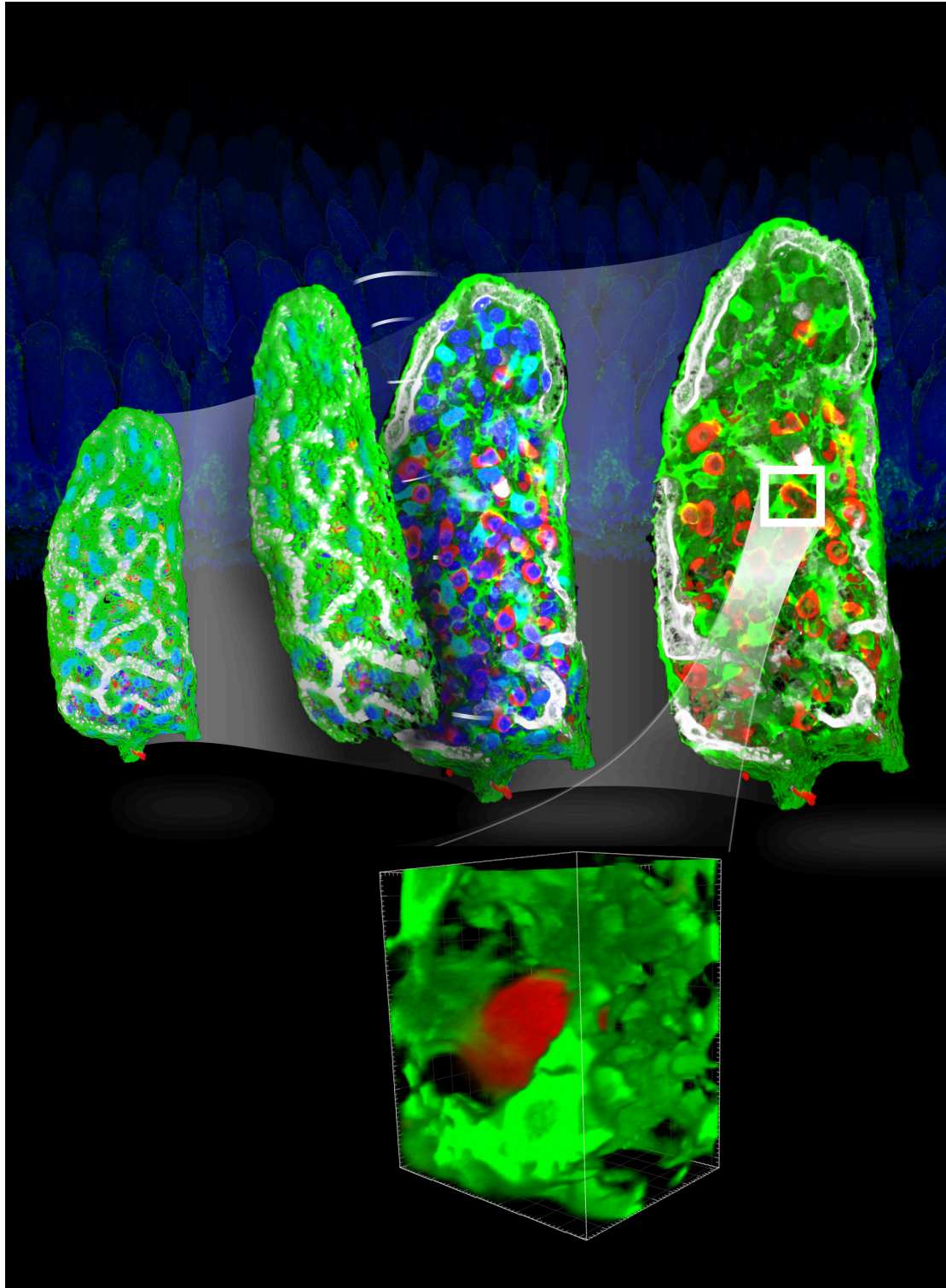
### 3 Abbreviations

|  |          |
|--|----------|
| A Proliferation-Inducing Ligand            | APRIL    |
| Adherent cell                              | AC       |
| Antibody                                   | Ab       |
| Antigen                                    | Ag       |
| B cell receptor                            | BCR      |
| B-cell-Activating Factor of the TNF family | BAFF     |
| Blood endothelial cell                     | BEC      |
| Bone marrow                                | BM       |
| Class switch recombination                 | CSR      |
| Cytidine deaminase                         | AID      |
| Dendritic cell                             | DC       |
| Eosinophil                                 | Eos      |
| Fibroblastic reticular cell                | FRC      |
| Follicular dendritic cell                  | FDC      |
| Gastrointestinal                           | GI       |
| Germ-free                                  | GF       |
| Germinal center                            | GC       |
| Intestinal fibroblast                      | iFB      |
| Intestinal lamina propria cell             | iLPC     |
| Intraepithelial lymphocyte                 | IEL      |
| Isolated lymphoid follicle                 | ILF      |
| Knock out mice                             | KO mice  |
| Lamina propria                             | LP       |
| Lymphatic endothelial cell                 | LEC      |
| Macrophage                                 | M $\phi$ |
| Medullary reticular cell                   | MedRC    |
| Mesenteric lymph node                      | mLN      |
| Peripheral lymph node                      | pLN      |
| Peyer's patches                            | PP       |
| Plasma cell                                | PC       |
| Plasmablast                                | PB       |
| Polymeric Ig receptor                      | pIgR     |
| Regulatory T cell                          | Treg     |
| Ribosomal RNA                              | rRNA     |
| Secondary lymphoid organ                   | SLO      |
| Secretory component                        | SC       |
| Small intestine                            | SI       |
| Smooth muscle cell                         | SMC      |
| Somatic hypermutation                      | SHM      |
| Specific-pathogen-free                     | SPF      |
| T follicular helper                        | Tfh      |
| T zone reticular cell                      | TRC      |
| T-dependent                                | TD       |
| T-independent                              | TI       |
| Tritiated thymidine                        | TTH      |



# Intestinal lamina propria fibroblasts – phenotype and function for IgA<sup>+</sup> plasma cells

François Renevey





## 4 Introduction

### 4.1 The gut: a huge exchange interface in perpetual contact with microorganisms and food antigens

The small and the large intestine are part of the gastrointestinal (GI) system specialized in the digestion and absorption of vital nutrients for the body. To optimize these functions, the structure of the intestine has evolved to maximize the surface area particularly in the small intestine (SI) where most part of the nutrient absorption takes place. Indeed, in addition to its impressive length of 6-7m for an adult human SI, the surface area is further increased by the presence of villi and microvilli to finally reach a total absorptive surface of about 400m<sup>2</sup> (Haase, 2005). Anatomically, the SI is longitudinally divided into three segments depicted in **Fig. 1A**. As the mouse model is used in this study, only the murine GI organization is shown. However, mouse and human GI is very similar in term of structure (Nguyen et al., 2015). The duodenum, immediately after the stomach, is the first and shortest portion. It is followed by the jejunum, which extends into the ileum, which, in turn, joins the ceacum, the first portion of the large intestine, at the ileocecal junction (**Fig. 1A**). Notably, the ceacum of mice is larger than its human counterpart probably due to its important involvement in fermentation of plant and vitamin production. In contrast, the human ceacum is similar to that of the colon with no clear function (Nguyen et al., 2015). Finally, humans have an appendix, which is not the case for the murine GI. In contrast to the small intestine, the large intestine, or colon, does not harbor villi (**Fig. 1B**). The GI tract is made up of four main layers: the mucosa, the submucosa, the muscularis, and the serosa (**Fig. 1B**). The serosa is the most external layer composed of connective tissue followed by two perpendicular layers of muscle, or muscularis. The connective tissue between the muscle sublayers contains blood and lymph vessels, as well as the myenteric (Auerbach) nerve plexus. The submucosa forms the next layer, which is rich in large blood and lymph vessels and is physically separated from the mucosa by a thin layer of smooth muscle cells (SMC), called the muscularis mucosae. Finally, the mucosa groups the lamina propria (LP), rich in smaller blood and lymphatic vessels and immune cells, and the epithelium, which is continuously regenerated (Mowat and Agace, 2014) (**Fig. 1B**). This last epithelial monolayer, mainly composed of enterocytes, ensures the transport of digested food molecules from the gut lumen into the LP where they can reach blood or lymph vessels for their dissemination throughout the body. The epithelium provides another critical function:

it is the only physical barrier between 100 trillion commensal microorganisms and the underlying 'sterile' LP.

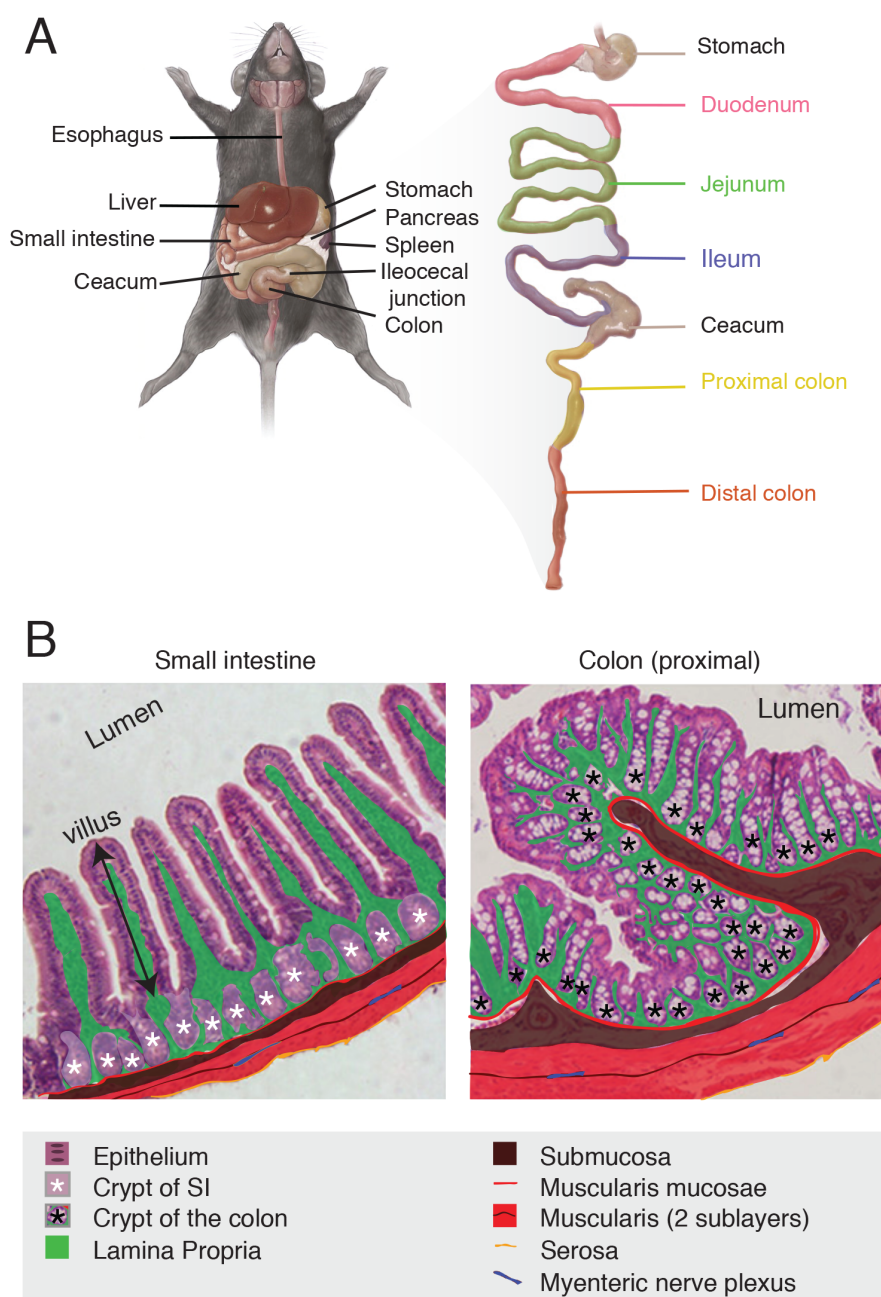


**Figure 1: Anatomy of the murine gastrointestinal (GI) tract.** (A) Left: the GI tract of a mouse and its disposition in the abdomen. The majority of the stomach is covered by the liver, which, along with the caecum, occupies the majority of the murine abdomen. Right: the different anatomical parts of the GI tract. (B) Thin sections of the jejunum (left) and the proximal colon of a mouse stained with hematoxylin (cell nucleus) and eosin (cell cytoplasm). The wall of the GI tract from the esophagus to the anal canal is organized in the same way with four layers of tissues (the important structures were highlighted with colors): 1) the *serosa* as the connective tissue (orange line); 2) the *muscularis* (red zone), composed by two perpendicular sublayers of muscle between which is found the myenteric nerve plexus (blue); 3) the *submucosa* (dark brown), separated from the mucosa by a thin muscle layer, called muscularis mucosae (red line); 4) the *mucosa* is composed of the epithelium (violet) and the underlying lamina propria (green), which embeds the crypts (star, in the SI; light zone in the colon). To optimize food absorption, the SI harbors numerous villi, which are absent from the colon. Figure adapted from Treuting et al. 2018 (A) and Zuo et al. 2014 (B).

The commensal microorganisms, including members from all three branches of life (bacteria, viruses, fungi), form the gut microbiota that is established soon after birth (Garrett et al., 2010; Putignani et al., 2014). Based on 16S ribosomal RNA (rRNA) sequencing-based metagenomic methods, more than a thousand different bacteria species have been identified in humans that coexist in a mutual symbiosis (Eckburg et al., 2005; Fagarasan et al., 2010). These microorganisms serve not only as natural competitors for opportunistic agents but also optimize processing and delivery of certain nutrients such as xyloglucans, short-chain fatty acid, and vitamins (Wang et al., 2017a; Nguyen et al., 2015). In addition, they are crucial for the development and regulation of parts of the gut immune system (Fagarasan et al., 2010; Hooper et al., 2012; Kato et al., 2014b; Randall and Mebius, 2014). However, the spread of these bacteria out of their niche constitutes a potential health threat, which can even lead to the host's death. In addition, the gut immune system has to deal with many non-commensal pathogens. Indeed, viruses, fungi, parasites or bacteria can colonize the mucosal surface and exploit this great exchange surface as gateway to enter the body and then spread systemically (Randall and Mebius, 2014). Therefore, to ensure containment of these bacteria in the lumen and maintain this host-microbiome homeostasis, the gut immune system has developed a set of diverse defense mechanisms involving innate and adaptive immune cells as well as non-immune cells (Garrett et al., 2010). The challenge of the gut immune system is to preserve the balance between effective immunity against invading pathogens and immune tolerance to commensals and food antigens to avoid unnecessary inflammation and the associated tissue damage (Randall and Mebius, 2014). Disruption of this crucial but delicate balance can result in dramatic inflammatory reactions, e.g., hyper-reactivity to food components (Meresse et al., 2012) or inflammatory bowel diseases (IBD), such as Crohn's disease or ulcerative colitis (Xavier and Podolsky, 2007).

### **4.2 The actors of the intestinal immune system**

To maintain gut immune defense and homeostasis, a large variety of mechanisms work hand in hand in the LP. Several epithelial cell types contribute to the first line of defense, as physical barrier but also by secreting various factors. Broad-spectrum antimicrobial peptides are produced constitutively by Paneth cells in the epithelial lining including  $\alpha$ -defensins, lysozyme C, phospholipases and C-type lectins such as Regenerating islet-derived 3-gamma (RegIII $\gamma$ ), which can also be produced by

enterocytes (Garrett et al., 2010; Mowat and Agace, 2014) (**Fig. 2A**). While most of these molecules regulate in part the microbiota size and composition, others, like

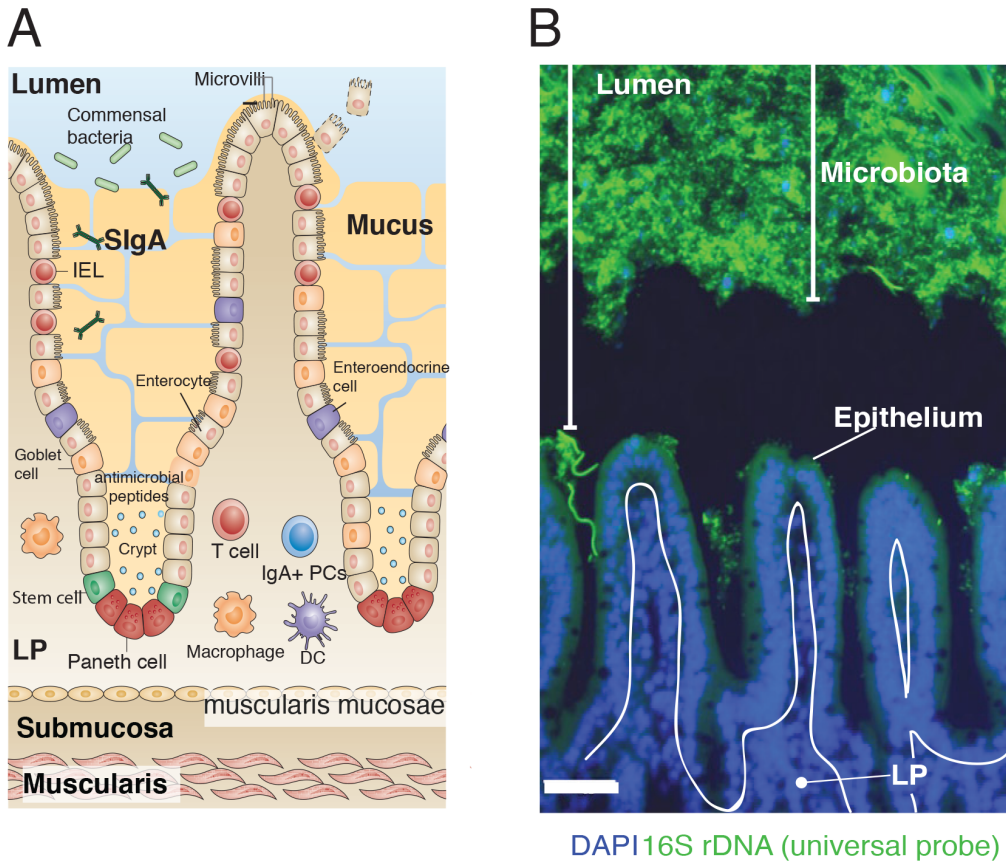


**Figure 2: The GI immune system maintains an impressive density of bacteria in the gut lumen.** (A) A magnified view of the mucosa of the small intestine. The lamina propria (LP) is found around the crypts as well as within the long thin villi. It contains numerous hematopoietic cells, including T cells, IgA<sup>+</sup> plasma cells (PC) secreting massive amount of soluble (S)IgA dimers, dendritic cells (DC) and macrophages. The LP is covered by an epithelium constituted in majority by absorptive enterocytes with microvilli providing a huge surface for absorption of nutrients. Intraepithelial lymphocytes (IEL), goblet cells (mucus-secreting cells) and Paneth cells (anti-microbial peptide-expressing cells) as well as stem cells (epithelium self-renewal) are also found in this layer (respective functions reviewed in Mowat and Agace, 2014). The mucus mostly created by goblet cells has a protective role for the mucosa. (B) 16S-RNA labeling using a 16S rDNA probe (green) highlights intestinal bacteria, which are responsible for a large part of the gut microbiota that is in addition composed of archaea, viruses, and fungi, that together form a dense and compact population in the lumen of the small intestine. The mucosa is revealed by a DAPI staining. Due to the secretion of the antimicrobial peptide RegIII $\gamma$ , the microbiota is physically separated from the epithelium. This image highlights the impressive achievement by the immune system in keeping the mucosa layer sterile and uninfamed despite the presence of only a single epithelial cell layer separating the LP of the gut from commensals. Scale bar: 50 $\mu$ m. Adapted from Mowat and Agace, 2014 (A) and Vaishnava et al., 2011 (B).

RegIII $\gamma$ , are, in addition, involved in the physical separation of the bacterial community from the epithelium (Vaishnava et al., 2011)(as visible in **Fig. 2B**). Moreover, massive production of mucus by goblet cells in the epithelium helps to protect and lubricate the GI tract as well as to drain out bacteria and other

components of the intestinal flora (Johansson and Hansson, 2013; Johansson et al., 2013)(**Fig. 2A**). These innate mechanisms of the epithelial lining work together with an impressive number of different innate myeloid cells and adaptive immune cells (activated T and B lymphocytes) that are found scattered within the LP, just below the epithelial layer, few within the epithelial layer itself (**Fig. 2A**) and many in various forms of organized lymphoid tissues draining various parts of the gut. Of note, the gut is the site with most of the immune cells in the body illustrating its importance for immune defense. In the following the various intestinal immune cells of the LP will be shortly described, starting with the innate immune cells.

Intestinal macrophages ( $M\phi$ ), dendritic cells (DC), and eosinophils (Eos) form a dense population of the myeloid cells and play a crucial role in gut homeostasis. Due to their migratory capacity DC drain gut antigens (Ag) from the LP to the mesenteric lymph nodes (mLN) to prime T cells. On the other hand, resident  $M\phi$  display a highly phagocytic phenotype and are believed to clear bacteria and participate in amplifying the inflammation and thereby activating neighbouring immune cells (reviewed in (Gross et al., 2015) and (Bain and Mowat, 2014)). Moreover, IL-10 expressing  $M\phi$  prevent excessive anti-bacterial innate immunity by limiting IL-23 synthesis in myeloid cells (Krause et al., 2015). Finally, Siglec-F<sup>+</sup> Eos constitute an important fraction of the intestinal myeloid compartment and participate in gut homeostasis (Chu et al., 2014; Jung et al., 2015; Carlens et al., 2009). Eos-deficient mice allowed highlighting the important role of these cells in Peyer's patch development, mucus production, IL-1 $\beta$  production and IgA response (Jung et al., 2015; Chu et al., 2014). In addition to these numerous innate cells, activated T cell populations are found throughout the gastrointestinal tract.

Two major T cell subsets home the intestinal mucosa, namely the intraepithelial CD8<sup>+</sup> T cells (so-called intraepithelial lymphocytes (IELs)), which are involved in barrier repair and defense against intestinal pathogens, and LP CD4<sup>+</sup> T cells. The latter can be further subdivided into pro-inflammatory Th1/Th2/Th17 and regulatory T cells (Treg). Th17 and Treg cells form an additional layer of control of the homeostasis illustrating the necessary equilibrium between effective immunity and preservation of tissue integrity. Indeed, while Th17 cells have been shown to drive mucosal protection against various extracellular bacteria and parasites (Korn et al., 2009; Ivanov et al., 2009; Sellge et al., 2010), Treg cells exert their effects through dampening inflammatory responses by secreting anti-inflammatory cytokines, such

as IL-10 (Maynard and Weaver, 2008). As this thesis focuses on IgA-secreting plasma cells they will be described separately in the following chapter.

### **4.3 Secretory IgA antibodies represent one of the major effectors ensuring mucosal homeostasis and defense**

The second important lymphocyte population of the LP is represented by effector B cells, namely IgA producing plasma cells (PC), that are responsible for the production of 80% of all secreted antibody (Ab) in the body, with much fewer IgM<sup>+</sup> (around 10%) and IgG<sup>+</sup> PC (less than 1%) being present. This IgA synthesis is sort of constitutive after birth as it is constitutively triggered by the microbiota and food Ag. After its synthesis by LP PC, IgA forms polymers, predominantly dimers. This is achieved by the incorporation of a 15-kDa polypeptide, the so-called joining (J) chain. IgA dimers are then secreted by the PC into the extracellular space of the LP. The J chain of the dimeric IgA is recognized by the polymeric Ig receptor (pIgR), which is constitutively expressed on the basolateral membrane of epithelial cells. This receptor allows the transcytosis of the polymeric IgA from the LP into the intestinal lumen where the pIgR is cleaved thereby releasing the IgA dimers (**Fig. 3A, point 1**). The cleaved extracellular part of pIgR, called the secretory component (SC) remains attached to the IgA making it more resistant against the proteolytic degradation in the gut lumen (reviewed in (Brandtzaeg, 2013; Pabst, 2012)).

#### **4.3.1 IgA function**

The main function of secreted IgA dimers is to neutralize microbiota and their toxins thereby keeping this danger away and preventing inflammatory responses (**Fig. 3A, point 1**). According to the traditional view the functions of secretory IgA can be divided into at least three major categories: Ag excretion, intracellular neutralization and immune exclusion (**Fig. 3A**). The Ag excretion may occur during the IgA transcytosis through the epithelial layer. Indeed, IgA can neutralize Ag within endosomes of epithelial cells modulating the immune status of these cells (**Fig. 3A, points 2 and 7**) and participating in the Ag secretion (**Fig. 3A, point 2**). The same phenomenon may take place when Ag reach the LP. Indeed, specific IgA secreted by PC can encounter antigen within the LP, bind them and aid in their excretion (**Fig. 3A, point 3**). However, most IgA functions take place after transcytosis into the intestinal lumen where it binds more than 40% of anaerobic commensals in a non-inflammatory manner thereby contributing to immune tolerance of commensals

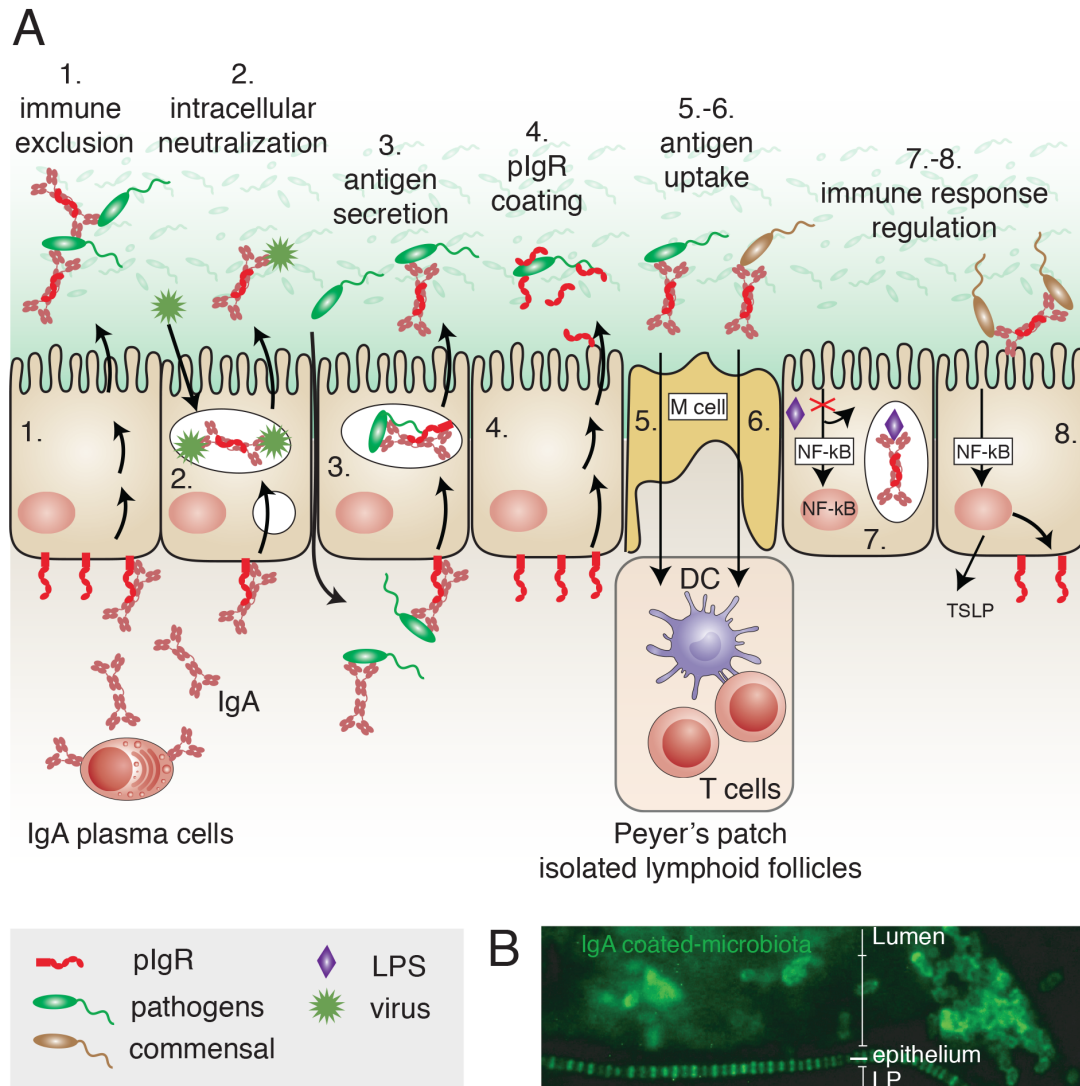


**Figure 3: IgA antibody dimers have been proposed to have numerous diverse functions in the LP and the lumen of the intestine.** (A) Summary of known functions of IgA, most of which contribute to keeping the mucosa sterile and thereby dampen proinflammatory immune responses. 1.: IgA is released into the lumen after transcytosis and mediates immune exclusion of the bound microbiota/pathogens. 2 and 3.: during the secretion process, IgA may encounter antigens either in the endosome of epithelial cells (2) or in the LP (3) and participate in their secretion into the lumen. 4.: The secretory component can also be released without IgA dimers and participate by its own to microbiota homeostasis by binding and excluding them. 5 and 6.: IgA can mediate the uptake of antigens via specialized epithelial cells, called M cells, found above Peyer's Patches leading to the development of a non-inflammatory immune response. 7.: Neutralization of bacteria-derived LPS in recycling endosomes by IgA abrogates NF- $\kappa$ B-mediated activation of pro-inflammatory genes. 8.: Cross talk between the bacteria and the intestinal mucosa is enhanced by IgA. Indeed, commensal strains coated by IgA can potentiate the responsiveness of the epithelium by modulating the expression of different cytokines, such as TSLP, and pIgR. Notably, IgA can directly modulate the metabolism and the virulence of pathogens. (B) Direct immunofluorescence IgA staining from the saliva with IgA illustrating the *in vivo* IgA coating of microbiota. Adapted from Cortésy, 2013 (A) and Brandtzaeg, 2013 (B).

(Brandtzaeg, 2013). One of the most referenced functions is immune exclusion which describes the secretory IgA ability to entrap Ag in mucus preventing their interaction with the epithelium and promoting their elimination by peristalsis (Fig. 3A, point 1).

Note that excess of unoccupied pIgR is released also by proteolytic cleavage to form so-called free SC which can participate to some immune functions within the lumen (**Fig. 3A, point 4**). However, immune exclusion due to IgA does not seem to be sufficient to prevent all infections (Mantis et al., 2011). Recent data showed that IgA might assist in Ag uptake across the epithelium via microfold (M) cells to initiate a response (**Fig. 3A, point 5 and 6**) or to modulate the expression of some immune proteins by epithelial cells (**Fig. 3A, point 7 and 8**) (Corthesy, 2013; Mantis et al., 2011; Pabst, 2012). In addition, IgA may share some functions with serum IgG *in vitro*. Indeed through cross-linking of IgA bound to the Fc $\alpha$ R, protective functions such as phagocytosis, degranulation (Motegi et al., 2000) and respiratory burst activity (Shen and Collins, 1989; Shen and Collins, 1989) can be initiated. Finally, IgA may have a more direct effect on pathogen metabolism and virulence (Corthesy, 2013), for example by reducing the bacterial fitness and motility and by decreasing the production of pro-inflammatory signals (Peterson et al., 2007; Cullender et al., 2013). So in a broad sense, IgA is important to orchestrate the beneficial tolerance established between the host and its commensal microbiome.

### 4.3.2 IgA deficiency in human

In humans, IgA deficiency (IgAD) is relatively common occurring in about 1 in 500 Caucasian individuals (Yel, 2010; Jorgensen et al., 2013). Most of the time IgAD is not absolute in humans, as IgA levels are reduced but not absent, and shows genetic associations with certain major histocompatibility complex (MHC) haplotypes (Corthesy, 2013; Wang and Hammarstrom, 2012) and mutations in the TACI (transmembrane activator and calcium-modulating cyclophilin ligand interactor) receptor (Martinez-Gallo et al., 2013). Nevertheless, human selective IgA deficiency was for a long time considered as an asymptomatic feature with mild phenotype. However, long-term studies revealed that 80% of patients are symptomatic when assessing complications more broadly (Jorgensen et al., 2013; Koskinen, 1996). These patients suffer from recurrent respiratory and gastrointestinal infections, autoimmunity, and intestinal disorders such as IBD and lymphoid hyperplasia (Aghamohammadi et al., 2009; Ludvigsson et al., 2014a; Ludvigsson et al., 2014b; Fagarasan et al., 2010). Surprisingly, a recent study demonstrated that IgAD patients display preserved global microbiome diversity with mild dysbiosis compared to healthy donors using a high-resolution metagenomic approach (Fadlallah et al., 2018). This result seems to be partially explained by compensatory mechanisms

including IgM secretion in IgAD patients, even though not absolutely all typical IgA targets are bound by gut IgM in IgAD patients (Fadlallah et al., 2018).

#### 4.3.3 IgA deficiency in mice

The importance of a proper IgA secretion in the intestine has been also highlighted by the characterization of murine models of IgA deficiency such as IgA KO, pIgR KO or J-chain KO (Mirpuri et al., 2014) (Harriman et al., 1999; Reikvam et al., 2012; Wijburg and Strugnell, 2006; Lycke et al., 1999). IgA deficiency in mice was associated with altered microbiota, increased susceptibility to induced colitis and injury, predisposition to certain types of infections, and lack of protective immunity against cholera toxin (CT) (Reikvam et al., 2012; Wijburg et al., 2006). Interestingly, altered microbiota composition was mainly observed in the SI, whereas colonic communities extracted from feces were much less affected by the absence of IgA (Fagarasan et al., 2002). This observation can also explain the preserved microbiome observed in IgAD patients (Fadlallah et al., 2018). Two other mouse strains have been useful to elucidate the function of IgA *in vivo*: the Activation-induced cytidine deaminase (AID) KO and AID<sup>G23S</sup> KI mice. AID is a key enzyme for both the class switch recombination (CSR) process allowing the exchange of the constant region typically from IgM/D to IgA, and for the somatic hypermutation (SHM) process allowing the generation of point mutations in the variable region of the antibody and thereby the generation of IgA of higher affinity (Keim et al., 2013). As a consequence, AID KO mice have no IgA but mainly IgM antibodies throughout the body. In the second strain (AID<sup>G23S</sup> KI), the mutant AID protein still catalyzes the isotype switch but no antibody hypermutation which implies that PC are able to produce a normal amount of IgA but their specificity cannot be improved over time. Interestingly, in AID KO and AID<sup>G23S</sup> KI, the microbiota showed an altered composition with expansion of anaerobes in the SI, such as segmented filamentous bacteria (SFB), as well as bacteria of the *Bacteroidales* and *Clostridiales* order, while no significant changes could be detected in the large intestine, in line with the findings of IgAD phenotype explained above. Moreover, the anaerobic bacteria expansion led to isolated lymphoid follicle (ILF; LP lymphoid structures described in more details in the next paragraph) hyperplasia and overstimulation of the immune system in non-mucosal secondary lymphoid organs (SLO) with an enormous expansion of germinal center (GC) B cells, despite a massive accumulation of IgM<sup>+</sup> B cells in the LP (Fagarasan et al., 2002; Suzuki et al., 2004; Fadlallah et al., 2018). All

together these studies clearly highlight the importance of IgA secretion and affinity maturation for proper regulation of the gut homeostasis, in addition to its evolutionary conservation and its massive production at the individual level (4-5g per day).

### **4.4 Induction of intestinal IgA responses and the migration of plasmablasts to the LP**

#### **4.4.1 Inductive sites**

According to the nomenclature of the Society for Mucosal Immunology (SMI) the gut immune system is divided into inductive sites and effector sites (<http://www.socmucimm.org/>; Brandtzaeg, 2009). Part of the inductive sites of the mammalian intestine are referred to as the gut-associated lymphoid tissues (GALT) and includes mainly Peyer's patches (PP) and Isolated lymphoid follicles (ILF) located close to the gut lumen (**Fig. 4**). MLN are also an inductive site of the mucosal immunity. However, they should not be called GALT structures according to the terminology recommended by the SMI as they do not sample Ag directly from the lumen via M cells but via the afferent lymph (Brandtzaeg, 2009; Brandtzaeg and Pabst, 2004) (**Fig. 4**). The intestinal effector sites include the LP and surface epithelia where IELs localize (Ganusov and De Boer, 2007; Pabst, 2012; Suzuki and Fagarasan, 2008). PP are classical SLO that develop on a stromal scaffold during gestation and therefore independently of gut colonization by bacteria which starts at birth. Despite their similarity, PP present some differences compared to conventional peripheral lymph nodes (pLN). PP are not encapsulated and localize right below a specialized epithelial cell lining called follicle-associated epithelium (FAE), containing microfold (M) cells that actively collect luminal Ag and distribute it to DC in the subepithelial zone which then induce in turn an immune response in the PP to be prepared for all potential invaders. Because of the constant microbiota exposure, GC are continuously present in PP, which is not the case for pLN in specific-pathogen-free (SPF) mice, which are defined as free of a specific list of pathogens and display a relatively high health status. GC are the site within SLO of B cell clonal expansion, CSR, and SHM, which together allow the generation of high-affinity memory B cells and PC responsible for antibody (Ab) responses. The second type of GALT are represented by ILF that form a heterogeneous array of small-sized lymphoid clusters scattered in great number throughout the gut LP (1000-1500 in mice and at least 30'000 in humans) (Mowat and Agace, 2014). In mice, these structures develop from

cryptopatches, which are small clusters containing lymphoid tissue inducer (LTi) cells and DC, but not  $CD3^+/CD4^+/CD8^+/B220^+$  cells that develop after birth in a microbiota-dependent manner (Kanamori et al., 1996; Pabst et al., 2005). ILF are also equipped with M cells and associated DC for Ag uptake and  $B220^+$  B cells. They can form GC but, in contrast to PP, have no clear T cell zone and harbor a higher proportion of innate lymphocytes as well as different DC subsets (Pabst, 2012). Interestingly, at

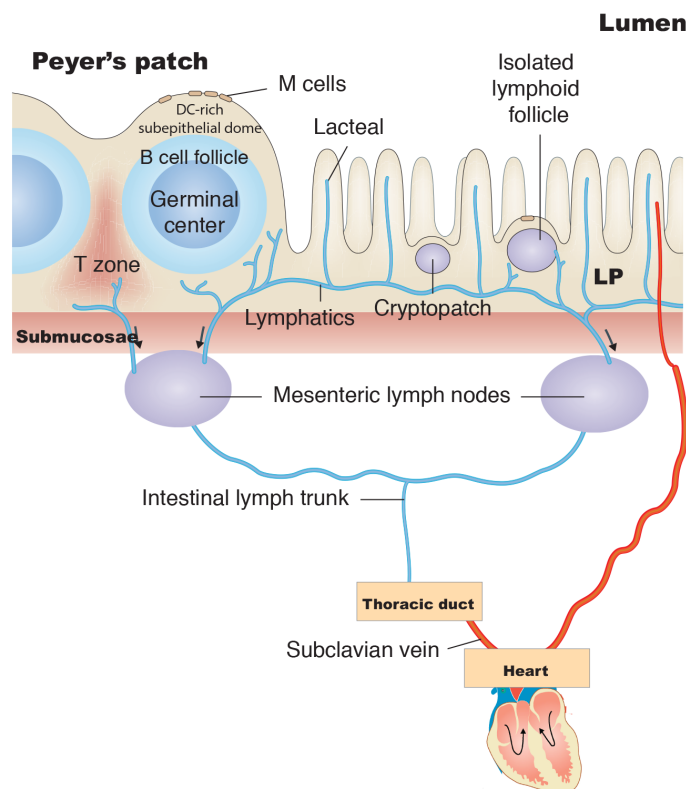


**Figure 4: Secondary lymphoid organs as sites of intestinal IgA response induction and their vessel connections with mesenteric lymph nodes and the lamina propria.** Schema illustrating the three induction sites for IgA responses: i.e. Peyer's patches, isolated lymphoid follicles (ILF) and the mesenteric lymph nodes (mLN). Peyer's patches consist of a DC-rich subepithelial dome where DC collect antigens provided by M cells localized in a specialized portion of the epithelium (follicle associated epithelium; FAE). During a T-cell dependent IgA-response induction, DC process and present antigens to  $CD4^+$  T cells to start a response and thereby the differentiation of primed B cells within the germinal center (GC) environment. Induction of B cell responses may also occur in ILF or mLN leading to the generation of  $IgA^+$  PC. Plasmablasts (PB), the migratory PC precursors, can leave these diverse inductive sites via local efferent lymphatics, join the intestinal lymph trunk and finally the bloodstream through the subclavian vein before reaching their effector site within the LP via the blood circulation where they become resident PC. Adapted from Pabst, 2012; Mowat and Agace, 2014.

steady state few ILF host GC and it is only when a bacterial overgrowth is detected that ILF develop a significant GC reaction. Therefore, ILF are thought to be a safety resource when immune response induction in PP is not sufficient (Knoop and Newberry, 2012; Lorenz et al., 2003; Pabst, 2015). Finally, mLN are very similar to pLN in terms of structure with the presence of capsule, lymphatic system, and similar

compartmentalization into T cell rich and B cell rich areas as well as the medulla as exit site. However, they share some characteristics with the PP because of their relationship with the intestinal immune system and flora. MLN are larger and contain more GC than pLN at steady state, even though GC are not present in all B cell follicles. MLN filter lymph draining from PP and ILF but also from a large part of the small intestinal LP, with each mLN draining a different segment of the intestine (Mowat and Agace, 2014).

### 4.4.2 IgA response

The induction of a mucosal IgA response is described in the following for PP. Epithelial M cells actively sample gut content and shuttle it to the underlying sub-epithelial dome rich in specialized DC but also T and B cells (**Fig. 4**) (Kucharzik et al., 2000; Pabst, 2012). Ag presented by DC can interact with T and B cells directly in the subepithelial dome region. Alternatively, DC can also migrate to the T cell area of the PP where they prime CD4<sup>+</sup> T cells that together with activated B cells form GC in the B cell follicle (Shreedhar et al., 2003; Reboldi et al., 2016). The activation of naïve B cells into IgA<sup>+</sup> PC is initiated once B cells have recognized their cognate native Ag via their IgM/IgD B-cell receptor (BCR), internalized and partially degraded their cargo. Then, B cells that successfully present antigenic peptides in the context of MHCII to previously primed Ag-specific CD4<sup>+</sup> T cells will initiate GC structures within follicles where CSR and somatic SHM can occur. GC B cells may interact with follicular dendritic cells (FDC) and a subset of CD4 T cells known as T follicular helper (T<sub>FH</sub>) cells (Kato et al., 2014b). In this T-dependent (TD) B cell activation, MHCII-T cell receptor (TCR) and CD40-CD40L interactions are thought to be critical to induce B cell proliferation and differentiation, including AID expression essential for CSR and SHM processes (Suzuki and Fagarasan, 2009). Activated GC B cells are prone to apoptosis and will die unless they obtain a survival cue from the GC environment. In this GC selection process, B cells with BCRs that have a higher affinity for the antigenic epitopes are selected to survive whereas B cells with low affinity or autoreactive BCRs are out-competed and die (Shlomchik and Weisel, 2012). These mechanisms lead to differentiation of B cells into plasmablasts (PB; the migratory precursor of plasma cells) that will preferentially express high affinity BCR of the IgA isotype.

Importantly, GC are not an absolute requirement for IgA CSR and IgA<sup>+</sup> PC generation. Indeed, CD40-deficient mice display a normal level of LP IgA<sup>+</sup> PC

accompanied with normal expression of AID and short-lived IgA post-switch circle transcripts (or CT $\alpha$ ) in PP, with only an impaired SHM despite the lack of GC (Bergqvist et al., 2006; Bergqvist et al., 2010). Similarly, CD40 deficiency in humans does not abolish IgA induction (Ferrari et al., 2001). AID-expressing B cells were also observed in TCR $\beta/\delta$ -deficient mice with IgA<sup>+</sup> PC populations being present in the LP, demonstrating the existence of both TD and T-cell-independent (TI) pathways for IgA<sup>+</sup> PC within intestines (Tsuji et al., 2008; Macpherson et al., 2000; Macpherson et al., 2001). Notably, IgA responses without T cells take more time to develop (Pabst, 2012; Kato et al., 2014a). As T zones are absent in ILF, TI antibody responses, including CSR but not SHM, are probably the predominant pathway ongoing in these sites, while TD responses dominate in PP. Notably, in CD40-deficient mice, IgA are largely unmutated and directed against TI Ag, while displaying multiple mutations in WT highlighting the important role of the TD response *in vivo* and the role of PP (Bergqvist et al., 2006). However, the relative TD/TI IgA response contribution is still difficult to determine experimentally.

The IgA predominance over the other isotypes in the LP is due to the particular microenvironment present in the different inductive sites, namely transforming growth factor (TGF)- $\beta$ 1, interleukin (IL)-21 and retinoic acid (RA) (Fagarasan et al., 2010; Suzuki and Fagarasan, 2009). Furthermore, many other cytokines are involved in the CSR process, including myeloid cell-derived APRIL (A Proliferation-Inducing Ligand) and BAFF (B-cell-Activating Factor of the TNF family) both of which have been shown to stimulate CSR from IgG to IgA in humans in a CD40-independent manner (Litinskiy et al., 2002), similar to findings with mice (Castigli et al., 2005). TACI and, to a lesser extent, BAFF-R have been shown to mediate the CSR by controlling AID expression induced by BAFF and APRIL (Katsenelson et al., 2007; von Bulow et al., 2001; Schneider, 2005; He et al., 2010; Pabst, 2012; Suzuki and Fagarasan, 2009). In line with this, 65% reduction of IgA<sup>+</sup> PC in the LP was observed in APRIL KO compared to littermate control upon oral vaccination (Castigli et al., 2004). Interestingly, low *april*–*taci* expression in ILF of young children compared to older healthy controls gives rise to a low number of IgA<sup>+</sup> PC accumulating in the SI, while *april*, *baff*, *bcma*, *taci* and *baff-r* expression was similar in the LP of these children, indicating IgA CSR in early infancy is inefficient in ILF because of the limited APRIL and TACI expression in these structures (Gustafson et al., 2014).

B cell responses cannot only be initiated in PP and ILF but also within mLN. Intestinal Ag carried by DC from the LP into mLN can induce IgA responses in either a TD or TI way (Cerutti et al., 2011; Pabst, 2012). Interestingly, mLN are not essential to mount a proper IgA response against some mucosal Ag such as cholera toxin (Bemark et al., 2012). It is highly controversial whether LP may also be a site allowing CSR (He et al., 2007; Gustafson et al., 2014; Brandtzaeg, 2013; Fagarasan et al., 2001; Lycke and Bemark, 2017). B-1 lineage cells, which are typically activated in the absence of T cell help, may enter LP from the peritoneal cavity and are thought to be a major source of TI IgA in mice with class switch potentially occurring within the LP (Fagarasan et al., 2010; Pabst, 2012).

Once IgA<sup>+</sup> PB/PC finalized their differentiation within PP or ILF, gut-homing receptors such as CCR9, CCR10 and  $\alpha_4\beta_7$  integrin are upregulated on PB/PC mainly due to RA signals. To leave PP, PB/PC upregulate sphingosine 1-phosphate receptor 1 (S1PR1) with IL-21 playing a major role in this process. IgA<sup>+</sup> PB/PC leave the PP (or ILF) via the efferent lymph, pass through mLN, wherein it has been proposed that they can undergo further differentiation (Lycke and Bemark, 2017), and return to the bloodstream at the junction of the thoracic duct and the left subclavian vein (Fagarasan et al., 2010; Macpherson et al., 2008; Pabst, 2012; Roth et al., 2014)(**Fig. 4**). The preferential mucosal localization of these PB and PC is determined by their expression profile of particular gut-homing receptors. The  $\alpha_4\beta_7$  integrin will interact with the mucosal addressin molecule MAdCAM-1 expressed by gut LP blood vascular endothelial cells (BEC) with tissue-specific homing being controlled by the expression of the chemokine receptors CCR9 and/or CCR10 which recognize the ligands CCL25 and CCL28, respectively (Macpherson et al., 2008). CCR9 – CCL25 seems to be the major axis for the small intestinal localization and more specifically for the observed location of PC in the lower half of the villus (Pabst et al., 2004). Once in the gut LP, PB undergo the final differentiation step into PC that can secrete large amounts of IgA (Cerutti et al., 2011). The fate of these IgA<sup>+</sup> PC is still not well understood. Indeed, relatively little is known on the migratory behavior as well as the half-life and the potential survival factors involved in the LP PC survival in contrast to the bone marrow (BM) and pLN. As this thesis focuses on the LP PC niches, I will first review the characteristics of PC niches in these other two sites.

## 4.5 Bone marrow plasma cell survival niche

Due to their high sensitivity to death when isolated from the BM (Minges Wols et al., 2002; Cassese et al., 2003) and their high turnover observed in peripheral lymphoid organs (Makela and Nossal, 1962; Cooper, 1961), PC were thought to be short-lived and last for maximum a couple of weeks once generated. However, this hypothesized short-lived feature of PC does not reflect the long-term maintenance of Ab titers observed in the serum. Therefore, the prevalent paradigm proposes that the long-term maintenance of Ag-specific antibody titers is ensured by periodic activation of Ag-specific memory B cells which generate new short-lived PC (Bernasconi et al., 2002; Bernasconi et al., 2003). However, since 1997, accumulating evidence suggested that at least a subset of PC could survive for a long period indicating that continuous production of serum Ag-specific Ab can be memory B cell-independent (Manz et al., 1997; Slifka and Ahmed, 1998; Slifka et al., 1998; Ahuja et al., 2008). Because of the considerable clonal expansion occurring during a GC reaction, long-lived PC were thought to arise mostly from TD GC responses (Chu et al., 2011a). However, long-term Ab titers and long-lived PC are also generated upon TI Ag stimulation without meaningful GC, indicating that long-lived PC can be generated independently of T cells (Bortnick et al., 2012; Foote et al., 2012; Taillardet et al., 2009). These findings led to the delicate question of what factors and/or parameters allow to some PC to become long-lived while others die rapidly. Recently, a study proposed that long-lived PC have metabolic advantages in comparison to short-lived PC, such as higher oxygen consumption and better glucose uptake capacity reflected by a higher Glut1 receptor expression (Shi et al., 2015; Corcoran and Nutt, 2016). Although the answer to the existence of a potential intrinsic capacity to survive is not found yet, it is clear that PC are not intrinsically long-lived and need external stimuli to avoid their default death fate.

The long-term maintenance of PC has been mostly studied in the BM where a spatially limited microenvironment, or survival niche, has been proposed to play the role of nursery for PC by providing them prosurvival factors (Radbruch et al., 2006; Roth et al., 2014; Tangye, 2011; Wilmore and Allman, 2017). Currently, it is believed that PB/PC generated upon Ag exposure leave their inductive site, such as pLN or spleen, and migrate into the BM where CXCL12-expressing VCAM-1<sup>+</sup> stromal cells, attract and retain them within a niche rich in survival factors (Wilmore and Allman, 2017). Indeed, murine and human BM PC survival is improved when co-cultured with stromal cells derived from BM (Minges Wols et al., 2002; Nguyen et al., 2018). PB

migrate more efficiently towards CXCL12 compared to mature B cells or PC, in agreement with their high CXCR4 (CXCL12 receptor) and low CXCR5/CCR7 expression (Hargreaves et al., 2001; Shi et al., 2015). Moreover, experiments using chimeric mice reconstituted with CXCR4KO fetal liver cells revealed that CXCR4-deficient PC fail to accumulate normally in the BM and are mislocalized in the spleen (Hargreaves et al., 2001). In line with this, analysis of CD19-Cre x CXCR4<sup>flox/flox</sup> mice revealed a dramatic reduction of CXCR4-deficient IgG<sup>+</sup>CD138<sup>+</sup> PC in the BM compared to control mice at steady-state (Tokoyoda et al., 2004). Furthermore, a role of CXCL12 as a survival factor in addition to its chemotactic activity has been also reported (Cassese et al., 2003) but this prosurvival effect was small and only described for *in vitro* PC cultures (Minges Wols et al., 2007).

In addition to CXCL12 chemotaxis, cell – cell interactions are thought to play an important role in the maintenance of the BM PC pool. BM PC have been shown to express various adhesion molecules including LFA-1, VLA-4 and CD44 (Minges Wols et al., 2002; Belnoue et al., 2012) and *in vitro* neutralization of PC binding to BM-derived stromal cells using anti-VLA-4 reduces PC survival, while anti-VCAM-1 does not (Minges Wols et al., 2002). Interestingly, combined *in vivo* neutralization of LFA-1 and VLA-4 causes a temporary but important loss (75% reduction) of NP<sub>25</sub>-specific PC in the BM (DiLillo et al., 2008). In contrast, confusing results were generated when CD44 was targeted on BM PC. Using two different Ab clones of CD44, namely IRAWB, an agonist Ab (Lesley et al., 1993a; Lesley et al., 1993b), and IM7, a neutralizing Ab (Zheng et al., 1995), Cassese and colleagues showed an unexpected prosurvival effect for both Ab clones on cultured BM PC (Cassese et al., 2003). In contrast, KM81 neutralizing Ab against CD44 showed no effect on BM PC in the hands of Minges Wols and colleagues (Minges Wols et al., 2002). In addition, neutralization of various CD44 isoforms (including CD44v6 and CD44v9) using Ab led to binding inhibition between immortalized PC lines and BM-derived stromal cells (Van Driel et al., 2002). Importantly, in this last study, the authors did not assess the PC survival in their binding assays, most probably because they used cell lines instead of *ex vivo* PC. All together, these *in vitro* data targeting CD44 need to be defined in the context of PC survival and adhesion, Finally, whether CD44 depletion *in vivo* causes mature PC to die has not been tested directly. Therefore, the function of CD44 in BM PC homeostasis still needs further exploration.

CXCL12 and ligands for LFA-1 and VLA-4, namely ICAM-1 and VCAM-1, respectively, have been shown, in many early studies, to be constitutively expressed

by BM stromal cells, which corroborates with their role in supporting BM-PC survival (Miyake et al., 1991; Jacobsen et al., 1996; Michigami et al., 2000). However, apart from CXCL12, VCAM-1 and ICAM-1 expression, a clear phenotypical and structural description of BM stromal cells *in vivo* has remained elusive for a long time with stromal cells most often defined as non-hematopoietic cells with plastic adherence capacity. Important advance came with the description of CXCL12-GFP reporter mice in which a large fraction of the CD31<sup>-</sup> BM stromal cells express GFP (Tokoyoda et al., 2004). This mouse model was then extensively analyzed to assess physical cell-cell contact and proximity showing that all B cell subsets including PC contact GFP<sup>+</sup> stromal cells (Tokoyoda et al., 2004; Holzwarth et al., 2018). Furthermore, a recent study dedicated to the description of CXCL12<sup>+</sup> cell networks in the BM highlights the complex structural organization and impressive density formed by the GFP signal of this reporter mouse (Gomariz et al., 2018). These studies clearly showed that the CXCL12-expressing cell network was underestimated, that they display a CD31<sup>-</sup> CD45<sup>-</sup> Ter119<sup>-</sup> PDGFRβ<sup>+</sup> mesenchymal cell phenotype, and interact with virtually all BM cell types (Gomariz et al., 2018). Furthermore, CXCL12<sup>+</sup> cells do not form a homogeneous cell type but seem to express differently some markers such as IL-7, VCAM-1, BP-1, or leptin receptor (LpR) (Cordeiro Gomes et al., 2016; Holzwarth et al., 2018). Interestingly, BM stromal cells can also produce IL-6 in response to BM PC coculture and IL-6KO BM stromal cells are substantially impaired in their ability to promote PC survival and function (Minges Wols et al., 2002). These results suggest that BM stromal cells react to PC interaction and can provide more survival factors than just CXCL12. Taken together these paragraphs highlight the important role of BM PC – BM stromal cell interactions in the formation of the BM PC pool.

However, it is believed that PC attraction and retention by themselves are not sufficient to maintain PC survival and that additional non-redundant cell-extrinsic PC survival factors are provided in this milieu. Multiple studies highlighted the role of BAFF, previously called BLyS, and APRIL in BM PC survival. Depletion of BCMA, the main APRIL receptor, led to an important loss of NP-specific PC in the BM (O'Connor et al., 2004; Peperzak et al., 2013) and to a reduced expression of the anti-apoptotic protein MCL-1 in PC (Peperzak et al., 2013). APRIL and BAFF were both shown to boost murine PC survival *in vitro*, even though APRIL was usually more efficient (Belnoue et al., 2008; O'Connor et al., 2004). Interestingly, the prosurvival effect of APRIL was only significant for human PC when they were combined with supernatant from BM stromal cells (Nguyen et al., 2018), while addition of BAFF to the stromal

cell secretome did not impact human PC survival suggesting that BAFF might be less important for human PC *in vitro* (Nguyen et al., 2018). Furthermore, transfer of PC into APRIL KO mice compromises their survival relative to WT hosts (Belnoue et al., 2008; Belnoue et al., 2012). Interestingly, APRILKO mice display a BM PC reduction only if TACI-Fc or BAFFR-Fc was injected in these mice. Moreover, BAFFR-Fc treatment alone had no impact on BM PC demonstrating that BM PC maintenance is dependent on the presence of BAFF and APRIL *in vivo* (Belnoue et al., 2008). All together, these data demonstrate that either APRIL or BAFF activity is critical for BM PC survival in mice while APRIL seems to be a better survival factor for human BM PC.

In contrast to BAFF and APRIL, IL-6 function in BM PC survival is still not clear, even though this molecule is studied since years in this context. Indeed, while IL-6 has been shown to be a potent survival factor *in vitro* for murine PC (Minges Wols et al., 2002; Cassese et al., 2003), IL-6 KO mice display no striking deficiency in BM PC survival as they showed no (Cassese et al., 2003) or a small defect in the Ag-specific PC population (Peperzak et al., 2013). On the other hand, transfer of tetanus toxoid specific PC into IL-6KO compared to WT mice did not reveal any difference in surviving PC (Belnoue et al., 2012). Notably, addition of IL-6 has been shown to help human BM PC survival and function *in vitro* in one study (Jourdan et al., 2014) but not another (Nguyen et al., 2018). Finally, apart APRIL, BAFF, and IL6, it should be emphasized that hypoxia, which is a physiological feature of the BM, augmented PC survival mediated by BM stromal cells and recombinant APRIL (Nguyen et al., 2018). Given the important and most described role of APRIL and/or BAFF and to a lesser extent IL-6 for PC survival, an important question was to identify the main cellular source of these soluble survival factors. Numerous cell types have been suggested to provide APRIL, BAFF or even IL-6 in the BM, including osteoclasts (Geffroy-Luseau et al., 2008), basophils (Rodriguez Gomez et al., 2010), megakaryocytes (Winter et al., 2010), and eosinophils (Eos) (Chu et al., 2011b). Consistent with this model, megakaryocyte and Eos-deficient mouse models display a reduction of approx. 50 and 70% of BM PC, respectively, whereas basophil-deficient mice show a reduced PC population only in the spleen (Rodriguez Gomez et al., 2010; Chu et al., 2011b; Winter et al., 2010). Interestingly, following the publication of Chu and colleague, BM Eos were placed, by different subsequent reviews (Chu and Berek, 2012; Corcoran and Nutt, 2016; Kometani and Kurosaki, 2015), as the main source of APRIL in BM and the main niche cells leading to the paradigm of the eosinophil-

driven PC survival. However, several recent studies demonstrated that *april* and *il6* transcripts, BM PC numbers, and IgM/IgG titers are normal in eosinophil-deficient  $\Delta$ dblGATA-1 mice at steady state (Bortnick et al., 2018; Haberland et al., 2018), but also after NP-CGG or TNP-OVA immunization, or in a Pristane-induced lupus model (Haberland et al., 2018). In line with this observation, anti-siglec-F Ab-mediated eosinophil depletion did not affect PC numbers (Bortnick et al. 2018). Moreover, Haberland and colleagues propose that APRIL and IL-6 is low in Eos and megakaryocytes but high in other myeloid cell types (Haberland et al., 2018). Furthermore, in contrast to the observation of Chu and colleagues, Zehentmeier and colleagues showed that only 10-11% of sessile PC contact dynamic and proliferating Eos using intravital microscopy of the BM niche (Zehentmeier et al., 2014). In conclusion, CXCL12-expressing CD31<sup>-</sup> BM stromal cells seem to form a stable niche playing the role of anchorage for BM PC and for other hematopoietic niche cells.

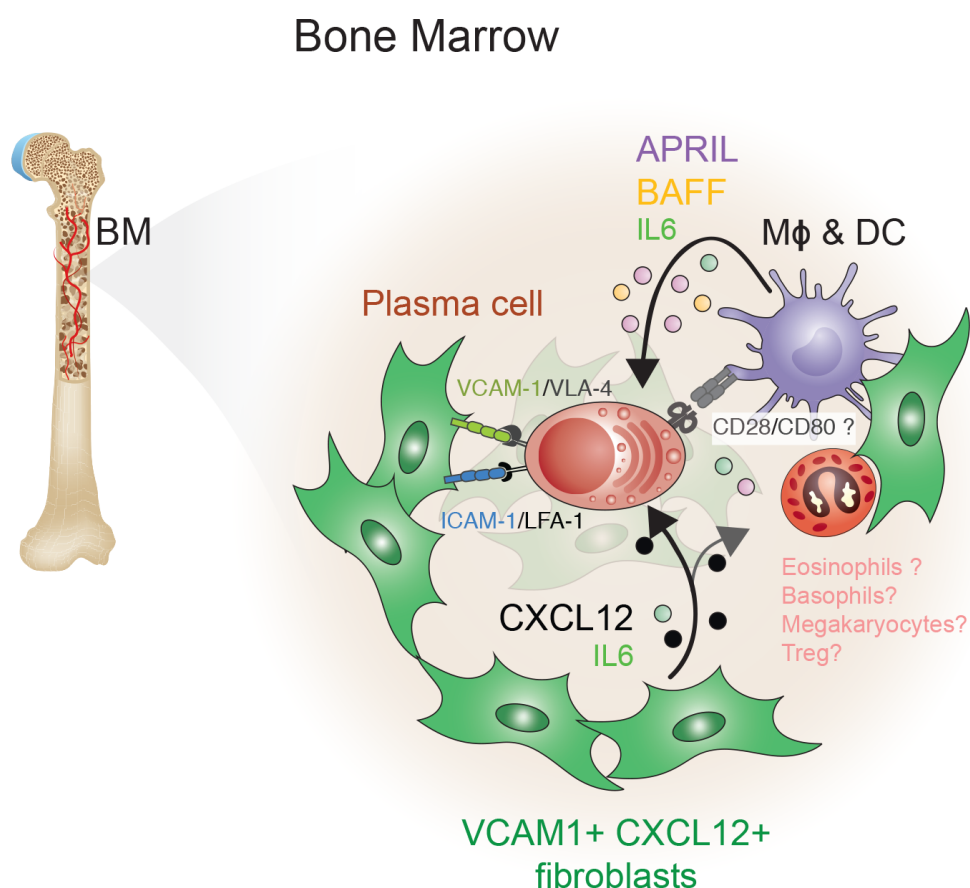


**Figure 5: Proposed PC survival niches in bone marrow (BM).** (A) BM PC survival niches. CXCL12<sup>+</sup>VCAM-1<sup>+</sup> fibroblasts attract (via CXCL12) and retain (via CXCL12, ICAM-1/LFA-1, and VCAM-1/VLA-4) PC but also other niche cells to form PC survival niches. Several studies suggest that myeloid cells, probably subsets of Mφ and DC, produce APRIL and BAFF, which are crucial for BM PC maintenance. Other cell types may also contribute to the production of these cytokines, including basophils, megakaryocytes, and eosinophils. Other interactions and cell types proposed to play a role in regulating PC homeostasis include CD28/CD80 and Treg cells.

APRIL and BAFF are still believed to be the major survival factors involved in BM PC survival, but the identity of the cells responsible for the limiting production of APRIL and/or BAFF still needs to be addressed further even though myeloid cells seem to be the best candidates.

As highlighted in this paragraph, scientists in this field have focused mostly on CXCL12, IL-6, APRIL and BAFF function, dedicating a lot of time to the identification of their cellular source. Although these molecules probably play crucial roles, other molecules and cell types could emerge as survival factors and niche cells in the future. In line with this, BM Foxp3 Treg have been described as an important regulator of the PC niche consistent with them contacting often PC in a dynamic manner. Moreover, Treg depletion using Foxp3-DTR mice leads to a 50% loss of PC number in the BM at steady state, while Eos were found in normal number (Glatman Zaretsky et al., 2017). Even though PC loss induced upon Treg depletion may be explained by the widespread inflammation, the investigation of new targets in the BM niche constitute an interesting area for future research. Finally, other survival factors have been described, including CD28 expressed by PC *in vivo* (Njau et al., 2012; Utley et al., 2014; Rozanski et al., 2015), as well as fibronectin and YWHAZ for human BM PC *in vitro* (Nguyen et al., 2018) showing that the characterization of the BM PC survival niche is still in its infancy. Based on the current literature a model of the BM PC survival niche is proposed in **Fig. 5**.

### **4.6 The transient PC niche of peripheral lymph nodes**

PC are not present constitutively in the pLN of SPF mice but they develop and accumulate there rapidly within days of infection or immunization to provide a first humoral protection before higher affinity plasma cells arise in GC to provide the long-term protection with PC homing to the BM. Although PC from pLN are not considered as long-lived, they still manage to home to the medullary cords of pLN and form an early PC response in this location, forming so-called extrafollicular PC foci, and secreting Ab for several days to 1-2 weeks. In contrast, when isolated from their microenvironment, they die in a couple of hours (Minges Wols et al., 2007), similar to BM PC. This suggests that the medullary cords of pLN have the potential to create a transient PC survival niche. Like in the BM, LN PB migrate from the B and T cell zones to the medullary cords where they differentiate into a more sessile PC, where they contact various cell types including myeloid cells and medullary cord-derived

fibroblasts or medullary fibroblastic reticular cells (MedRC) (Fooksman et al., 2014; Huang et al., 2018). The whole fibroblastic compartment of the pLN (as well as thymus, spleen, and other lymphoid tissues) are referred as fibroblastic reticular cells (FRC) and have been shown to form different functional and geographical subsets including among others Marginal zone FRC (MRC), T zone FRC (TRC), and previously mentioned Medullary FRC (MedRC). The functional description of most of these subsets has been covered by this recent review (Fletcher et al., 2015), while MedRC have been described only recently (Fooksman et al., 2014; Huang et al., 2018; Takeuchi et al., 2018). Interestingly, the medulla of pLN has been shown to be

## Peripheral lymph node

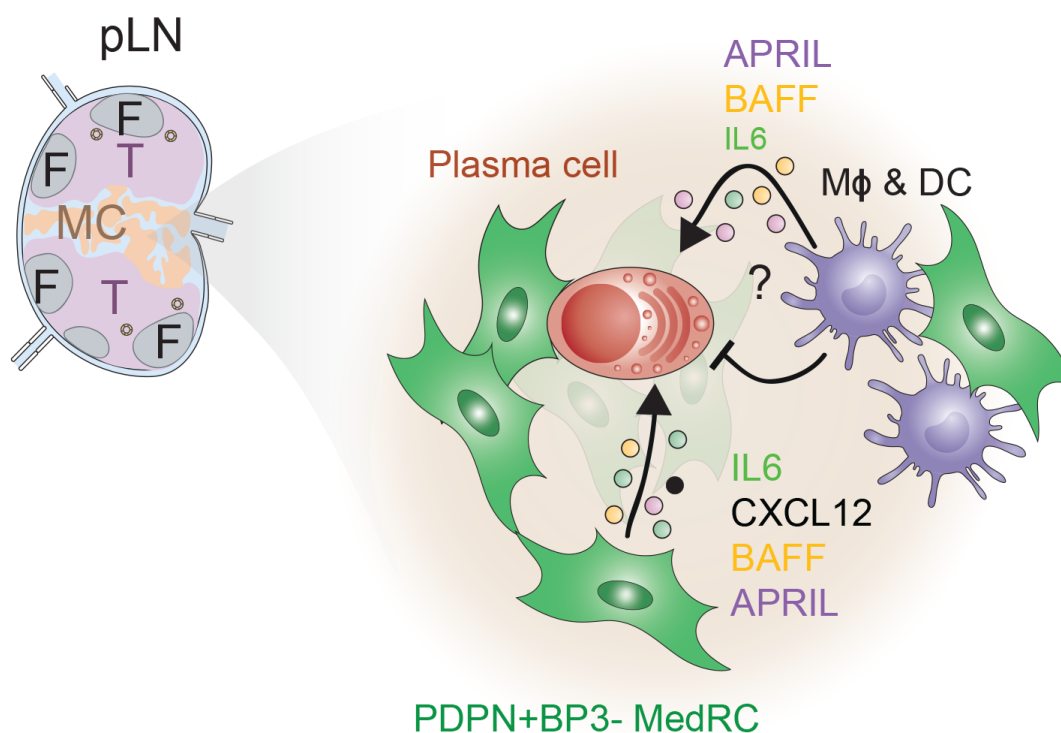


**Figure 6: Proposed PC survival niches in activated peripheral lymph nodes (pLN).** PB/PC survival niche in activated pLN. Upon infection, for example in the skin, PC develop in the draining pLN and accumulate within the medullary cords (MC) where they secrete antibodies during several days. PDPN<sup>+</sup>BP3<sup>-</sup> fibroblasts of the LN medulla (MedRC) interact with PC and promote their survival by providing IL-6, CXCL12 and possibly BAFF. Both MedRC and myeloid cells produce important amounts of APRIL and IL-6, but their role in PC survival is still incompletely understood *in vivo*. Abbrev.: F: B cell follicles; T: T cell zone; MC: medullary cords.

enriched in transcripts for *april*, *taci*, and *bcma* as well as *cxcl12* compared to B and T zones, using combination of microdissection and RT-qPCR techniques (Mohr et al., 2009; Zhang et al., 2018). These data suggest that similar mechanisms may be involved in extrafollicular PC survival in LN as in BM leading to the same question

concerning the source of these factors. Zhang and colleagues demonstrated that pLN-derived FRC, can express *april*, *baff*, *cxcl12* and *il-6* mRNA (Cremasco et al., 2014; Rodda et al., 2018; Zhang et al., 2018). We went further in this analysis by using a flow cytometry-based approach using a combination of several markers to segregate podoplanin<sup>+</sup> (PDPN, also known as gp38) BP-3-expressing TRCs from PDPN<sup>+</sup> BP-3<sup>-</sup> MedRC (Sitnik et al., 2016; Huang et al., 2018). This gating strategy allowed us to show that sorted MedRC express a high level of *baff* and *cxcl12* transcripts relative to myeloid, T, and B cells and constitute the main source of *IL-6*. In line with this, sorted MedRC promoted PC survival in an IL-6-dependent manner (Huang et al., 2018). Notably, *april* and *il-6* mRNA was shown to be highly expressed by myeloid cells (Mohr et al., 2009; Huang et al., 2018; Zhang et al., 2018). In our study, IL-6KO mice showed a reduction of PC d5.5 upon immunization, which was slightly less marked on d8.5 (Huang et al., 2018). Despite these mRNA data, no consensus emerged so far about the cell type(s) crucial for this niche. The use of different myeloid cell depletion models *in vivo* led to a decreased (Kumar et al. 2015), similar (Hebel et al., 2006) or increased PC number (Fooksman et al., 2014). Interestingly, we observed a synergistic prosurvival effect on LN PC when they were cocultured with MedRC and myeloid cells compared to MedRC alone or myeloid cells alone, suggesting a functional crosstalk between these two cell types (Huang et al., 2018). There data clearly indicate that further studies are important to understand the role of myeloid cells versus fibroblast subsets in LN PC homeostasis *in vivo*, including the factors involved. In conclusion, even though extrafollicular PC from pLN medullary cords are considered as short-lived compared to BM PC, they still need survival factors involving a niche comparable to the BM, involving both fibroblasts and innate immune cells (**Fig. 6**).

### **4.7 IgA plasma cell survival niche in the intestinal lamina propria**

In the intestinal LP, the PC life span is thought to be much shorter than for their BM counterpart. Indeed, newborn mice treated for 20 days with tritiated thymidine (TTH) revealed that TTH<sup>+</sup> IgA<sup>+</sup> PC frequencies drop rapidly from 100% (day 0) to 2% 35 days after the last TTH injection, while no TTH<sup>+</sup> IgA<sup>+</sup> PC were detected after 60 days under physiological conditions (Mattioli and Tomasi, 1973). This result was reproduced in adult mice using BrdU labeling years later and a similar result was obtained, namely a rapid decrease of BrdU<sup>+</sup>IgA<sup>+</sup>PC in the LP in a similar period of

time (Kamata et al., 2000). Moreover, one can easily imagine that the constitutive activation of PP and mLN by the microbiota leads to ongoing GC reactions generating constantly new IgA<sup>+</sup> PB that will delocalize the previously generated PC in the spatially limited LP niche. However, recent reports indicated that at least a subpopulation of IgA<sup>+</sup> PC has the potential to be long-lived. Indeed, Hapfelmeier and colleagues generated a *E. coli* triple auxotrophic mutant, called HA107, that colonizes efficiently germ-free (GF) mice but in a transient manner, being undetectable 72 hours after the last colonization when the mice become GF again. Importantly, HA107-treated mice display no measurable decrease in IgA secretion 112 days after exposure, despite the frequencies of GL7<sup>+</sup> GC B cells in mLN and PP returning to GF levels within 2 to 6 weeks after HA107 colonization (Hapfelmeier et al., 2010). Examination of human intestinal biopsies kept alive in culture demonstrated that even though IgA<sup>+</sup> PC numbers drop to 50% between day 1 and 5, the remaining PC persisted until day 20 and continued secreting IgA into the culture medium (Mesin et al., 2011). Lemke and colleagues used a coadministration of cholera toxin (CT) and OVA to generate a strong mucosal antibody response and test PC survival in a vaccination setting. They used an EdU pulse-chase strategy to label proliferating cells during a window of 12 days after boost immunization. CT- and OVA-specific EdU<sup>+</sup>IgA<sup>+</sup> PC were still detected 9 months after the boost in the LP, despite the ongoing B cell response in inductive sites. Importantly, the decrease of EdU<sup>+</sup> PC frequencies was quite rapid during the first three months with a drop from 90% to less than 5% on day 72, while only 1.5 and 0.2% were detected 4 and 9 months later, respectively (Lemke et al., 2016). Importantly, it is now well-accepted that IgA<sup>+</sup> PC represent 40 to 50% of the PC pool in the BM of mice (Youngman et al., 2002) and human at steady-state (Mei et al., 2009), suggesting a substantial contribution of mucosal PC to the BM PC pool. In the Lemke paper, CT- and OVA-specific IgA<sup>+</sup> PC in the BM were still found in the BM 9 months after the boost immunization (Lemke et al., 2016). These studies revealed that IgA<sup>+</sup> PC have the potential to be long lived *in vivo* in the context of strong immune response in mice and that part of these cells can also home the BM niche. In humans, using the advantage of mixed gender (which allows distinction between donor and recipient by labeling X/Y chromosomes) pancreatic-duodenal transplantation (Horneland et al., 2015), Landsverk and colleagues showed, that CD38<sup>+</sup>CD138<sup>+</sup> PC from the donor remained in the LP more than 1 year after the transplantation (Landsverk et al., 2017). Of note, three LP PC subsets were described, namely CD19<sup>+</sup> PC, CD19<sup>-</sup>CD45<sup>+</sup> and CD19<sup>-</sup>CD45<sup>-</sup> PC, with the majority of them expressing IgA, but showing different potential to remain in the SI. Indeed, while CD19<sup>+</sup> PC were dynamically

exchanged, the CD19<sup>-</sup>CD45<sup>+</sup> subset showed little and the CD19<sup>-</sup>CD45<sup>-</sup> PC subset no replacement. Measurement of Carbon-14 concentrations in DNA revealed that CD19<sup>-</sup>CD45<sup>-</sup> PC had a median age of 22 years (Landsverk et al., 2017). As most people are infected by rotavirus in their early childhood, rotavirus specific PC can be easily detected in humans and they were found to be highly enriched in the CD19<sup>-</sup> PC subsets. All together these different data from *in vitro* and *in vivo* investigations of murine and human LP PC demonstrate that, despite the high yield of PB generation, intestinal PC can survive for months to years in the gut. In other words, the LP most likely provides longterm survival niches for IgA PC, similar to the BM.

In contrast to BM and pLN, the niche cells and survival signals keeping IgA secreting PC alive have been poorly studied in the gut. APRIL has been shown to be expressed in the LP of the SI and colon in mice (Barone et al., 2009) and humans (Gustafson et al., 2014). Epithelial cells seem to represent the main source of APRIL in mouse and human intestine as based on histological protein stainings (Chu et al., 2014; Lemke et al., 2016; He et al., 2007), while other studies confirmed APRIL expression in epithelial cells but without comparing this expression with other LP-derived cells (Barone et al., 2009; Wang et al., 2017b). Mucosal neutrophils may also contribute APRIL, especially in the human tonsil (Huard et al., 2008). TACI-Fc injection (every second day for two weeks) reduced LP IgA<sup>+</sup> PC number about 60% under physiological condition (Kunisawa et al., 2013). However, as mentioned above, APRIL and BAFF are also involved in the IgA CSR making the distinction between CSR and survival function of these two molecules challenging. Two studies could exclude CSR process *in vitro* and demonstrate prosurvival effect of APRIL on IgA<sup>+</sup> PC in mucosa. Indeed, soluble oligomerized APRIL can boost the survival of purified tonsillar PC (Huard et al., 2008). In the second study, by blocking BCMA and IL-6, Mesin and colleagues decreased the IgA secretion from cultured human intestinal biopsies, suggesting that APRIL and IL-6 produced in the biopsy tissue promote PC survival or function (Mesin et al., 2011). These first studies suggest that, similar to the BM, APRIL is an important player of the LP PC survival niche (**Fig. 7**).

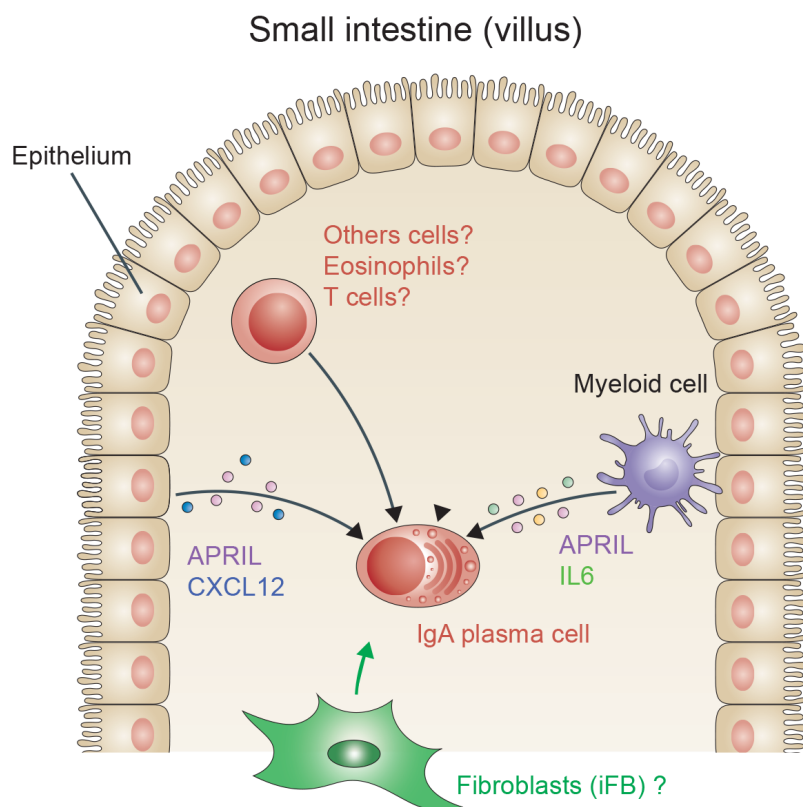


**Figure 7: Hypothetical PC survival niche in the intestinal LP.** Epithelial cells have been put forward in several studies as the major source of APRIL. CXCL12 seems to be released by the epithelium as well. Myeloid cells, and more specifically neutrophils, can also contribute APRIL within that niche. The involvement of eosinophils in this niche is controversial. Intestinal fibroblasts (iFB), other stromal cells or T cells have not been described yet in the context of IgA<sup>+</sup> PC survival. Adapted from Pabst, 2012

Although epithelial cells (and potentially some myeloid cells in the underlying LP) have been identified as APRIL source, no direct evidence has clearly demonstrated a role for APRIL, or other factors, from these cells in the promotion of LP PC survival *in vivo*. Also, the potential role of the numerous LP cell types on the *in vitro* or *in vivo* survival of the neighboring IgA<sup>+</sup> PC has been poorly explored. Several groups studied the role of intestinal eosinophils in this process *in vivo*, but reached different conclusions (Chu et al., 2014; Jung et al., 2015; Forman et al., 2016). The first study by Chu and colleagues showed that eosinophil-deficient  $\Delta$ dbIGATA-1 mice have a 70% decrease of BM PC (Chu et al., 2011a) and approx. a 50% decrease of LP IgA<sup>+</sup> PC (Chu et al., 2014). Based on these findings Siglec-F<sup>+</sup> eosinophils were rapidly accepted as typical PC niche cells in BM and LP making contact with PC and providing IL-6 and APRIL. Two other studies confirmed the impaired accumulation of IgA<sup>+</sup> PC in the SI of eosinophil-deficient mice (Jung et al., 2015; Forman et al., 2016), while no IgA<sup>+</sup> PC population difference was observed in the colon between eosinophil-deficient and control mice (Forman et al., 2016). However, Jung and

colleagues explained this phenotype differently than by an impaired PC survival. Indeed, they explained the *in vitro* and *ex vivo* observations of Chu et al. by a CD11b<sup>+</sup> SI DC contaminating their “purified” eosinophil samples used in coculture and transcript quantification. Using a corrected gating strategy, Jung and colleagues demonstrated that sorted eosinophils do not express APRIL and that the presence of eosinophils in culture does not promote IgA PC survival. Based on the PP phenotypes that they and Chu et al. observed along with the direct involvement of eosinophils in the TGFβ-dependent IgA class switch (Chu et al., 2014), they proposed that the IgA<sup>+</sup> PC pool reduction observed in ΔdbpGATA-1 mice may be due to an impairment of PP development combined with IgA class switch defects in PP (Chu et al., 2014; Jung et al., 2015). In conclusion, the eosinophil involvement in the IgA<sup>+</sup> PC survival niche remains to be further elucidated. Among the other candidate PC survival (or retention) factors, very little is known for the intestine. In contrast to the BM, CXCL12 seems to be mostly expressed by the epithelium and very rare within the LP (Agace et al., 2000). Similarly little is known about the role of LP stromal cells in IgA<sup>+</sup> PC survival, including intestinal fibroblasts, despite the evidence for their prominent role in the PC niches of the BM and LN (**Fig. 5, 6 & 7**).

### 4.8 Intestinal fibroblasts

Populations of non-hematopoietic (CD45<sup>-</sup>) non-endothelial (CD31<sup>-</sup>Lyve1<sup>-</sup>) and non-epithelial (EpCAM<sup>-</sup>) mesenchymal cells have been described for the LP of the small and large intestine but the lack of a general consensus on how to define and identify intestinal fibroblasts has given rise to the description of various populations termed either stromal cells, fibroblasts, mesenchymal cells, myofibroblasts, pericryptal stromal cells or telocytes. In fact, characterization of the intestinal LP architecture started with electronic microscopy studies in the ‘80s and 90s’ providing the first description of basement membranes and the subepithelial fibroblast-like cells (Komuro, 1985; Toyoda et al., 1997; Furuya and Furuya, 2007). These first electron microscopy-based data were then rapidly completed with antibody-based techniques done by Powell and colleagues resulting mostly in the identification of CD45<sup>-</sup> CD31<sup>-</sup> cells being either vimentin<sup>+</sup> α-smooth muscle actin (αSMA)<sup>-</sup> fibroblasts or αSMA<sup>+</sup> desmin<sup>+</sup> myofibroblasts (Pinchuk et al., 2010; Powell et al., 2011).

αSMA<sup>+</sup> myofibroblasts were found mostly around the crypts and to a limited extent in the subepithelial area of the human villi (Powell et al., 2011) while being absent from villi in mice (Bernier-Latmani et al., 2015). αSMA<sup>+</sup> myofibroblasts have been

proposed to be important for the proper development of the epithelial layer, but also for tissue repair and tissue organization, inflammation as well as tumorigenesis (Mifflin et al., 2011; Saada et al., 2006). In addition, these myofibroblasts were thought to be the predominant source of the Cox-2 dependent immunoregulator PGE2 during inflammation (Edwards and Smock, 2006) and of IL-33 (Mahapatro et al., 2016).

Alternatively, Thy1 (CD90) has been used to identify human intestinal fibroblasts and  $\alpha$ SMA<sup>+</sup> myofibroblasts *in vitro* and *in vivo* (Pinchuk et al., 2008; Bradley et al., 2009). In parallel, Thy1 was also used as alternative marker for murine myofibroblasts. Functionally, murine Thy1<sup>+</sup> myofibroblasts were shown to up-regulate the tolerogenic PD-L1 protein upon TLR4 activation *in vitro* (Beswick et al., 2014).

$\alpha$ SMA<sup>+</sup> cells represent only a small subset of stromal cells in the LP with these markers being expressed also by other cell types. Recently, several studies showed that intestinal fibroblasts express PDPN (Vicente-Suarez et al., 2015) similarly to pLN, splenic, and thymic fibroblasts (Link et al., 2007; Luther et al., 2000). Indeed, PDPN and CD31 co-staining can be used to identify PDPN<sup>+</sup>CD31<sup>-</sup> fibroblasts, CD31<sup>+</sup> PDPN<sup>+</sup> lymphatic endothelial cells (LEC) and CD31<sup>+</sup> PDPN<sup>-</sup> blood endothelial cells (BEC) (Peduto et al., 2009; Stzepourginski et al., 2015; Vicente-Suarez et al., 2015). Intestinal PDPN<sup>+</sup>CD31<sup>-</sup> fibroblasts (named iFB in this work) were observed in the whole LP from the duodenum to the colon filling the mucosa from the sub-epithelial area of the villi to the muscle layers (Stzepourginski et al., 2015) suggesting that most of the iFB are labelled by PDPN. This new technology to isolate and selectively analyze iFB has allowed to attribute new functions to this cell type. For example, PDPN<sup>+</sup>CD31<sup>-</sup> fibroblasts were found to express ICAM1 and VCAM1 and to produce constitutively RA and GM-CSF that imprint mucosal DC by inducing their own RA production which, in turn, induces gut-tropism and functional differentiation of T cells in mLN (Vicente-Suarez et al., 2015). It has been also shown that human and mouse PDPN<sup>+</sup>ICAM-1<sup>+</sup>CD31<sup>-</sup> iFB express oncostatin M (OSM) receptor and that iFB react to hematopoietically derived OSM by upregulating genes related to leukocyte chemotaxis (including CCL2, CXCL1, and CXCL10) and inflammatory cytokines (IL-6). Interestingly, OSM and OSM receptor expression was in IBD diseases and correlate with the histopathological severity (West et al., 2017). In addition, this study revealed that pharmacological blockage of OSM significantly reduced colitis in a mouse model of anti-TNF-resistance (West et al., 2017).

However, it is not known whether  $\alpha$ SMA<sup>+</sup> myofibroblasts/smooth muscle cells or Thy1<sup>+</sup> fibroblasts belong to the PDPN<sup>+</sup> iFB or form separate FB populations. In addition, it is also unclear whether the functional roles attributed to  $\alpha$ SMA<sup>+</sup> or Thy1<sup>+</sup> fibroblasts can be applied to the entire iFB population or whether they constitute specific features for these FB subsets. Along those lines, recent studies started to identify phenotypical and functional subsets among PDPN<sup>+</sup> iFB. For example, the CD34/PDPN combination allows distinguishing CD34<sup>-</sup> PDPN<sup>+</sup> iFB in the villi of the SI from pericryptal CD34<sup>+</sup> PDPN<sup>+</sup> iFB (Stzepourginski et al., 2017). CD34<sup>+</sup> PDPN<sup>+</sup> iFB do not express  $\alpha$ SMA and are positioned around Lgr5<sup>+</sup> stem cells providing the niche factors Wnt2b, Gremlin1 and R-spondin1 that promote stem cell proliferation, maintenance and differentiation onto the different epithelial cell types (Stzepourginski et al., 2017). Furthermore, CD34<sup>+</sup> PDPN<sup>+</sup> iFB are activated by intestinal injury, upregulating niche factors, proinflammatory cytokines and growth factors (Stzepourginski et al., 2017). In addition, CD34<sup>+</sup> PDPN<sup>+</sup> iFB has been shown to participate in the immune response against *Listeria monocytogenes* by providing IL-11 to the epithelium, which leads to an accelerated intestinal villus epithelium renewal, while decreasing E-cadherin-expressing goblet cells, thereby locking *Listeria monocytogenes* portal entry (Disson et al., 2018). Other studies characterized PDGFR $\alpha$ <sup>+</sup> Foxl1<sup>+</sup> subepithelial cells as niche cells for epithelium using reporter mice (Aoki et al., 2016; Shoshkes-Carmel et al., 2018). These Foxl1<sup>+</sup> cells, called telocytes, form a polarized monolayer providing Wnt2b and R-spondin3 (Wnt pathway activator) at the crypt base and Dkk3 (Wnt pathway inhibitor) toward the villus tip (Shoshkes-Carmel et al., 2018). Interestingly, some Foxl1<sup>+</sup> cells express PDGFR $\alpha$  and CD34 in mice and humans suggesting that they form a subset of the PDPN<sup>+</sup>CD34<sup>+</sup> iFB described above with a similar supportive function for the epithelium (Vannucchi et al., 2013; Shoshkes-Carmel et al., 2018; Greicius et al., 2018). Of note, PDGFR $\alpha$  seems to be expressed throughout the entire LP from SI to colon suggesting that its expression is not restricted to subepithelial telocytes and could be a good iFB marker together with PDPN (Shoshkes-Carmel et al., 2018; O'Rourke et al., 2016). Finally, a subset of CD31<sup>-</sup>PDPN<sup>+</sup> iFB has been reported to express the atypical chemokine receptor 4 (ACKR4), a receptor binding and scavenging CCL19/21 and CCL25 (Thomson et al., 2018). Stromal cells express ACKR4 in highly restricted areas where they can facilitate leucocyte trafficking (Nibbs and Graham, 2013). Although ACKR4 has been shown to be important for Langerhans cell and DC migration from the skin to the draining LN, Thomson and

colleagues did not observe impaired DC migration in the intestine and mLN of ACKR4 KO mice at steady-state or after R848 (molecule that activates immune cells through TLR7/8 engagement)-induced DC mobilization (Thomson et al., 2018). Instead, they observed ACKR4<sup>+</sup>PDPN<sup>+</sup> iFB exclusively in the deep LP in close proximity to BEC and LEC. In addition, ACKR4<sup>+</sup>PDPN<sup>+</sup> iFB express PDGFR $\alpha$ , ICAM-1 and CD34, indicating that these iFB are the same cells than as previously described by Stzepourginski and colleagues (Thomson et al., 2018; Stzepourginski et al., 2017). But, in addition to their role in epithelial stem cell homeostasis, ACKR4<sup>+</sup>PDPN<sup>+</sup>CD34<sup>+</sup> iFB express an array of genes encoding for endothelial cell regulators (Thomson et al., 2018). All together, these very recent studies highlight the requirement for a unified terminology of iFB in order to assess in more detail their heterogeneity as well as their function for neighboring immune cells. As mentioned above, iFB are crucial for the epithelium barrier maintenance and seem to participate in different aspects of the gut immune system, which make these cells a fascinating new avenue of research and a good candidate as component of the IgA PC niche.

## 4.9 Aims of this thesis

As described in the introduction, the organization and heterogeneity of iFB is only partially understood. In addition, iFB have not been proposed to play any role in PC survival. However, two previous lab members (Stefanie Siegert and Chen-Ying Yang) have produced preliminary data showing that collagen1 $\alpha$ 1<sup>+</sup>PDPN<sup>+</sup> iFB form a network throughout the LP where IgA-expressing PC localize and constitute the main local source of BAFF and CXCL12, besides being also a source of APRIL. Therefore, in my thesis project I pursued the following aims:

1. I wanted to investigate and define the structural organization of the iFB network *in vivo* using three-dimensional (3D) high-resolution confocal microscopy and using an iFB reporter mouse, namely the collagen1 $\alpha$ 1-GFP mouse strain.
2. To characterize iFB heterogeneity and try to unify the already existing iFB terminology and literature I wanted to screen various FB markers (PDPN,  $\alpha$ SMA, Thy1, CD34, PDGFR $\alpha$ , VCAM1, etc), both by histology and flow cytometry. As part of this question I wanted to establish an efficient isolation protocol for hematopoietic and non-hematopoietic cells of the intestine.
3. The cell types forming a physical PC survival niche for IgA PC in the LP are poorly known. Therefore, I wished to define in a quantitative manner the spatial organization of this niche by investigating the relative positioning of IgA<sup>+</sup> PC relative to iFB and other mucosal cell populations.
4. As *in vivo* tools are currently missing to target specifically survival factors in iFB, I wanted to establish an *in vitro* co-culture assay to be able to screen cell types and survival factors that might be involved in IgA PC survival and function.
5. Finally, I aimed to take the findings from these *in vitro* screening experiments and try to test their role for IgA PC survival *in vivo*.

## 5 Results

### 5.1 Fibroblasts of the lamina propria form a dense network in which IgA<sup>+</sup> PC reside and represent a rich source of PC survival factors.

To evaluate the potential functions of intestinal fibroblasts (iFB) in IgA<sup>+</sup> PC homeostasis, I first characterized the physical distribution and organization of iFB and other cells relative to IgA<sup>+</sup> cells in the LP. Fibroblasts are well known to be the major cell type involved in the production and processing of extracellular matrix (ECM) components in SLO but also throughout the body. Therefore, high collagen production may be considered the best criterion for defining a cell as fibroblast. Thus, in collaboration with Jeremiah Latmani-Bernier, I analyzed the intestine of mice transgenic for collagen-1 $\alpha$ 1-GFP (col-GFP) using a recently reported whole mount staining technique followed by confocal microscopy and 3D image reconstruction (Bernier-Latmani et al., 2015; Bernier-Latmani and Petrova, 2016). I observed a dense GFP<sup>+</sup> iFB network throughout the LP that displays a constitutively active collagen-1 $\alpha$ 1 promoter, from the proximal SI to the distal colon (**Fig.8A**). The iFB network was found throughout the villi, where the IgA<sup>+</sup> PC localize, but they also form a cellular scaffold around crypts of the small intestine (SI) and colon (**Fig. 8A; Annex 1A and B**; dashed line and stars) providing presumably a structural support for epithelial stem cells, Paneth and goblet cells as well as enterocytes, from the very bottom of the crypts (**Annex 1A**; layer 1) to the last level of the crypts (**Annex 1A**; layer 2 and 3). This wide iFB distribution was also seen in the colon with the whole LP around the crypts showing a dense network of iFB (**Annex 1B**), including in the regions rich in IgA<sup>+</sup> PC (**Fig.8A**). IgA<sup>+</sup> PC in the SI were found mostly in villi and were almost completely excluded from pericryptal areas (**Fig. 8A**), suggesting that the PC survival niche is spatially restricted, in contrast to iFB which are found throughout the LP. Moreover, the density of IgA<sup>+</sup> PC is high in the first two-thirds of the villi, while relatively low towards the tip of the villi (**Fig. 8A**). As no villi exist in the colon, the IgA<sup>+</sup> PC were found to be distributed around the colonic crypts, again surrounded by collagen-1 $\alpha$ 1-GFP<sup>+</sup> iFB (**Fig. 8A**).

As previous studies have shown that intestinal fibroblasts can be identified by their CD31<sup>-</sup> and PDPN<sup>+</sup> phenotype (Vicente-Suarez et al., 2015; Peduto et al., 2009; Stzpourginski et al., 2015), I tested whether these PDPN<sup>+</sup> iFB and the GFP<sup>+</sup> iFB I have identified here using col-GFP mice belong to the same population. Histological

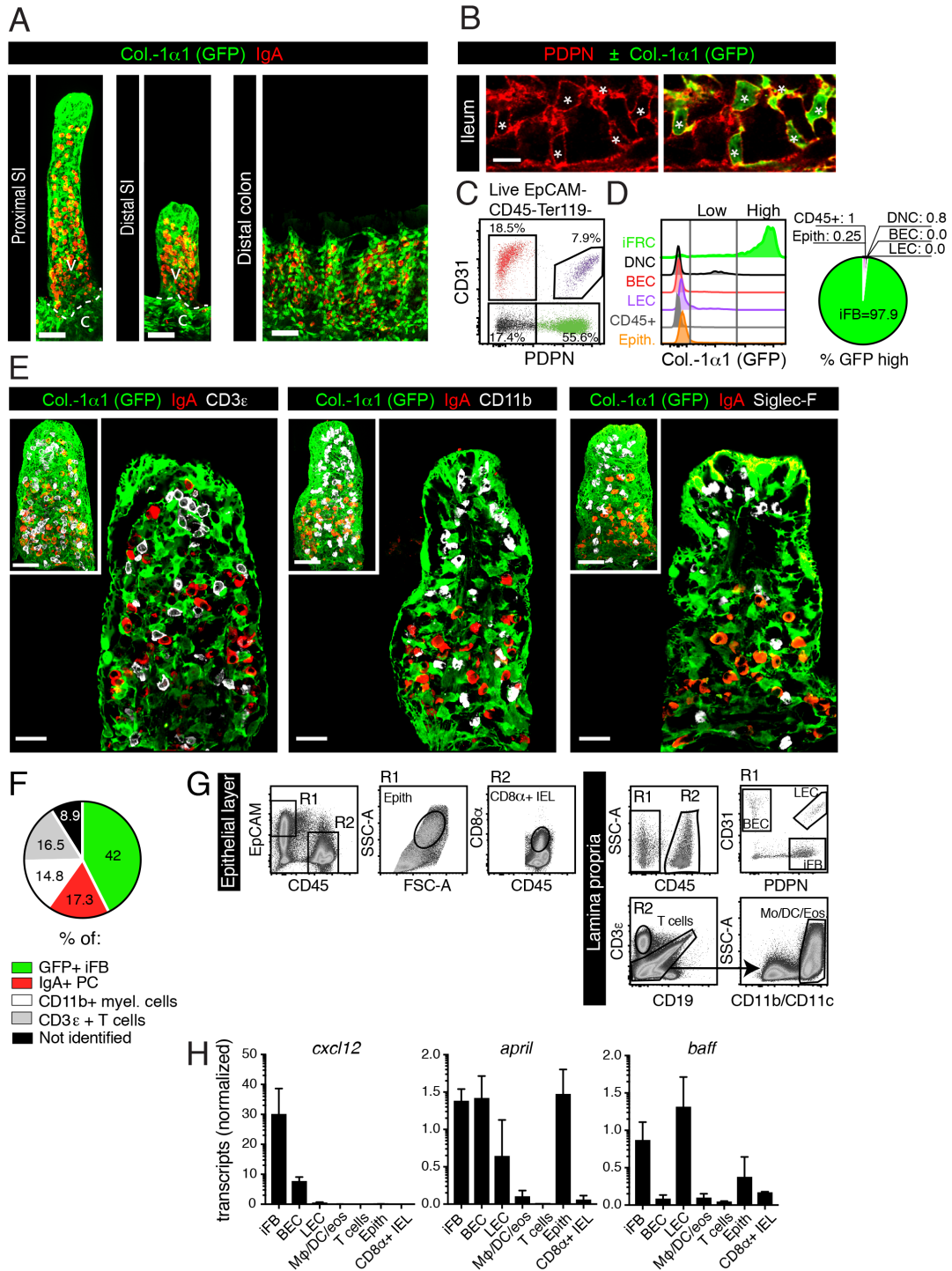


**Figure 8: IgA<sup>+</sup> plasma cells in the intestine are embedded within a dense fibroblastic network that produces collagen I and plasma cell (PC) survival factors. (A, B, E)** Representative confocal microscope images of intestine from adult collagen1 $\alpha$ 1-GFP (col-1 $\alpha$ 1-GFP) transgenic mice after epithelial layer elimination and whole-mount immunostaining. **(A)** 3-dimensional (3D) reconstruction of images showing the lamina propria (LP) of the small intestine (SI) or of the colon. col1 $\alpha$ 1-GFP expression (green) identifies intestinal fibroblasts (iFB) that form a dense meshwork for IgA<sup>+</sup> PC (red) localizing within the villi in the proximal and distal SI, or around crypts in the colon. iFB are not only found in the villus (v) but also in pericryptal areas (c) of the SI. Representative for images from more than 5 mice (n=5). **(B)** Co-expression of surface protein podoplanin (PDPN) and cytoplasmic GFP by iFB in ileum as assessed by confocal imaging (2D). Representative for images obtained from 2 mice (n=2). Similar data were obtained for the other SI segments (not shown). \* indicate individual iFB. **(C)** Flow cytometrical analysis of EpCAM<sup>+</sup>CD45<sup>-</sup>Ter119<sup>-</sup> intestinal cells from enzymatically digested distal

---

jejunum of col-1 $\alpha$ 1-GFP mice. Dot plot shows how the four stromal subsets were distinguished according to their CD31 and PDPN expression. Representative of more than 7 experiments with each 1-3 mice. **(D)** Histograms showing GFP expression by LP stromal cells (iFB, LEC, BEC, DNC), hematopoietic cells (CD45<sup>+</sup>) and epithelial cells (EpCAM<sup>+</sup>). The pie diagram depicts the sources responsible for the GFP<sup>high</sup> signal. Pool of six mice. **(E)** IgA PC (red) distribution and positioning in villi of the ileum relative to GFP<sup>+</sup> iFB (green), CD3 $\epsilon$ <sup>+</sup> T cells, CD11b<sup>+</sup> myeloid cells, and Siglec-F<sup>+</sup> eosinophils (all in white). The reduced upper left images show the entire 3D villi, while the main images display a villus reconstruction with three to five confocal layers only (5-7  $\mu$ m) and are displayed in the Imaris 'Blend' mode. Images are representative for villi from three mice. **(F)** Numbers of indicated cell types were counted in 3D whole-mount images of distal SI villi as shown in E, and are shown as ratio, calculated from 3-5 villi per mouse, n=3 mice. **(G)** Gating strategy used for cell sorting to analyze the transcripts levels as in H. Pre-gated on single live Ter119<sup>-</sup> cells. **(H)** iFB, LEC, BEC, CD45<sup>+</sup> hematopoietic cells and EpCAM<sup>+</sup> epithelial cells were sorted from distal SI and their transcript levels of indicated cytokines measured by RT-qPCR (means $\pm$ SD, n=3-5 mice) and normalized relative to a housekeeping gene (*hprt*). Scale bars: 50 $\mu$ m, A; 10 $\mu$ m, B; 40 $\mu$ m (3D), 20 $\mu$ m (semi-2D), E.

analysis showed that GFP<sup>+</sup> iFB in the SI always express PDPN on their surface (**Fig. 8B**). Similar to the GFP signal, PDPN expression is all over the LP and the submucosa in the SI and colon (**Annex 1C**), and largely absent in the muscle layers (**Annex 1C, stars**), while potentially being expressed in the serosa (**Annex 1C, filled arrow-head**) and in the space between the two perpendicular muscle layers (**Annex 1C, empty arrow-head**). In addition to histological analysis, GFP expression was assessed by flow cytometry on distal SI (second half of jejunum and ileum) digested by the method described by (Stzepourinski et al., 2015). This isolation method proved to be better than our previous isolation method using collagenase IV for 20 min, as indicated by a better iFB survival and higher iFB numbers (data not shown). Four distinct Ter119<sup>-</sup> EpCAM<sup>-</sup> CD45<sup>-</sup> stromal cell subsets were distinguished, namely CD31<sup>-</sup>PDPN<sup>-</sup> double negative cells (DNC), CD31<sup>+</sup>PDPN<sup>-</sup> blood endothelial cells (BEC), CD31<sup>+</sup> PDPN<sup>+</sup> lymphatic endothelial cells (LEC) and CD31<sup>-</sup> PDPN<sup>+</sup> iFB (**Fig. 8C**). Among all intestinal LP cells (iLPC), only iFB displayed a high activity of the collagen-1 $\alpha$ 1 promoter whereas a GFP<sup>lo</sup> signal was detected in DNC (**Fig. 8D, left panel**). Backgating on GFP<sup>hi</sup> populations highlighted iFB as the almost unique source of GFP<sup>hi</sup> expression, or by extension for collagen-1 $\alpha$ 1 transcripts, in the distal SI (**Fig 8D, right panel**). These data demonstrate that CD45<sup>-</sup>CD31<sup>-</sup>PDPN<sup>+</sup> iFB and collagen-1 $\alpha$ 1<sup>hi</sup> iFB are the same cells and that Col-GFP mice represent an excellent reporter selectively identifying PDPN<sup>+</sup> iFB, allowing their convenient visualization and study.

Using Col-GFP mice and whole mount staining to visualize the iFB compartment within entire intestinal villi, I next addressed the cellular composition of the PC niche in the murine SI. Importantly, the whole-mount protocol contains a removal step of the epithelium monolayer allowing homogenous and strong antibody stainings within the LP (see material and methods), but which implies that we cannot observe EpCAM<sup>+</sup> cells, intraepithelial CD3 $\epsilon$ <sup>+</sup> lymphoid cells, and CD103<sup>+</sup>CD11b<sup>+</sup> DC, which

are enriched in the epithelium (data not shown). Besides iFB that form a dense network in the villus segment where IgA<sup>+</sup> PC localize, we observed also the presence of CD3 $\epsilon$ <sup>+</sup> T cells, CD11b<sup>+</sup> myeloid cells (regrouping DC, M $\phi$ , and eosinophils) and Siglec-F<sup>+</sup> eosinophils, a subset of intestinal CD11b<sup>+</sup> cells (Jung et al., 2015). As 3D reconstructions might be misleading when the proximity is assessed, optical stacks of 4-7 $\mu$ m thickness were generated from villus images (**Fig. 8E**). Due to their abundance, CD3 $\epsilon$ <sup>+</sup> T cells and CD11b<sup>+</sup> myeloid cells seem to be often in the neighborhood of IgA<sup>+</sup> PC, in contrast to Siglec-F<sup>+</sup> eosinophils (**Fig. 8E**). Strikingly, all these immune cells always appear to directly contact with GFP<sup>+</sup> iFB that form a dense network inside the LP of the villus thereby occupying much of the space surrounding IgA<sup>+</sup> PC, thereby possibly restricting PC contact with other cells (**Fig. 8E**). To get a quantitative assessment of the cellular composition of villi in the distal SI, the individual cell types were counted on 3D images. Each villus contained approximately 100 iFB, and 20-50 cells for each of the other cell subsets (**Annex 1D**). This means that more than 40% of all DAPI<sup>+</sup> cells in the villus were found to be iFB, while IgA<sup>+</sup> PC, CD3 $\epsilon$ <sup>+</sup> T cells and CD11b<sup>+</sup> myeloid cells, and represent 17.3%, 16.5% and 14.8% of total cells, respectively (**Fig. 8F**). Together, these four cell types constitute more than 90% of all cells found within the villus segment of the LP, with 8.9% of cells not being identified using this approach. Obviously, the cell numbers assessed here for the distal SI may be different for the duodenum and proximal jejunum where villi are much longer but iFB appear to be also a very frequent cell type at those sites, as shown in **Fig. 8A**. In summary, this histological analysis of the IgA<sup>+</sup> PC niche composition revealed that iFB form a large part of the physical PC niche and provide support for our hypothesis that they might play an important role in PC attraction, retention and/or maintenance. T cells and myeloid cells appear to be further components of this niche, although at lower frequency than iFB.

Next, we wanted to assess the contribution of the different LP cell types identified histologically to the production of factors important for PC survival and homeostasis. Strong production of survival factors might be considered an even better definition for niche cells than the relative numbers. Current knowledge on PC survival niches in BM and pLN indicates that soluble factors such as CXCL12, APRIL, BAFF and IL-6 might play a critical role in IgA<sup>+</sup> PC attraction and homeostasis. Previous work suggested that epithelial cells and/or eosinophils are the main source of APRIL in the SI suggesting these cells may be important regulators of IgA<sup>+</sup> PC homeostasis (Chu et al., 2014; Lemke et al., 2016). Using the gating strategy depicted in **Fig. 8G**, Chen-

---

Ying Yang (a former PhD student in the lab) and I sorted EPCAM<sup>+</sup> epithelial cells and CD45<sup>+</sup>CD8a<sup>+</sup> IEL from the epithelial layer of the distal SI, and 5 cell populations from the LP, including iFB, BEC, LEC, myeloid cells and T cells. Sorted iFB (EPCAM<sup>+</sup>CD45<sup>-</sup>CD31<sup>-</sup>PDPN<sup>+</sup>) were observed to be the major source of *cxcl12* transcripts with BEC (CD31<sup>+</sup>PDPN<sup>-</sup>) being the only other source but contributing more modestly (**Fig. 8H**, first graph). All CD45<sup>-</sup> stromal cell types from the LP and epithelial layer were found to abundantly express *april* transcripts at 5-10 times higher levels than in myeloid cells (CD45<sup>+</sup>CD11b<sup>+</sup>CD11c<sup>+</sup>) which included eosinophils (**Fig. 8H**, second graph). Our findings do not fully support the previous conclusions that eosinophils and epithelial cells are the major cell types providing APRIL (Chu et al., 2014), as iFB, BEC and LEC provide similar levels as epithelial cells. Finally, we identified iFB and LEC as the main source of *baff* transcripts with epithelial cells showing lower levels (**Fig. 8H**, third graph). Strikingly, the pool of myeloid cells containing DC, M $\phi$  and eosinophils was not only low for *cxcl12* and *april* but also for *baff* transcripts (**Fig. 8H**, third graph). In summary, the various stromal cell types seem to be the providers of factors potentially mediating PC attraction and survival, while myeloid and T cells do not seem to be directly involved in this process, despite their partial colocalization with IgA<sup>+</sup> PC. As iFB produce not only all three PC factors, but also constitute the major structural component of the PC niche, being much closer to PC than epithelial cells, we considered iFB as a strong candidate for regulating IgA<sup>+</sup> PC survival and possibly function.

## 5.2 iFB in the subepithelial layer are distinct from iFB in the core of the villus

As the initial histological characterization of iFB shown in **Figure 8E** has revealed an iFB layer lining the epithelium, but also a more scattered iFB distribution in the villus core next to IgA<sup>+</sup> PC, I aimed to define further the structural differences between iFB found within villi of col-GFP mice. High resolution 3D confocal imaging of GFP expression confirmed the existence of a highly organized 3D iFB network with evidence for two iFB subsets that differ not only in their location, but also in their size and cell morphology (**Fig. 9A** and **9B**). The subepithelial iFB population displays a flat shape with highly interconnected cellular processes that also appear to contact neighboring iFB of the same layer (**Fig. 9A** and **Fig. 9B**; filled arrow head). In the core of the villus, so below the layer with subepithelial iFB and blood vessels, and

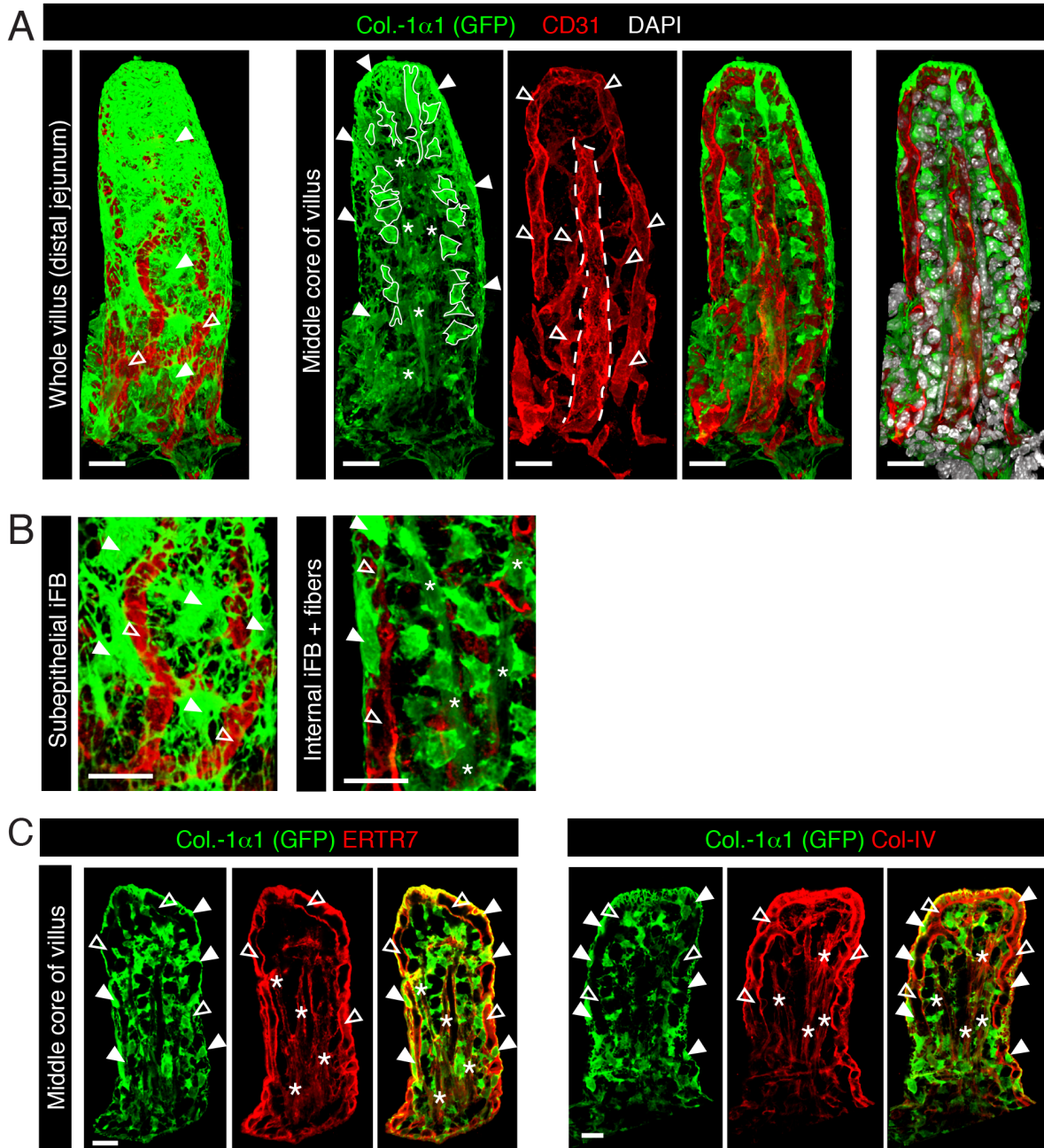


**Figure 9: iFB form a highly organized 3D cell network throughout the LP and below the epithelial barrier.** Representative confocal microscope images of the distal jejunum from col-GFP mice after epithelial layer elimination and whole-mount immunostaining. **(A)** Structural organization of intestinal stromal cells in a whole 3D reconstruction of a villus (left image) or the same villus opened through its center (other images) using the Imaris Blend mode. Col-1 $\alpha$ 1-expressing iFB (green) are subdivided into three cell types based on morphology and localization: subepithelial iFB (filled arrow head), internal iFB (white lines) and elongated GFP<sup>low</sup>  $\alpha$ SMA<sup>+</sup> smooth muscle cells (stars). BEC (empty arrow head) and LEC (dashed line) are stained with CD31 (red). **(B)** Magnified view of the three iFB types introduced in A highlighting their different cell morphologies. Symbols as in A. 8 to 10 $\mu$ m confocal reconstruction **(C)** Middle core of villi showing the costaining of collagen-1 $\alpha$ 1 (green) with either ERTR7 or Collagen-IV (red) next to subepithelial iFB (filled arrow head) and fibers (stars;  $\alpha$ SMA<sup>+</sup>) but not internal iFB. ERTR7 and Col-IV stainings are observed also around blood vessels identifying the basement membrane (empty arrow head). Data are representative of at least three independent experiments with n=3 mice. Scale bars: 20 $\mu$ m, A & B; 30 $\mu$ m, D.

---

around the CD31<sup>+</sup> central lymphatic vessel, called lacteal, is a zone with iFB that are more roundish and show less branches than subepithelial iFB (**Fig. 9A**, second panel with outlined cells; **Fig. 9B**, right image) but still form an interconnected iFB network (**Fig. 9C**, left image). This more frequent iFB population in the villus core is also the one contacting IgA<sup>+</sup> PC and most other immune cells found inside the villus (**Fig. 8E**; **Fig. 9A**, right image with DAPI staining).

One function of iFB is the deposition of extracellular matrix (ECM) structures, as indicated by the exclusive GFP expression by iFB in Col-GFP reporter mice. Whole mount staining with antibodies to ERTR7 and col-IV highlighted most strongly the basement membranes associated with the subepithelial iFB layer and the blood vessels in the outer LP layer (**Fig. 9C**), with a weaker staining showing the basement membrane of the central lacteal (**Fig. 9C**; **Fig. 9A**, lacteal highlighted with dashed line). No evidence was obtained for other matrix-based structures such as conduits, as observed in spleen and LN. As consequence iFB do not seem to fully enwrap these matrix structures, possibly explaining the different cell morphology compared with FRC in spleen and LN. Subepithelial iFB were nevertheless tightly associated with the basement membrane of the epithelial layer (**Fig. 9C**) on one side, and often associated with the basement membrane of CD31<sup>+</sup> blood vessels on the other side (**Fig. 9A** and **Fig. 9B**, empty arrow heads). The more centrally located iFB (or internal iFB) were found to be also matrix associated, either with the blood or lymphatic vessel or both (**Fig. 9A**; lacteal highlighted with dashed line). This second layer of internal iFB shows also associations with GFP<sup>lo/-</sup> smooth muscle cell (SMC) fibres (**Fig. 9A-C**, stars), which express  $\alpha$ SMA and are arranged around the CD31<sup>+</sup> lacteal (Bernier-Latmani et al., 2015). Interestingly, SMC were also strongly associated with the ERTR7 and col-IV expression (**Fig. 9C**, stars). In summary, iFB are found associated with the basement membranes that they most likely produce. These iFB exist in at least two subsets, with only the one in the villus center being close to IgA<sup>+</sup> PC.

### **5.3 Stromal cells in the LP of the SI are highly heterogeneous as assessed by flow cytometric and histological analysis.**

The histological investigation of Col-GFP mice described above suggested the existence of two GFP<sup>+</sup> iFB subsets that, however, could not be differentiated in flow cytometry based on their GFP expression level (**Fig. 8D**). Previous reports have

proposed that  $\alpha$ SMA, CD90 (Thy1) and CD34 allow to identify or subdivide intestinal fibroblasts by histology or flow cytometry. To elucidate iFB heterogeneity in the SI and compare our iFB identification strategy using GFP and PDPN with the data reported in the literature, I performed a flow cytometrical analysis of EpCAM<sup>-</sup> CD45<sup>-</sup> CD31<sup>-</sup> cells isolated from distal SI, combining multiple markers for intestinal fibroblasts in one labeling, namely PDPN, CD90,  $\alpha$ SMA as well as Collagen-1 $\alpha$ 1 (GFP), size (FSC-A) and granularity (SSC-A). All six parameters showed considerable heterogeneity in their values suggesting the potential existence of multiple iFB subsets (data not shown). In order to reduce the complexity of six dimensions into a two-parameter graph, a t-SNE (T-distributed stochastic neighbour embedding) algorithm was applied on the data generated using FlowJo software. Different subsets were then identified based on the every possible combination of the six markers mentioned above. This approach revealed in a step-wise fashion eight different clusters that were manually color-coded in the tSNE graph corresponding to potentially eight distinct cell types or cell states (**Fig. 10A**). The detailed features of each cluster are highlighted in histograms with the corresponding color (**Fig. 10A**). Of note, this flow cytometric analysis was not only performed on PDPN<sup>+</sup>GFP<sup>+</sup> iFB but also included double-negative cells (DNC), so CD31<sup>-</sup>PDPN<sup>-</sup> cells, which not only are distinct due to the absent PDPN expression but also express no or very low levels of GFP and correspond to the grey/black/purple/pink groups in **Figure 10A**.

The two cell clusters colored in gray and black have not yet be confirmed to be live cells. According their size and granularity distribution (smaller than naïve T cells) and lack of positive markers (**Fig 10A**), these recorded events are most probably dead cell fragment, debris or non-lysed erythrocytes. In support with their debris/dead cell identity, my preliminary evidence from experiments in non-GFP mice suggest that these events do not incorporate the calcein-AM, a live cell dye activated by the esterase activity present in live eukaryotic cells (data not shown). In future, the technical problems should be solved to combine the GFP signal with the calcein-AM to circumvent this issue.

The populations expressing intermediate to high GFP levels included three main groups colored in dark and light green as well as red. The GFP<sup>hi</sup> iFB cells of the dark green group comprise the biggest group with 42% of all isolated cells in this analysis and are the cell type with the highest PDPN expression. The stromal cells in the light green group show lower expression levels for GFP and PDPN, compared to the dark

---

green group, and corresponding to 17% of all cells (**Fig. 10A**). Finally, the cells colored in red show lower PDPN expression along with intermediate GFP levels but very high  $\alpha$ SMA therefore most likely corresponding to smooth muscle cells or myofibroblasts which are rare in cell isolates (4%) but may exist as a second rare subset (2.8%) shown in the orange group expressing similar  $\alpha$ SMA and PDPN levels but lacking GFP expression (**Fig. 10A**). Notably, I could not clearly distinguish GFP<sup>int</sup> and GFP<sup>hi</sup> iFB by histology. Only GFP<sup>int</sup>  $\alpha$ SMA<sup>hi</sup> cells showed clearly an intermediate level of GFP compared to surrounding iFB. The use of an anti-GFP to amplify the GFP signal in 3D histology could reduce the GFP<sup>int</sup> and GFP<sup>hi</sup> level difference measured by flow cytometry (without anti-GFP). Indeed, the anti-GFP needs to penetrate through the tissue that might lead to differential staining level independently of the actual GFP expression within the cells. In line with this hypothesis, subepithelial iFB were often observed with a slightly higher GFP signal compared to internal iFB (data not shown).

Several more surface markers were investigated that previously have been associated with iFB, including CD34, PDGFR $\alpha$ , ICAM-1, and VCAM-1. CD34 and PDGFR $\alpha$  have been associated with pericryptal iFB and/or subepithelial telocytes (Vannucchi et al. 2013; Stzepourginski et al. 2017; Shoshkes-Carmel et al. 2018) while ICAM-1/VCAM-1 expression have been associated with iFB (Vicente-Suarez et al., 2015). GFP<sup>+</sup> iFB were gated (**Fig. 10B**; dashed line in left graph), and analyzed for these markers. The CD34 and PDGFR $\alpha$  expression analysis indicated two clearly distinguishable subsets, with only one large subset (> 70%) expressing these markers, while ICAM-1 and VCAM-1 expression analysis showed one broader peak with 55-78% of iFB being positive suggesting smaller differences between cells (**Fig. 10B**). Among these four markers, CD34 and PDGFR $\alpha$  expression may be most interesting to further analyze with PDGFR $\alpha$  expression being highly restricted to iFB (**Fig. 10B** and data not shown).

This stromal cell characterization by flow cytometry allowed to identify marker combinations that could then be tested in histology to localize the cell types in situ. Thy1 has been proposed as a (myo)fibroblast marker (Pinchuk et al., 2008; Bradley et al., 2009) but our flow cytometry analysis showed the lack of PDPN and GFP expression among Thy1<sup>+</sup> cell populations (**Fig 10A, purple and pink groups**) suggesting Thy1 is not a fibroblast marker in murine 'naive' intestine of B6 mice. Indeed, by flow cytometry the anti-Thy1.2 antibody labelled LEC and a population of

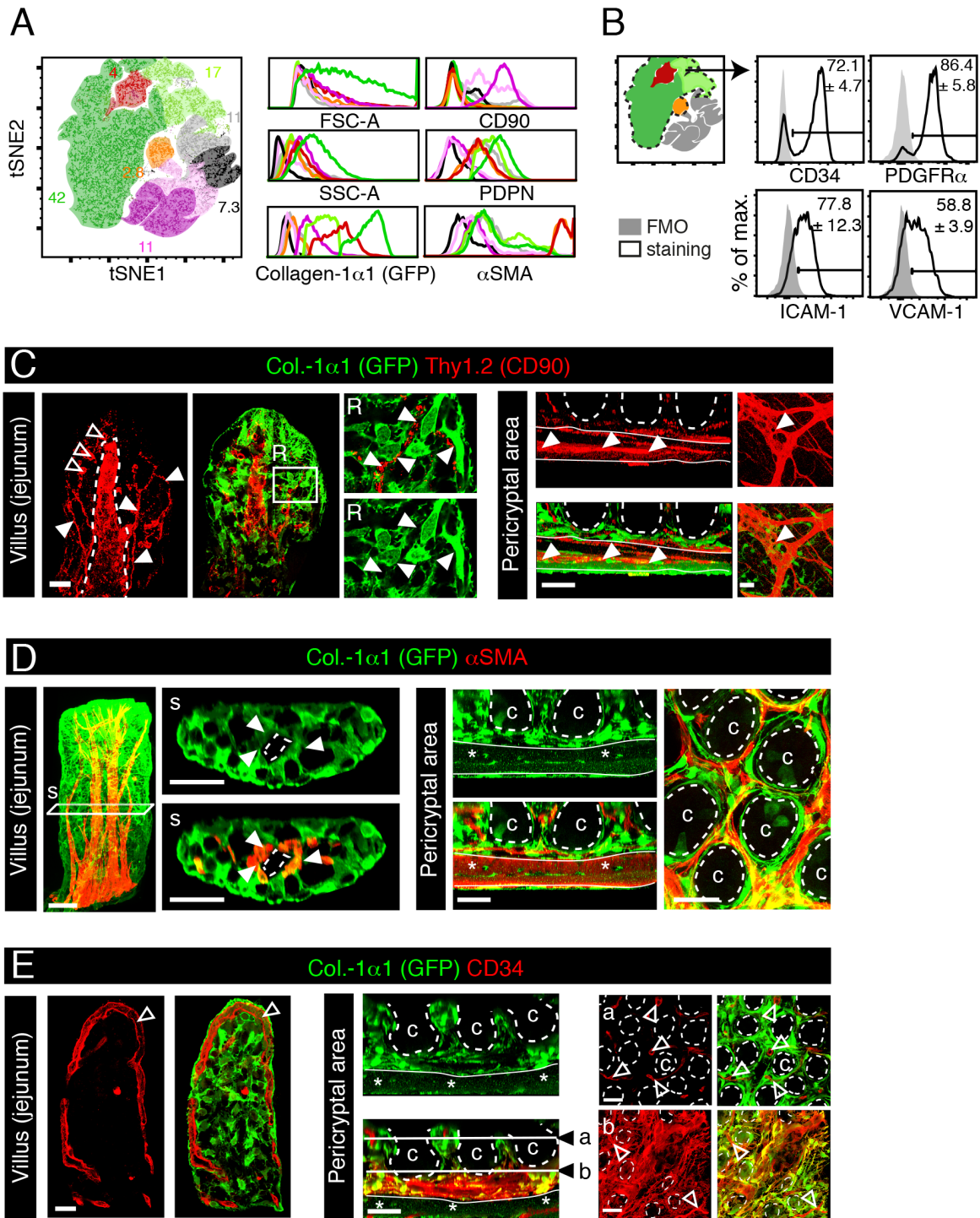


**Figure 10: iFB in the SI are highly heterogeneous and distinct from smooth muscle cells and endothelial cells.** **A)** Flow cytometric tSNE (t-Distributed Stochastic Neighbor Embedding) analysis of non-endothelial/non-epithelial stromal cells (EpCAM<sup>+</sup>CD45<sup>+</sup>Ter119<sup>-</sup>CD31<sup>-</sup>) isolated from the LP of the distal SI of col-GFP mice. 6 parameters were taken into account: FSC-A and SSC-A Collagen1 $\alpha$ 1-GFP, CD90 (Thy1), PDPN and  $\alpha$ SMA, revealing at least distinct stromal cell subsets. Black/grey populations correspond probably to cellular debris. Representative of five independent experiments. **(B)** PDPN<sup>+</sup> GFP<sup>+</sup> iFB populations identified in tSNE analysis in A (surrounded by dashed line) were analyzed by flow cytometry for further mesenchymal markers, as shown in the histograms for CD34 PDGFR $\alpha$ , ICAM-1 and VCAM-1. Representative of four independent experiments. **(C-E)** Representative confocal microscope images of the jejunum from col-1 $\alpha$ 1-GFP mice after epithelial layer elimination and whole-mount immunostaining. **(C)** GFP signal and Thy1.2 (CD90) expression by iFB and T cells/lymphatics/neurons, respectively. In the left image and the region of interest (R) of the

---

villus: filled arrowheads point to Thy1<sup>+</sup> nerves, empty arrowheads to roundish Thy1<sup>+</sup> T cells, and the dashed line show the Thy1<sup>+</sup> lacteal (lymphatic). In the pericryptal images on the right side: dashed lines delimit the mucosa/submucosa and filled arrowheads point to the Thy1<sup>+</sup> myenteric plexus. Data are representative of at least three independent experiments. **(D)** Villus in 3D side view on left side: GFP signal (green) and  $\alpha$ SMA (red) expression distinguish iFB (green) from smooth muscle cells (green and red, filled arrowheads), shows their different distribution and organization within the LP. The 2D image on right side is an optical thin section (s) of left image showing the top view: Dashed line indicates the boundary of the lacteal. In the pericryptal area, a side view is shown on left and a top view on right side. Dashed lines surround the crypts (c); the two perpendicular smooth muscle layers (red, stars) are framed by two filled lines. **(E)** Villus on left side: CD34 expression by blood endothelial cells (empty arrowhead) and GFP signal by iFB showing their different organization and distribution within the LP. For the pericryptal area, a side view is shown on left and a top view on right side with two optical sections at two different depths shown: a (at the top of the crypts) and b (bottom of the crypts). The thin full lines delimit the submucosa from the muscularis, the dashed lines delimit the crypts (c). Data are representative of at least three independent experiments. Scale bars: 20 $\mu$ m for villus and 40 $\mu$ m for pericryptal area images.

T cells (data not shown). High-resolution histology on whole mount preparation corroborated the flow data showing Thy1.2 staining on lymphocytes (**Fig. 10C**, empty arrow head) and the central lacteal in the villus but not on GFP<sup>+</sup> cells (**Fig. 10C**, dashed line). In addition, histology images revealed long and very thin Thy1.2<sup>+</sup> structures in the villus consistent with them being neurons (**Fig. 10C**, filled arrow head) with Col1 $\alpha$ 1<sup>+</sup> iFB being tightly associated (**Fig. 10C**, R square, filled arrow head). Furthermore, pericryptal and muscular layer images showed that Thy1 labelled the Col1 $\alpha$ 1<sup>-</sup> myenteric plexus localizing between the two perpendicular muscle layers (**Fig. 10C**, pericryptal area, filled arrow head). These findings demonstrate that Thy1 stains LP T cells, LEC and enteric neurons but not iFB in mice at steady state.

$\alpha$ SMA has been extensively used in the literature to identify myofibroblasts in murine and human tissue sections. However,  $\alpha$ SMA has been reported to be expressed by many other cell types such as smooth muscle cells and pericytes, in different organs including the gut. Flow cytometrical analysis showed that  $\alpha$ SMA<sup>hi</sup> cells form two populations according their Col1 $\alpha$ 1 promoter activity, being GFP<sup>low</sup> or GFP<sup>-</sup>, while all are PDPN<sup>int</sup>Thy1<sup>-</sup> (**Fig. 10A**; red and orange clusters). Histological analysis confirms that  $\alpha$ SMA<sup>hi</sup> cells derived from the villus can express low levels of GFP but form flame-like structures (**Fig. 10D**), surrounding the central lacteal (**Fig. 10D**, s section, filled arrow head) characteristic of smooth muscle cells (Bernier-Latmani et al. 2015).  $\alpha$ SMA<sup>hi</sup> cells are also all around the crypts but, importantly, do not interact directly with them as GFP<sup>+</sup>  $\alpha$ SMA<sup>-</sup> iFB are closer to the crypts (**Fig. 10D**, pericryptal area, dashed line, c). Finally,  $\alpha$ SMA labelled clearly the two Col1 $\alpha$ 1<sup>-</sup> perpendicular muscle layers (**Fig. 10D**, pericryptal area, stars). These data show that  $\alpha$ SMA<sup>hi</sup> cells form a highly organized but linear cell network that is distinct from the 3D meshwork-like cell

network formed by Col1 $\alpha$ 1<sup>+</sup> PDPN<sup>+</sup> iFB, with both networks physically interacting. Therefore, at steady state,  $\alpha$ SMA<sup>hi</sup> staining seems to be restricted to smooth muscle cells but not to myofibroblasts. Even though  $\alpha$ SMA<sup>hi</sup> cells express PDPN and Col1 $\alpha$ 1 at low level, their structural organization suggest that these cells are responsible of the physical strength and contraction of the villi (Choe et al., 2015).

CD34 expression by stromal cells identifies crypt-related fibroblasts as well as BEC (Vannucchi et al. 2013; Stzepourginski et al. 2017; Shoshkes-Carmel et al. 2018). Here, we confirm that by histology CD34 signals are found on GFP<sup>+</sup> iFB deep in the LP next to crypts containing epithelial stem cells where they form a dense network from the bottom of the crypts (**Fig 10E**, pericryptal area, layer b) to the underlying CD34<sup>-</sup> GFP<sup>-</sup> muscle layer (**Fig 10E**, pericryptal area, star), indicating that CD34 is also expressed in the submucosa of the SI. Within villi of the distal SI the CD34 marker was only detected on blood vessels but totally absent from neighbouring GFP<sup>+</sup> iFB (**Fig 10E**, villi, empty arrow head). Nevertheless, our flow cytometry experiments indicate that CD34<sup>+</sup> iFB represent 72.1 % of isolated GFP<sup>+</sup>PDPN<sup>+</sup> iFB (**Fig. 10B**, population selected by dashed line). It is currently unclear whether CD34<sup>+</sup> iFB are really that frequent in our histological sections relative to CD34<sup>-</sup> iFB within villi or whether this is a result of a more efficient isolation of iFB from the crypt regions compared to the ones from the villi.

Because CCL19 expression is one of the most studied features FRC in spleen and LN (Gunn et al., 1998; Luther et al. 2000) and a CCL19Cre-mouse line is available for genetic in vivo experiments (Ludewig et al., 2012), we investigated in CCL19Cre x ROSA26-eYFP reporter mice whether iFB share the CCL19 promoter activity with SLO-derived FRC. However, no Cre-induced eYFP signal was detected in isolated intestinal stromal cells, in contrast to lymph node FRC (**Annex 2A**). Histological analysis performed on these mice confirmed the absence of CCL19 promoter activity in villi of the SI. While most of the LP was eYFP<sup>-</sup>, rare eYFP<sup>+</sup> clusters were observed scattered throughout the LP presumably representing cryptopatches or isolated follicles (**Annex 2B**). Finally, iFB isolated from the SI were also investigated for two other FB markers for FDC and FRC in SLO, CD35 and BP3 (CD157), however, the villi and LP did not show any expression (**Annex 2C**).

All together these data demonstrate that PDPN<sup>+</sup> GFP<sup>+</sup> iFB represent the main iFB population in which different subsets can be identified such as deep LP CD34<sup>+</sup> iLP and CD34<sup>-</sup> iFB of the villi. The various approaches have however failed to reveal a way of differentiating subepithelial iFB from villus-internal iFB. FoxL1-cre mice may

---

help resolve that issue (Aoki et al., 2016; Shoshkes-Carmel et al. 2018).  $\alpha$ SMA<sup>hi</sup> cells seem to distinguish smooth muscle cells from typical iFB. However, these three cell types have the potential to share some features including the expression of Col1 $\alpha$ 1 or GFP, PDPN (**Fig. 10A**), PDGFR $\alpha$  and desmin (data not shown).  $\alpha$ SMA<sup>hi</sup> cells seem also to share the col-IV and ERTR7 expression with iFB (**Fig. 9C**). Finally, we demonstrated that, at least in mice, Thy1 expression is not a good marker for iFB in steady state.

#### **5.4 iFB and myeloid cells promote PC survival and IgA production in a contact dependent manner.**

As little is known on the cells and factors mediating IgA<sup>+</sup> PC survival and function, my aim was to establish an *in vitro* co-culture assay that is fairly physiological in its cellular composition but that would allow the efficient screening of different LP cell types we have identified within the PC niche as well as known PC survival factors (**Fig 11A**). First, I wished to determine whether iFB can promote PC survival and IgA secretion. To this end, I isolated intestinal LP cells (iLPC) from col-GFP jejunum and ileum (**Fig. 11A**; step 1) that I enriched for iFB using magnetic-activated cell sorting (MACS) for CD45<sup>-</sup> (**Fig. 11A**; step 2). As a negative control population, I MACS-enriched CD11b/c<sup>+</sup> myeloid cells that are also adherent cells but expected not to promote IgA<sup>+</sup> PC given their lack of transcripts for PC attraction and survival as shown in **Figure 8H**. In a later stage we also started co-culturing both iFB and myeloid cells, to assess whether iFB and myeloid cells that are both found in the PC niche *in vivo* would work more efficiently together than when cultured alone. The cell suspensions obtained were seeded at a fixed cell concentration into a 96 well plate before removing non-adherent cells after 2 hours to further enrich for iFB and myeloid cells. These different cell types were then cultured for 5 days to promote their recovery and normal cell morphology after the enzymatic isolation, and to allow iFB expansion (**Fig. 11A**; step 3). At day 4.5, the purity of GFP<sup>+</sup> iFB was assessed in the three types of cultures (iFB alone, myeloid cells alone or its mixture), using microscopy and flow cytometry, with cultures typically having around 99%, 12% and 55% of GFP<sup>+</sup> cells, respectively (**Fig. 11B** and **C**). Notably, the density of the cells in each condition was around 90-95% (**Fig. 11B**). Additional markers were also investigated on adherent iFB and myeloid cells. As expected, GFP<sup>+</sup> iFB were mainly GFP<sup>+</sup>CD45<sup>-</sup>CD31<sup>-</sup>PDPN<sup>+</sup> (**Fig. 11D**) and expressed ICAM-1 and VCAM-1 while being negative for MAdCAM-1 (**Fig. 11E**). Flow cytometrical characterization of adherent

## Results

---

myeloid cells revealed that they are not CD103<sup>+</sup> DC or Siglec-F<sup>+</sup> eosinophils but F4/80<sup>+</sup>CD11b<sup>+</sup>CD11c<sup>+</sup> M $\phi$  (**Fig. 11E**). Even though CD11b and CD11c could be expressed by DC, the F4/80<sup>+</sup>CD11b<sup>+</sup>CD11c<sup>+</sup> phenotype is restricted to M $\phi$  according to the literature (Cerovic et al., 2014; Gross et al., 2015; Bain and Mowat, 2014; Stagg, 2018). In this thesis, the adherent myeloid cells will be referred to as M $\phi$ . At d 5 of culture, iLPC were isolated from WT mice (**Fig 11A**, step 4) and depleted for plastic-adherent cells (AC), mainly iFB and M $\phi$ /DC, by letting them adhere to plastic dishes during 2 h of culture (**Fig 11A**, step 5). Non-AC, including IgA<sup>+</sup> PC that represent approximately 20% of this new cell suspension, were co-cultured alone or on top of iFB, M $\phi$ , or its mixture (**Fig 11A**, step 6). 24h later IgA<sup>+</sup> PC numbers were assessed by flow cytometry to monitor PC survival and IgA production to measure PC function. Initially, virtually all PC died in the assays, with little influence by iFB. To prolong PC survival, I used bcl-2 transgenic cells which allowed to reproducibly observe an improvement of IgA<sup>+</sup> PC survival when cocultured with iFB (data not shown). With increasing practice, faster and more gentle PC preparation, the level of PC survival mediated by iFB improved. Finally, I could switch back to non-transgenic PC and

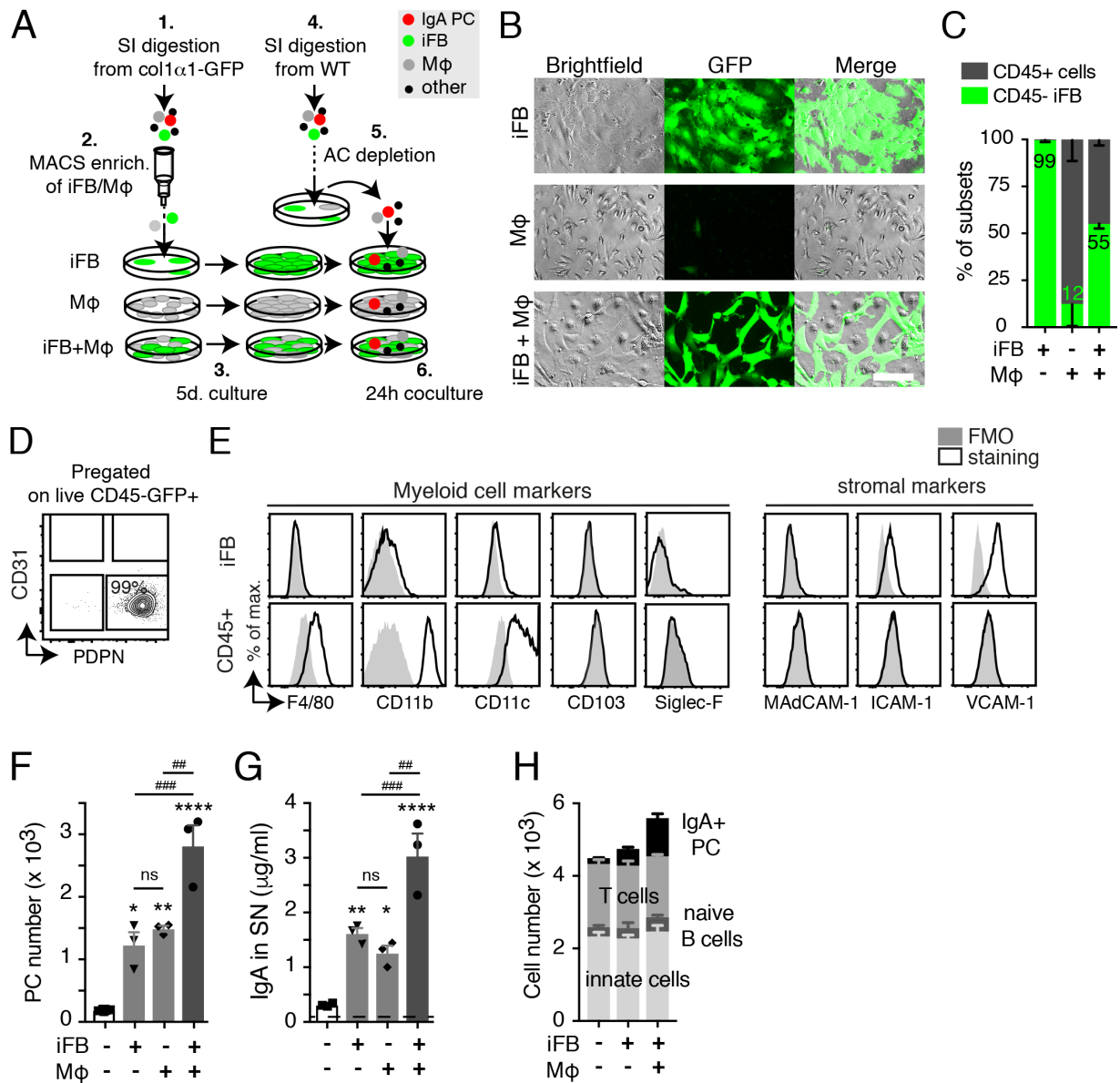
---

### Figure 11: In vitro screening for cells promoting PC survival and IgA secretion identifies iFB and macrophages as best support cells.

(A) Drawing showing the six-step procedure to screen cell types for their potential to support PC survival and/or IgA production. Steps 1-3: Cells were isolated from enzymatically digested distal SI of Col-GFP mice, then iFB and/or M $\phi$  from this cell suspension enriched by MACS and cultured for 5 days. Steps 4-6: LP cells (iLPC) isolated from the digested distal SI of wt mice were depleted of iFB and other adherent cells (AC) by culturing them for 2h on plastic surface, then the non-adherent cells containing IgA<sup>+</sup> PC were cultured on top of iFB and/or M $\phi$ , and after 24 hours IgA<sup>+</sup> PC survival assessed by flow cytometry and IgA secretion into the supernatant (SN) by ELISA. (B) After the first three steps explained in A (day 5 of culture), the iFB presence was assessed by microscopy using the GFP marker, with M $\phi$  being GFP<sup>-</sup> but visible in phase contrast mode. Shown are also controls where only iFB or M $\phi$  were enriched from the jejunum of Col-GFP mice. (C) After the first three steps explained in A, the frequencies of GFP<sup>+</sup> iFB versus CD45<sup>+</sup> hematopoietic cells (enriched in macrophages as depicted in E) were assessed by flow cytometry for the three indicated conditions. The numbers indicate the % of iFB in the culture. (D) Confirmation by flow cytometry of the PDPN<sup>+</sup> CD31<sup>-</sup> iFB identity among CD45<sup>-</sup> cells of adherent GFP<sup>+</sup> cells after 5 days of culture of previously MACS-enriched iFB cells. (E) Histograms showing the further flow cytometric characterization of 5 day cultured iFB and myeloid-enriched CD45<sup>+</sup> cells for myeloid versus stromal cell markers. (F-H) After the six steps indicated in A, including the coculture for 24h, the outcome was investigated in three different ways. Either no support cells were given to PC-containing iLPC, only iFB, only M $\phi$ , or both cell types, as indicated. (F) Numbers of surviving PC (CD45<sup>+</sup>CD3<sup>-</sup>CD11c<sup>-</sup>CD138<sup>+</sup>IgA<sup>+</sup>FSC<sup>hi</sup>) as assessed using flow cytometry. (G) IgA secretion in SN collected from samples like in F, as assessed by ELISA. (H) Number of indicated non-iLPC types that survived after 24 h of coculture as quantified by flow cytometry. It shows the presence of most LP cell types in cultures but with only iFB and myeloid cells promoting PC survival with no effects on the survival of the other cell types: PC, CD45<sup>+</sup>CD138<sup>+</sup>IgA<sup>+</sup>FSC<sup>hi</sup>; T cells, CD45<sup>+</sup>CD3e<sup>+</sup>FSC<sup>lo</sup>; naïve B cells, CD45<sup>+</sup>CD19<sup>+</sup>CD138<sup>-</sup>IgA<sup>-</sup>FSC<sup>lo</sup>; and DC/Eos/Mo pool: CD45<sup>+</sup>CD11b<sup>+</sup>CD11c<sup>+</sup>FSC<sup>hi</sup>SSC<sup>hi</sup>. All data are representative of at least three independent experiments. Error bars represent SD (n = 3–4); \*/#P < 0.05, \*\*/##P < 0.01, \*\*\*/###P < 0.001. \*, compared with surviving PC number cultured without AC (first column); #, compared with PC cultured in the indicated condition. 

observe PC survival in presence of iFB, although with an efficiency clearly below (2-3X) the one with bcl-2 tg IgA<sup>+</sup> PC. However, the fold increase in surviving PC between no support cells and iFB support was comparable in the two systems. Hence, in the following experiments presented the data were generated with WT IgA<sup>+</sup> PC.

Flow cytometrical analysis showed that almost all IgA<sup>+</sup> PC (FSC<sup>hi</sup>CD45<sup>+</sup>CD19<sup>-</sup>CD138<sup>+</sup>IgA<sup>+</sup>) died when cultured alone for 24h, but many IgA<sup>+</sup> PC were rescued when co-cultured with purified iFB (**Fig. 11F**), 4-5 fold more surviving IgA<sup>+</sup> PC as compared with IgA<sup>+</sup> PC cultured alone, corresponding to 6-8% of all IgA<sup>+</sup> PC plated. This increased PC survival was translated by a similar increase in IgA accumulation



in the supernatant (SN) (**Fig. 11G**). Surprisingly, a similar PC number survived when PC were cultured with M $\phi$  (6-8%). An even greater surprise was that a significantly greater PC number, approximately 12 - 15% of plated IgA<sup>+</sup> PC, survived when co-cultured with both iFB and M $\phi$  despite a similar density of support cells. This finding suggests that these two types of support cells can potentiate each other as niche cells to prevent PC death in this *in vitro* assay (**Fig. 11F**). This synergistic effect was confirmed also for the amount of IgA secreted (**Fig. 11G**). To investigate whether the improvement in cell survival was of general nature affecting all cell types, I measured also the number of other cell types that were plated along with PC as part of the non-adherent iLPC. Indeed, only IgA<sup>+</sup> PC numbers were markedly increased by the presence of iFB and/or M $\phi$ , while CD3 $\epsilon$ <sup>+</sup> T cells, CD19<sup>+</sup>B220<sup>+</sup> B cells (presumably naive B cells) or non-adherent CD11c<sup>+</sup> cells showed no or minor changes in cell number upon coculture (**Fig. 11H**). Importantly, the presence of these other iLPC types in the coculture assay cannot rescue PC survival on its own when no iFB or M $\phi$  were cultured alongside (**Fig. 11F** and **11H**). This observation indicates that CD3 $\epsilon$ <sup>+</sup> T cells, CD19<sup>+</sup>B220<sup>+</sup> naïve B cells and non-adherent innate immune cells, including CD11c<sup>+</sup> cells, are not sufficient to mediate PC survival and function *in vitro* suggesting that iFB and M $\phi$  have unique properties allowing this effect.

As mentioned above and depicted in the **Fig. 11H**, variable numbers of CD19<sup>+</sup>B220<sup>+</sup> B cells are present in the co-culture mix leaving open the possibility that these B cells can differentiate in a short time into IgA<sup>+</sup> PC and thereby contribute to the differences in PC numbers observed *in vitro*. To assess the role of this pathway in my *in vitro* culture assay, I depleted CD19<sup>+</sup> B cells by MACS right after the AC elimination (as part of step 5 in scheme shown in Fig. 11A) (**Fig. 12A**; left panel), in order to eliminate the potential source of *in vitro* generated IgA<sup>+</sup> PC. This new AC/B cell-depleted mix displayed the same IgA<sup>+</sup> PC survival pattern (**Fig. 12A**; right panel) that we observed in the previous setting (**Fig. 11F, G**), namely the iFB effect as well as the synergistic iFB - M $\phi$  effect which were both corroborated by the measurement of IgA production in the SN. Furthermore, CFSE labeling experiments confirmed that there is barely any proliferation observed among IgA<sup>+</sup> PC, in settings with or without B cell depletion (**Fig. 12B**). These results demonstrate that our co-cultures are a readout for PC survival and not PB proliferation or *in vitro* PC differentiation from CD19<sup>+</sup> B cell precursors.

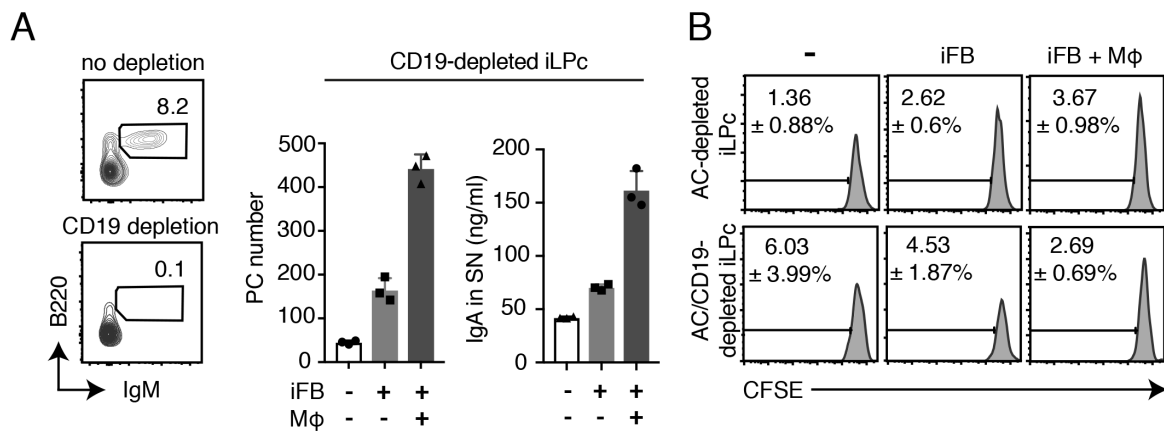


**Figure 12: Differentiation of mature B cells or plasma blast proliferation do not contribute to IgA<sup>+</sup> PC numbers measured in the PC co-culture assays in vitro.** (A) Flow cytometry analysis. Left panel: Density plots to control for the efficiency of the MACS-based depletion of CD19<sup>+</sup> B cells by labeling of two alternative mature B cell markers, namely B220 and IgM, before and after the depletion. Right panel: 24h of co-culture of CD19/AC-depleted intestinal LP cells (iLPC) with the indicated AC populations. Left histogram shows the numbers of surviving PC (CD45<sup>+</sup>CD3<sup>+</sup>CD11c<sup>-</sup>CD138<sup>+</sup>IgA<sup>+</sup>FSC<sup>hi</sup>) as assessed using flow cytometry; right histogram shows the IgA secretion in the culture SN as measured by ELISA. Representative of two independent experiments. (B) AC or CD19/AC-depleted iLPC were labeled with CFSE and then cultured in the indicated conditions for 24h. Histograms show CFSE signal intensity as assessed by flow cytometry in IgA<sup>+</sup> PC/PB. Representative of two independent experiments.

Because the IgA<sup>+</sup> PC survival data reported above were generated using a cell mixture containing 80% of cells other than PC, we also wondered whether iFB and Mφ promoted PC survival indirectly through other cell types present in the culture, such as T cells or innate cells, and that on their own are insufficient to promote PC survival but may improve PC homeostasis indirectly. To test this hypothesis, I performed a 24h co-culture of iFB and Mφ with flow cytometry sorted CD11b/c<sup>-low</sup> FSC-A<sup>hi</sup> IgA<sup>+</sup> PC (**Annex 3A and B**). Analysis of PC survival and IgA production clearly showed that iFB and Mφ can promote PC survival and function in an efficient manner (**Fig. 13A and B**) comparable to the assay that include the other immune cells (**Fig. 11F, G**), indicating iFB and Mφ directly mediate the prosurvival effects. Moreover DAPI/annexin-V co-staining showed that iFB rescued PC from apoptosis as they increased markedly the proportion of living (DAPI<sup>+</sup>) non-apoptotic (Annexin-V<sup>-</sup>) IgA<sup>+</sup> PC with the joint support by iFB and Mφ further improving the proportion of live PC (**Fig. 13C**). These annexin-V data together with the findings using CSFE further strengthen the notion that iFB and Mφ have an effect on PC survival rather than on their proliferation or on memory B cell differentiation. As Siglec-F<sup>+</sup> eosinophils have been previously suggested as niche cells (Chu et al., 2014), I performed a co-culture of iFB and Mφ with sorted IgA<sup>+</sup> PC in which sorted eosinophils were added or not

(Annex 3A and B). In this assay, addition of purified eosinophils with PC did not strengthen the prosurvival effect by iFB and M $\phi$  (Fig. 13D), while being still present after 24 h coculture (data not shown). Therefore, while eosinophils have been shown by others to be crucial for SI homeostasis and IgA<sup>+</sup> PC pool maintenance (Chu et al., 2014; Jung et al., 2015), they are dispensable for IgA<sup>+</sup> PC survival *in vitro* as already suggested by Jung and colleagues (Jung et al. 2015). Our finding goes well with the mRNA analysis for survival factors showing a very limited implication of the myeloid cell compartment in the production of the three PC survival factors investigated (Fig. 8H).

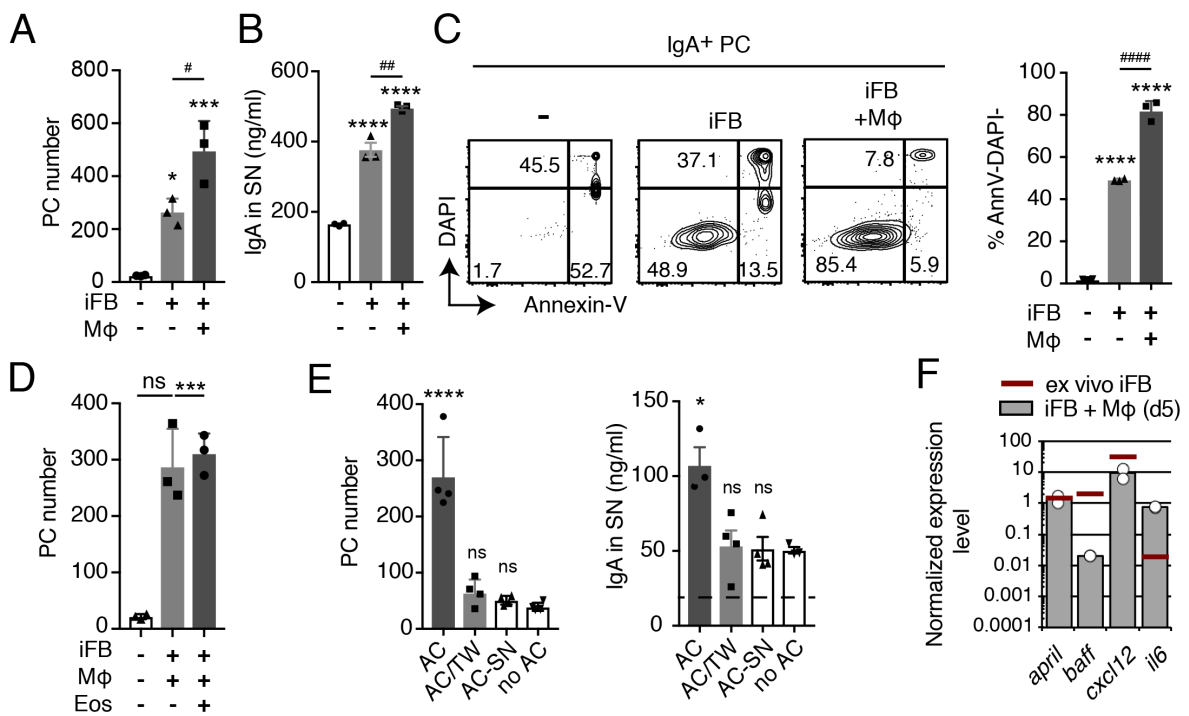


**Figure 13: iFB and adherent M $\phi$  keep PC alive via a contact dependent mechanism. (A-D)** Sorted CD3<sup>+</sup>CD11c<sup>+</sup>CD19<sup>+</sup>IgA<sup>+</sup>FSC<sup>hi</sup> PC were cultured for 24h under the indicated conditions. **(A)** Surviving IgA<sup>+</sup> PC were counted by flow cytometry. **(B)** Secreted IgA in SN of these cultures was quantified by ELISA. **(C)** IgA<sup>+</sup> PC were assessed as being live (DAPI<sup>-</sup>AnnexinV<sup>-</sup>), apoptotic (DAPI<sup>-</sup>AnnexinV<sup>+</sup>) or dead (DAPI<sup>+</sup>AnnexinV<sup>+</sup>) with proportions shown as % in the dot plot, and % live cells in bar graph on right side. **(D)** The contribution of sorted CD11c<sup>low</sup>CD11b<sup>+</sup>SSC-A<sup>hi</sup> Eos to PC survival mediated by iFB and M $\phi$  was assessed as in A. **(E)** AC-depleted iLPC were cultured in direct contact with iFB/myeloid cells (AC), separated by a permeable membrane called transwell (AC/TW), with AC-conditioned SN (AC-SN) or cultured alone (no AC). The number of surviving plasma cells is shown in the left graph and the IgA secreted into the SN in the right graph. **(F)** Transcript level of *april*, *baff*, *cxcl12*, and *il6* from sorted *ex vivo* iFB (red line level) and 5 days-cultured AC (grey bar). A, B, C and E are representative of at least three independent experiments. D and F are representative of two independent experiments. Error bars represent SD (n = 3–4); \*/#P < 0.05, \*\*/#P < 0.01, \*\*\*/###P < 0.001. \*, compared with surviving PC number cultured without AC; #, compared with PC cultured in the indicated condition. ns: not statistically significant.

As soluble factors, such as APRIL, BAFF, CXCL12 or IL6, are often considered as the main PC survival factors *in vitro* (Huard et al., 2008; Mesin et al., 2011; (Nguyen

et al., 2018) and *in vivo* (O'Connor et al., 2004; Peperzak et al., 2013; Belnoue et al., 2008), I performed a transwell (TW) experiment to see whether similar mechanisms are involved in our *in vitro* settings. Strikingly, the pro-survival effect of AC (iFB + M $\phi$ ) was completely abolished when PC were separated from them by a permeable membrane (**Fig. 13E, AC/TW**) demonstrating that the proximity with feeder cells is mandatory for IgA<sup>+</sup> PC survival and function. In line with this, PC survival was not rescued when PC were cultured with medium preconditioned by AC (**Fig. 13E, AC-SN**). Notably, *april*, *cxcl12* and *il-6* transcripts are expressed by 5 days-cultured AC at the same level than *ex vivo* sorted iFB (**Fig. 13F**), indicating that these factors are likely to be present in the SN. Because these factors have been extensively studied in the context of BM PC survival, I wanted to confirm the TW experiments using neutralizing molecules or specific KO AC. However, attempts to neutralize IL6 and APRIL/BAFF, using anti-IL6 and TACI-fc respectively, did not show any effect on IgA<sup>+</sup> PC survival and function (**Table 1**), confirming the TW experiments. Because the

**Table 1: soluble factor inhibitors and recombinant proteins**

| molecule tested | IgA+ PC # | IgA in SN   | other effect | exp. # |
|-----------------|-----------|-------------|--------------|--------|
| anti-IL-6       | →         | →           | N.O          | 4      |
| TACI-fc         | →         | →           | N.O          | 3      |
| anti-PGE2       | 25% ↘     | not checked | N.O          | 1      |
| rIL-6           | →         | →           | N.O          | 3      |
| rBAFF (60mer)*  | →         | →           | N.O          | 3      |
| rIL-17          | →         | →           | N.O          | 1      |
| rIL-22          | →         | →           | N.O          | 1      |
| rIL-33          | →         | →           | N.O          | 1      |

N.O.: nothing observed // → no effect // ↘ reduction // ↗ increase compared to ctrls

#: cell number

\*: when added on top of AC-depleted iLPC alone or on top of AC-AC-depleted iLPC cocultured

IgA<sup>+</sup> PC population has been shown to be strongly reduced in IL-6KO mice at steady state and upon infection (Ramsay et al., 1994), I wanted to investigate IL-6 function further *in vitro* and *in vivo*. WT and IL-6 KO AC were compared in their ability to support IgA<sup>+</sup> PC survival and function *in vitro*. No difference in IgA<sup>+</sup> PC numbers was

## Results

observed after 24h of coculture in the two settings (**Fig. 14A**). Interestingly, IgA secretion was higher when PC were in contact with WT AC compared to IL6KO AC suggesting a role for IL-6 in ab production or secretion instead of PC survival (**Fig. 14B**). This reduced IgA production was associated with a reduced surface IgA level (**Fig. 14C**). Of note, WT and IL-6KO AC display a similar proliferation and morphology in culture (data not shown and **Fig. 14D**). Finally, naive IL6KO mice harbored a similarly sized IgA<sup>+</sup> PC population in the distal SI compared to naive WT mice (**Fig. 14E**) suggesting that IL-6 does not play a limiting role for PC homeostasis *in vitro* or *in vivo* during steady state. Finally, attempts to boost PC survival with different cytokines, including IL-6, showed no impact on PC survival (**Table 1**).

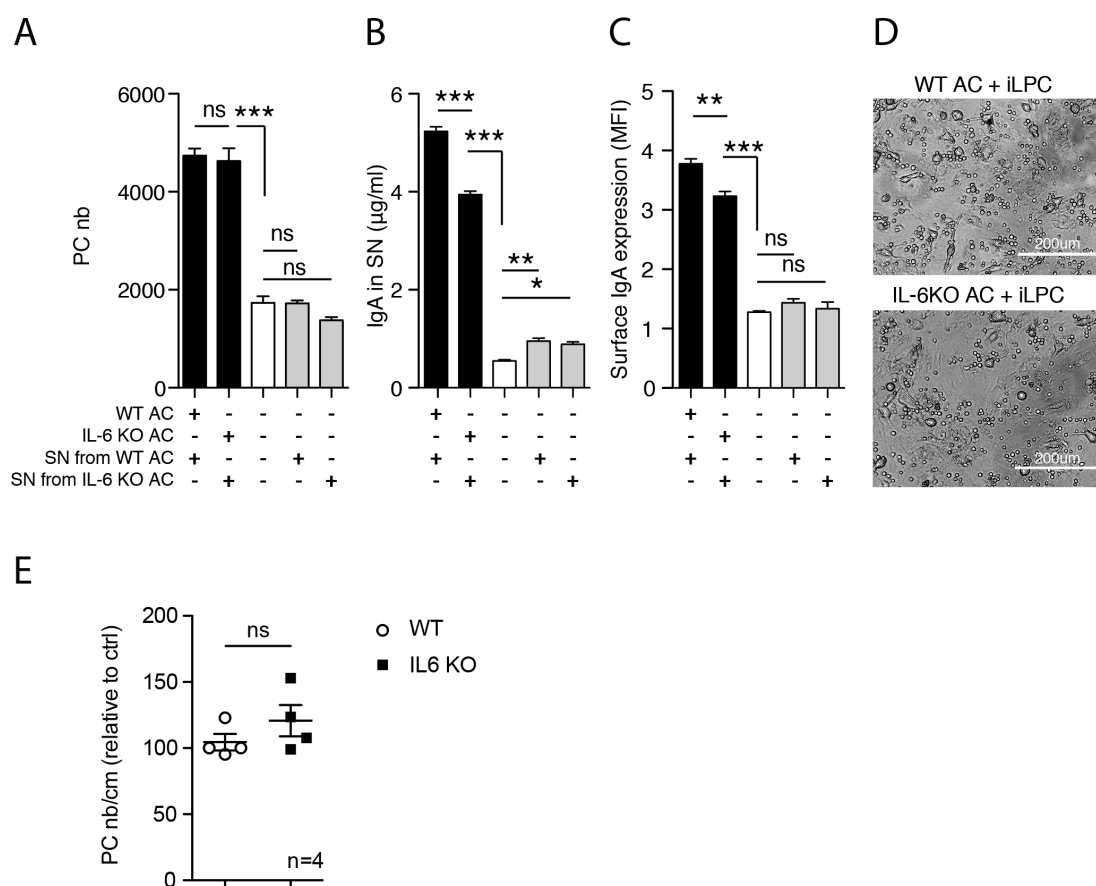


**Figure 14: IL6 is not essential for the survival of IgA<sup>+</sup> PC but boosts their IgA expression and secretion.** (A-D) Coculture experiment performed as described in Fig. 11A but AC from WT and IL-6KO mice were used instead of col-GFP mice. (A) Number of surviving IgA<sup>+</sup> PC as assessed by flow cytometry. Co-culture was performed once, n=4. (B) Levels of secreted IgA as measured by ELISA in the SN collected from A. (C) Surface IgA MFI on IgA<sup>+</sup> PC collected from A, as assessed by flow cytometry. (D) Microscopy images of WT AC and IL-6KO AC coculture with WT iLPC. Scale bars: 200µm. (E) IgA<sup>+</sup> PC number in the distal SI of sex- and age-matched adult WT and IL-6KO after three weeks of co-housing. IgA<sup>+</sup> PC were quantified by flow cytometry after intestinal LP digestion and normalized to the length of the organ isolated. Data shown represent the pool of two experiments with a total of 4 mice.

---

Another PC survival factor BAFF, was found to be strongly reduced in my cultured AC at the mRNA level compared to the *ex vivo* expression level measured in iFB (**Fig. 13F**) suggesting it may not play a role in the survival assay. Consistent with this notion, neutralization of BAFF and APRIL using TACI-Fc had no effect on iFB-mediated PC survival (data not shown). Similarly, recombinant BAFF 60mer did not improve the survival of PC in absence of support cells (**Table 1**). All these data negative data regarding the role of soluble factors are in line with the TW experiments showing that the proximity between AC and PC is essential.

All together these results demonstrated that iFB and M $\phi$  promote PC survival and IgA production directly through a mechanism requiring cell contact with IgA<sup>+</sup> PC or soluble factors requiring close proximity but not classical soluble factors. In addition, the synergy of iFB and M $\phi$  (AC) revealed an interesting functional interaction that strengthens their respective pro-survival effect on IgA PC that is not further improved by the presence of eosinophils.

## 5.5 The IgA PC niche is constituted of one or several PC that are showing cell-cell contacts with multiple iFB

As cell-cell interactions seem to be required for the prosurvival effect of iFB and M $\phi$  on IgA<sup>+</sup> PC *in vitro*, we sought to determine in the jejunum of Col-GFP mice with which cells IgA<sup>+</sup> PC had direct contacts. I showed previously in my thesis that IgA<sup>+</sup> PC selectively localize to villi in the SI while being mostly absent from the pericryptal area (**Fig. 8A**). By using the combination of IgA, DAPI and GFP labeling, we could show that every IgA<sup>+</sup> PC had six cells in its direct/physical neighborhood including GFP<sup>+</sup> iFB (**Fig. 15A** and **Fig 15B**). Next, I quantified the contribution of every cell types for the direct PC contact. iFB were found to represent the main cell type interacting physically with IgA<sup>+</sup> PC, with virtually every PC showing direct contacts with at least two iFB but 50% of PC were embedded by three or more iFB (**Fig. 15C**, first row, and **Fig. 15D**). Interestingly, 50% of IgA<sup>+</sup> PC interact with another IgA<sup>+</sup> PC, whereas 20% of them interact directly with two other PC (**Fig. 15C** and **15D**). In the majority of villi analyzed, clusters of 4-5 IgA<sup>+</sup> PC were found in which one given PC shows contacts with 3-4 other IgA<sup>+</sup> PC (**Fig. 15C**, second row), especially at the villus base (data not shown). In contrast, the frequency of PC contacting CD11b<sup>hi</sup> myeloid cells was only about 25% (**Fig. 15D**). Of note I also identified a CD11b<sup>low</sup> population that can interact with IgA<sup>+</sup> PC (data not shown). Unfortunately, the labeling of this CD11b<sup>o</sup> population was not stable enough through the different experiments to

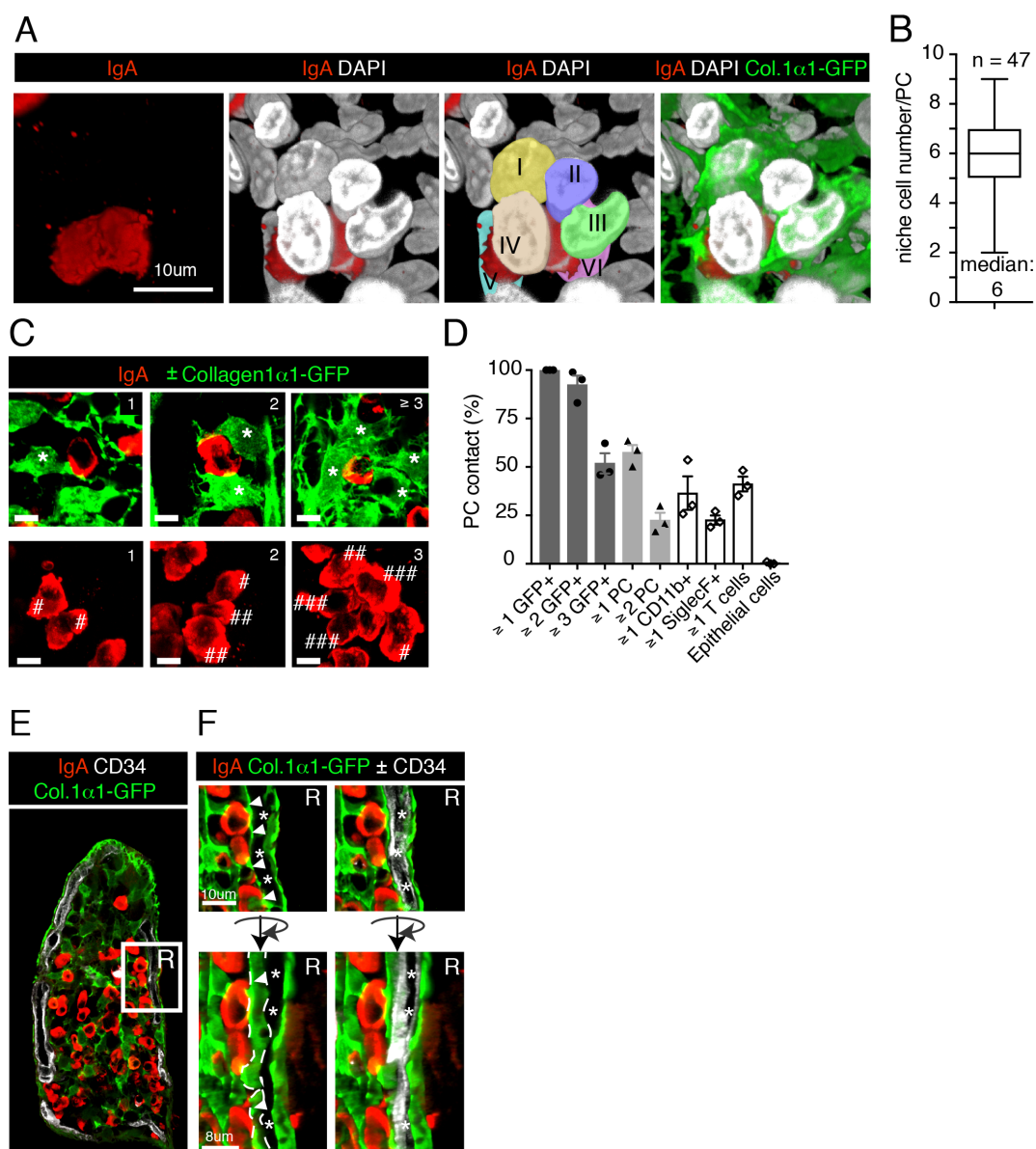


**Figure 15: iFB are the most prevalent cell type forming the anatomical niche for PC in the small intestine with an IgA<sup>+</sup> PC typically contacting two iFB directly.** Distal SI villi of col1 $\alpha$ 1-GFP mice were imaged by confocal microscopy after epithelial layer elimination and whole-mount immunostaining. **(A)** Representative 3D images showing one IgA<sup>+</sup> PC (red) surrounded by six cells (DAPI<sup>+</sup> nuclei in white), with several of them being GFP<sup>+</sup> iFB (green). **(B)** Total number of cells contacting one given PC, and called 'niche cells'. 47 independent PC were analyzed from three mice, 4 to 6 villi per mice. **(C)** Upper row: Representative images showing one IgA<sup>+</sup> PC (in red) contacting one, two or more than three GFP<sup>+</sup> iFB (in green; \* indicating an iFB) in left, middle or right image, respectively. Lower row: Representative images showing interaction of PC with other PC. The number of # corresponds to the number of PC that the labeled PC touches. Data are representative of three independent experiments, with one mouse per experiment and 4-6 villi per mouse. **(D)** Cumulative analysis of images as in A and C to measure the frequency of PC contacts with a particular cell type, with 5-8 villi per mouse analyzed from 3 mice. **(E)** Distribution in a villus of IgA<sup>+</sup> PC (red) relative to CD34<sup>+</sup> BEC (white) and GFP<sup>+</sup> iFB (green) in a 3D reconstruction (depth of 5-7 $\mu$ m). **(F)** Magnification of the region R selected in E +/- CD34 staining showing iFB forming a sheath (arrow heads and dashed line) around CD34<sup>+</sup> blood vessels (white, stars). The orientation of the lower images is turned on its axis by a few degrees (right images) to highlight the virtually complete separation of the CD34<sup>+</sup> BEC from IgA PC by iFB. Data are representative of at least three independent experiments. Scale bars: 10 $\mu$ m, A & F; 8 $\mu$ m, F; 5 $\mu$ m, C

perform a consistent contact analysis but it is obvious that these cells might increase the percentage of PC interacting with myeloid cells. Siglec-F<sup>+</sup> eosinophils and CD3 $\epsilon$ <sup>+</sup> T cells formed PC contacts with only 20% and 35-40% of PC, respectively, suggesting they do not form an important component of each PC niche (Fig. 15D). Epithelial cells are physically isolated from LP PC by the basement membrane (Fig. 9C), subepithelial iFB/telocytes and blood vessels (Fig 9A and B; Fig. 15E and F). As BEC and LEC were found to express transcripts of *cxcl12*, *april* and *baff*, I assessed whether PC were physically close to GFP<sup>-</sup> endothelial cells. I observed that most IgA<sup>+</sup> PC localized at a distance from the CD34 blood vessel cage structure (Fig. 15E), while some PC were in close proximity (Fig. 15E; R region). However, high magnification images revealed that iFB (Fig. 15F; arrows or dashed line) enwrap blood vessels (Fig. 15F; stars) thereby preventing direct PC contact with blood endothelial cells. Furthermore, I previously showed that BEC are surrounded by an ERTR7/Col-IV<sup>+</sup> basement membrane that forms a thin mesh contributing to the further isolation of BEC from PC (Fig 9C; empty arrows). For the LEC, many  $\alpha$ SMA<sup>+</sup> smooth muscle cell (SMC) fibers, which are embedded in ERTR7/Col-IV<sup>+</sup> basement membrane, isolate them from PC.

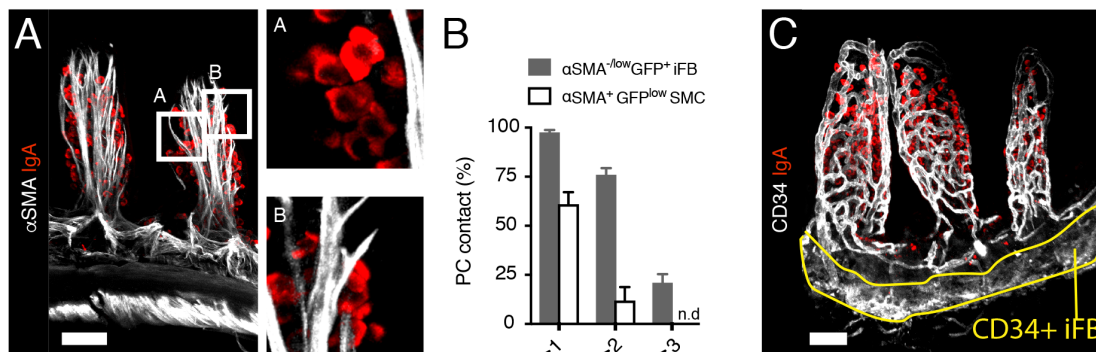


**Figure 16: IgA<sup>+</sup> PC contact iFB more frequently than  $\alpha$ SMA<sup>+</sup> smooth muscle cells; and IgA<sup>+</sup> PC do not localize adjacent to CD34<sup>+</sup> iFB that are found in the pericryptal area. (A-C)** Confocal microscope image analysis of distal SI villi of col-GFP mice after epithelial layer elimination and whole-mount immunostaining. **(A)** IgA and  $\alpha$ SMA costaining showing that some PC do not interact directly with  $\alpha$ SMA<sup>+</sup> cells (area A) while others do (area B). **(B)** Similar quantification as in fig. 15D counting the number of contacts between a PC and different  $\alpha$ SMA<sup>+</sup> iFB or  $\alpha$ SMA<sup>+</sup> smooth muscle cells (SMC). 4-5 villi per mouse were analyzed, n=3 mice. **(C)** IgA costaining with CD34 highlighting both iFB (yellow lined region around crypts) and blood vessels. Representative of at least four independent experiments. Scale bars: 50 $\mu$ m (A); 40 $\mu$ m (C). N.D.: not detectable.

Finally, we assessed cell contacts between IgA<sup>+</sup> PC and  $\alpha$ SMA<sup>+</sup>GFP<sup>low</sup>SMC. 40% of IgA<sup>+</sup> PC were not found in direct contact with SMC (Fi. 16A; A and 16B) while the remaining 60% of PC showed cell contact with one SMC and rarely with two SMC

(**Fig. 16A**; B and **16B**). In contrast, also in this tissue analysis all IgA<sup>+</sup> PC contacted at least one  $\alpha$ SMA<sup>+</sup>GFP<sup>+</sup> iFB with more than 70% and 20% contacting two and three of them, respectively (**Fig. 16B**). As anticipated knowing the different localization of IgA<sup>+</sup> PC (**Fig 8A**) and CD34<sup>+</sup> iFB (**Fig. 10E**), IgA<sup>+</sup> PC were not found in proximity of CD34<sup>+</sup> iFB (**Fig. 16C**). In conclusion, iFB represent the major component of the IgA<sup>+</sup> PC niche based on number, cell contacts and evidence for a PC promoting activity. Myeloid cells may complete this niche with little evidence for other cell types.

### 5.6 IgA PC survival is CD44 dependent *in vitro*.

Given the importance of cell-cell interactions or close proximity in IgA<sup>+</sup> PC survival *in vitro* and the large contact area observed between PC and iFB *in vivo*, we tested whether the neutralization of well-established adhesion molecules affected IgA<sup>+</sup> PC survival by AC (**Table 2**). I have previously described that ICAM-1 and VCAM-1 are expressed by iFB (**Fig. 10B**) with these molecules being ligands for LFA-1 ( $\alpha$ L $\beta$ 2) and VLA-4 ( $\alpha$ 4 $\beta$ 1) integrins that previously had been shown to regulate BM PC maintenance *in vitro* (Minges Wols et al., 2002) and *in vivo* (DiLillo et al., 2008). I saw no reduction in PC survival when these molecules were targeted with neutralizing antibodies to either ICAM-1, VCAM-1, or  $\alpha$ L (**Table 2**). However, blocking  $\alpha$ 4 slightly reduced PC survival (**Table 2**), as described later in more detail. However, targeting VCAM-1 induced a significant and reproducible reduction of CD45 mean fluorescence intensity (MFI) (**Table 2**). Blocking PDPN on iFB also failed to reveal any difference in AC-induced PC survival (**Table 2**).

**Table 2: interaction inhibitors**

| Ab tested         | IgA+ PC # | IgA in SN | other effect             | exp. # |
|-------------------|-----------|-----------|--------------------------|--------|
| anti-ICAM-1       | →         | →         | N.O                      | 2      |
| anti-VCAM-1       | →         | →         | CD45 MFI ↓               | 3      |
| anti- $\alpha$ L  | →         | →         | N.O                      | 2      |
| anti- $\alpha$ 4  | 10-30% ↓  | 5-10% ↓   | 10% ↓ T /CD11c+ cell #   | >5     |
| anti-PDPN         | →         | →         | N.O                      | 1      |
| anti-CD44 (IM7)   | 40-50% ↓  | 30-40% ↓  | 20-30% ↓ T/CD11c+ cell # | 4      |
| anti-CD44 (KM201) | 60-80% ↓  | 40-60% ↓  | 10-20% ↓ CD11c+ cell #   | >5     |

N.O.: nothing observed // → no effect // ↓ reduction // ↑ increase compared to ctrls

#: cell number

---

In reviews, CD44 is often associated with PC maintenance in the bone marrow (BM) niche whereas its neutralization *in vitro* showed contradictory effects. Indeed, CD44 targeting with  $\alpha$ CD44 IM7/IRAWB clones boosted BM PC survival (Cassese et al., 2003) while another Ab (clone KM81) had no effect on BM PC survival (Minges Wols et al., 2002). By using two different concentrations of the  $\alpha$ CD44 blocking antibody (Ab) - clone KM201 - known to interfere with the hyaluronic acid binding capacity of CD44 (Zheng et al., 1995; Ishiwatari-Hayasaka et al., 1999), I observed a striking decrease in IgA<sup>+</sup> PC numbers which was dose dependent: using 5 $\mu$ g/ml and 10 $\mu$ g/ml of KM201 antibody reduced the PC number by 40% and 75%, respectively (**Fig. 17A**, left histogram), with a corresponding decrease in IgA levels in the SN (**Fig. 17A**, right histogram). As I had used iFB and Mo (AC) as support cells in the experiments shown in Figure 17A, I reproduced these data with purified iFB cocultured with IgA<sup>+</sup> PC in presence or absence of KM201 antibody. The results revealed a similar reduction in PC numbers (**Fig. 17B**) as in settings with AC (**Fig. 17A**), demonstrating that iFB interact with IgA<sup>+</sup> PC in a CD44-dependent manner leading to improved PC survival. Because some  $\alpha$ CD44 antibodies have been shown to induce direct intracellular signaling within the target cells, I verified whether the KM201 antibody could induce PC death on its own. Thus, isolated AC-depleted iLPC were exposed to 10 $\mu$ g/ml KM201 or isotype control antibody for 4h or 24 h followed by the flow cytometric analysis of IgA<sup>+</sup> PC survival. This assay demonstrated that KM201 does not induce PC death by itself and that the observed effect is dependent on the presence of iFB and M $\phi$  (**Fig. 17C**). This result corroborated with the literature showing that KM201 binding to CD44 doesn't induce downstream intracellular signaling (Ishiwatari-Hayasaka et al., 1999). Notably, KM201 Ab induced also a low but reproducible reduction of T cells and CD11c<sup>+</sup> myeloid cells *in vitro* (**Table 2**).

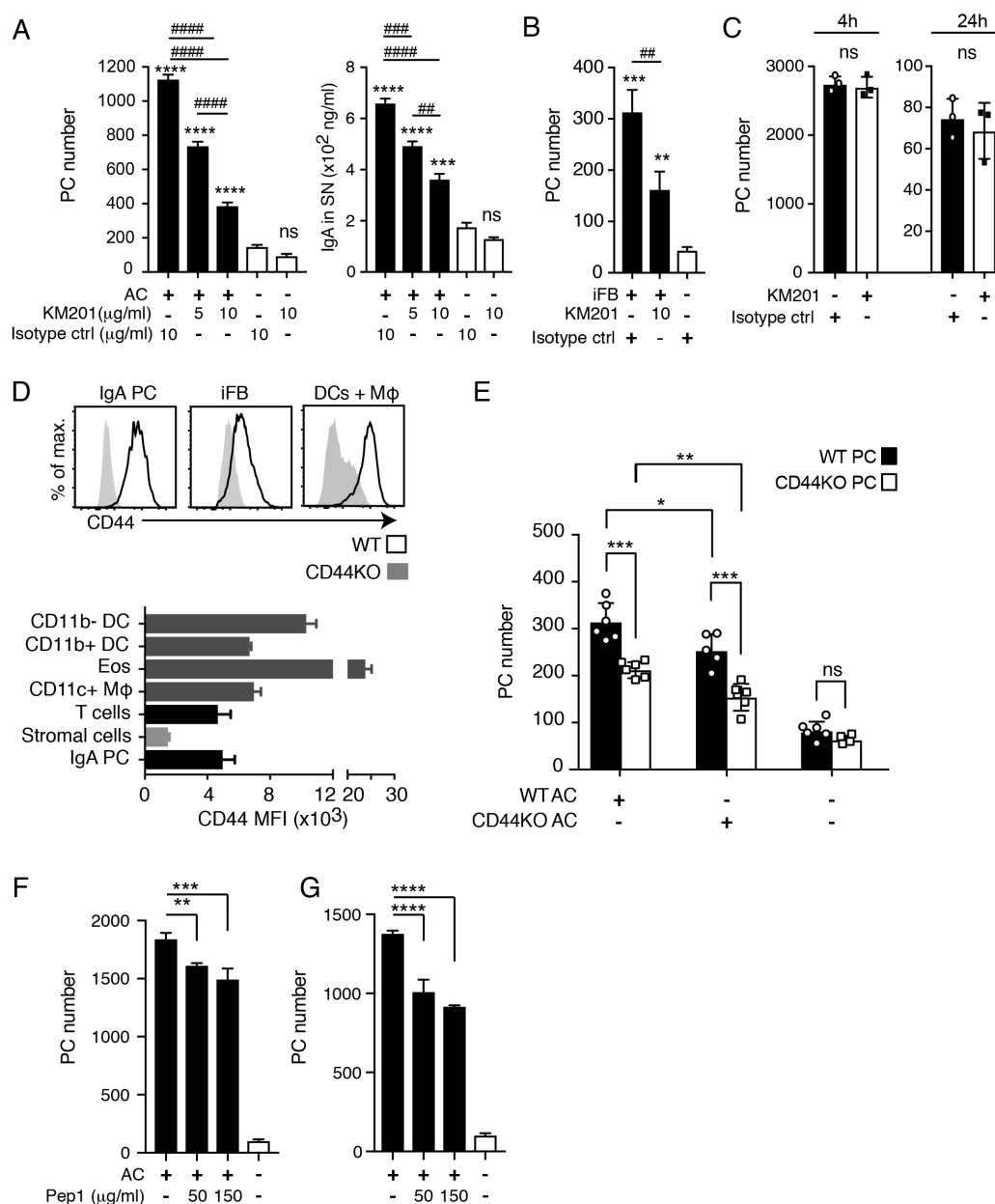


**Figure 17: CD44 on both IgA+ PC and support cells is critical for PC survival *in vitro*.** (A-B) *Ex vivo* WT iLPC cultured for 24h with or without 5 days-cultured AC (A) or MACS-enriched iFB (B) in the presence of the indicated concentration of CD44-neutralizing antibody (clone KM201) or isotype control antibody (ctrl). PC number in left graph and IgA titer in SN shown in right graph were determined by flow cytometry and ELISA, respectively. (C) AC-depleted iLPC were cultured in absence of support cells but with 10μg/ml of αCD44 (KM201) or isotype ctrl antibody for 4 or 24h followed by PC survival assessment by flow cytometry. (D) Flow cytometry histograms showing surface CD44 expression (black line) by *ex vivo* IgA<sup>+</sup>PC, iFB and myeloid cells (Mφ and DC). The corresponding CD44KO cells were used as a negative control (grey shading). Below: Bar graphs depicting the CD44 expression level by various intestinal cell types as assessed by flow cytometry. Signals from the CD44KO counterparts of every cell type were subtracted to calculate the mean fluorescence index (MFI). (E) *Ex vivo* WT and CD44KO AC were cultured for 5 days before adding AC-depleted iLPC from either WT or CD44KO mice. Surviving CD138<sup>+</sup>IgA<sup>+</sup>PC numbers were assessed by flow cytometry after 24h of co-culture. (F) The indicated concentration of Pep1 was incubated for 2 hours on 5 days-cultured AC before washing. AC-depleted iLPC were then added for a 24h coculture before IgA survival assessment. (G) As in F but the pep1 molecule was maintained throughout the coculture. Data are representative of four (A), two (B, C, F, & G) or three (D & E) independent experiments. Error bars present SD (n = 3-4); \*/# P < 0.05, \*\*/## P < 0.01, \*\*\*/### P < 0.001. \*, compared with PC cultured without AC (first column); #, compared with PC cultured in the indicated condition. In E: \*, compared with PC cultured in the indicated conditions.

---

Because we could not completely abrogate PC survival induced by AC using KM201 antibody, we looked for other survival factors that might play a role independently of CD44. When screening various neutralizing antibodies I had noticed that a high dose (30 $\mu$ g/ml) of neutralizing ab against  $\alpha_4$  integrin significantly reduced IgA<sup>+</sup> PC survival and IgA production (**Annex 4** and **table 2**). Co-neutralization of CD44 and  $\alpha_4$  showed a small additive effect in all experiment performed (data not shown) suggesting that the survival niche is a multifactorial microenvironment. However, the statistical significance of these results was only reached in one experiment out of three. As CD44 neutralization had given more striking effects than  $\alpha_4$  neutralization, I focused in the following on the role of CD44 in PC survival.

First, I wished to define by flow cytometry whether PC express CD44 or whether it is present on the support cells, or on both. All cell types were found to express CD44 at their cell surface although at different levels with IgA<sup>+</sup> PC and myeloid cells expressing high levels while iFB expressed lower levels (**Fig. 17D**). Among the immune and stromal cells investigated, only PDPN<sup>+</sup>CD31<sup>+</sup> LEC do not express CD44 (data not shown) demonstrating its ubiquitous distribution. As CD44 is expressed on both PC and AC in our *in vitro* settings as well as *in vivo*, we thought to assess whether IgA<sup>+</sup> PC survival and function are more dependent on CD44 expressed by PC, AC or a combination of both. Thus, I used iLPC isolated from the distal SI of CD44KO versus WT mice to generate the 5 d-cultured AC monolayers. Next a second isolation was carried out to add IgA<sup>+</sup> PC, either isolated from WT or CD44KO mice, on top of the AC layer, or without feeder cells. This *in vitro* experiment revealed that CD44KO PC are more prone to death than their WT counterpart, independently of the CD44 presence on feeder cells (**Fig. 17E**, black versus white bar comparison). Furthermore, WT PC were slightly reduced when co-cultured with CD44KO AC instead of WT AC, showing that CD44 expression by AC plays also a role in IgA<sup>+</sup> PC maintenance *in vitro* (**Fig. 17E**, white bar comparison). This result was confirmed by CD44KO PC co-cultured with normal or CD44KO AC, as WT AC rescuing slightly more PC than CD44KO AC (**Fig. 17E**, white bar comparison), demonstrating that CD44 on AC contributes also to PC survival. In summary, CD44 on both AC and IgA<sup>+</sup> PC is important for PC survival but with CD44 expression on PC playing a bigger role.

CD44 is involved in numerous cell-cell and cell-matrix interactions mediated by various different ligands of CD44, most notably ECM components such as collagen,

fibronectin, laminin, chondroitin sulfate, and hyaluronic acid (HA) as the most studied ligand (Goodison et al., 1999; Ponta et al., 2003; Misra et al., 2015). As the KM201 Ab clone is known to efficiently neutralize CD44 binding to HA binding (Lesley et al., 1990), I wanted to assess whether blocking of HA can reproduce the KM201 effects observed in PC survival. Therefore, I inhibited potential CD44 binding to HA using pep-1 which is a 12-mer peptide inhibitor of HA that was previously shown to specifically bind to soluble, immobilized and cell-associated forms of HA (Mummert et al., 2000). 1h neutralization of HA in AC cultures with 50 and 150 $\mu$ g/ml Pep-1 - followed by a washing step to remove the unbound inhibitor peptide - shows a small but significant reduction of PC survival after 24 h coculture (**Fig. 17F**). Longer neutralization of HA with the same concentrations of pep-1 but without removal of pep-1 from the medium results in a more important reduction in IgA<sup>+</sup> PC of approximately 40% (**Fig. 17G**). Nevertheless, neutralization of the CD44-HA axis cannot fully reproduce the effects observed with KM201 antibody (**Fig. 17A**) suggesting the involvement of additional CD44 ligands. Of note, the use of higher concentrations of Pep-1 disrupted the monolayer integrity indicating that the CD44-HA axis plays also a role in iFB-iFB or iFB-M $\phi$  interactions (data not shown). As an alternative approach to test the role of AC-derived HA in IgA<sup>+</sup> PC survival and function, I used hyaluronidase to digest HA in 5 day-cultures of AC. We hypothesized that degradation of HA into shorter fragments should impair IgA<sup>+</sup> PC survival. Interestingly, when the culture medium was not changed after a 2h hyaluronidase digestion, IgA<sup>+</sup> PC survival after 24h was improved compared to control treated samples (**Fig. 18A** and **Table 3**), with the AC monolayer supporting well the HA digestion (**Fig. 18B**). These results suggest that HA fragments have a prosurvival effect on IgA<sup>+</sup> PC and could be a mechanism of PC niche adaptation to its environment. Unfortunately, attempts to downregulate HA production by blocking hyaluronic acid synthases with 4-methylumbelliferone (4-MU) failed as the integrity of the AC monolayer was strongly disturbed upon this treatment not allowing healthy PC-AC coculture conditions (**Table 3**). Finally, experiments using plastic dishes coated with commercial ECM components (collagen and fibronectin) or AC-derived matrix did not rescue PC survival *in vitro* (**Table 3**). Notably, culture of AC on fibronectin-coated plastic dishes reduced PDPN expression by iFB which correlated with a significant reduction in IgA<sup>+</sup> PC survival and function (**Table 3**). Together, the results suggest that part of the CD44-mediated prosurvival effects are mediated by

HA which is likely to be produced by the support cells and can stimulate the survival and function of CD44<sup>+</sup> PC, and possibly also of CD44<sup>+</sup> AC.

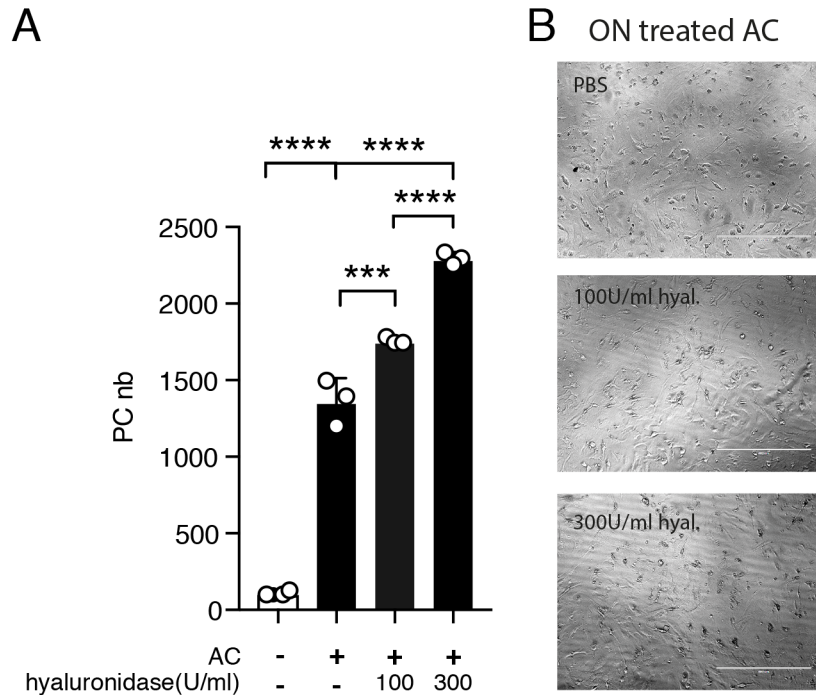


**Figure 18: HA fragments generated upon hyaluronidase treatment increase rather than decrease IgA<sup>+</sup> PC survival and IgA secretion.** (A) Adherent cells (AC) were treated with the indicated concentration of hyaluronidase (hyal) for two hours to digest HA before adding AC-depleted iLPC. After 24h the numbers of IgA<sup>+</sup> PC were quantified by flow cytometry. Data shown are representative of two independent experiments, n=3. \*\*\*P < 0.001, \*\*\*\*P<0.0001 indicate the significance between the conditions indicated. (B) Microscopy images of AC treated 24h with PBS or the indicated concentration of hyaluronidase. Images are representative for three independent experiments. Scale bars: 400µm.

**Table 3: soluble factor inhibitors and recombinant proteins**

| molecule tested       | IgA+ PC # | IgA in SN | other effect           | exp. # |
|-----------------------|-----------|-----------|------------------------|--------|
| Fibronectin collagenI | →         | →         | N.O                    | 3      |
| Fibronectin + AC      | 25% ↓     | 10% ↓     | PDPN MFI on iFB ↓      | 2      |
| Pep-1                 | 30%* ↓    | 25%* ↓    | N.O                    | 2      |
| Hyaluronidase         | 30%* ↗    | 20%* ↗    | N.O                    | 3      |
| 4-MU**                | —         | —         | AC monolayer destroyed | 2      |
| AC-derived ECM***     | →         | →         | N.O                    | 3      |

N.O.: nothing observed // → no effect // ↓ reduction // ↗ increase compared to ctrls

\*: When culture medium was not changed  
 \*\*: 4-methylumbelliferone, HA synthase inhibitor  
 \*\*\*: When 5 day cultured AC were removed either by EDTA or triton

## 5.7 IgA PC homeostasis is impaired in CD44KO mice.

Having identified CD44 as important PC survival molecule in our *in vitro* screen, we wished to investigate whether this pathway is also playing a limiting role for IgA PC *in vivo*. Despite the almost ubiquitous CD44 expression, mice deficient in all CD44 isoforms show only very few immune defects, such as a reduced Th1 memory response (Protin et al., 1999). I first checked CD44-deficient mice macroscopically but did not observe any obvious differences in the length and appearance of the SI, colon and cecum relative to WT mice cohoused for 3-4 weeks to reduce potential differences in the intestinal microbiome (data not shown). Then I assessed by whole-mount staining of the jejunum and ileum whether IgA<sup>+</sup> PC numbers were altered. CD44KO mice displayed a 40% reduction in IgA-expressing cells per villus (**Fig 19A**) with a clear trend to a localization only in the lower half of the villus. The isolation and quantification of IgA<sup>+</sup> PC by flow cytometry confirmed a 40-50% reduction in IgA<sup>+</sup> PC numbers within the distal SI (**Fig 19B**). Strikingly, this IgA<sup>+</sup> PC loss in CD44KO mice was observed to be associated with an even stronger reduction in IgA secreted into the intestinal lumen, as assessed by fecal IgA analysis (**Fig. 19C**), while IgA titers in the serum were not different relative to control mice (**Fig. 19D**). As the LP contains also IgG-switched and to a greater extent unswitched IgM<sup>+</sup> PC/B cells, I quantified these two populations using whole-mount staining and imaging. Surprisingly, IgG<sup>+</sup> and IgM<sup>+</sup> PC numbers were not significantly changed in CD44KO relative to WT mice (**Fig. 19E and F**) indicating that their homeostasis is not or less impaired by the lack of CD44 as compared to IgA<sup>+</sup> PC. IgG titers in the serum were also not impaired suggesting that at steady-state other PC niches such as the one in the BM are not sensitive to the lack of CD44 and continue to produce normal amounts of IgG which then distribute systemically via the blood circulation (data not shown).

As virtually all cell types express CD44, we wondered whether other cell types were affected in numbers or organization in tissues of CD44KO mice. In contrast to IgA<sup>+</sup> PC, CD3 $\epsilon$ <sup>+</sup> T cells were present in normal numbers in iLPC isolates analyzed by flow cytometry (**Fig. 19G**), consistent with their normal frequency and localization in the LP in whole-mount images (data not shown). Moreover, no differences in numbers were observed in iLPC isolates for eosinophils or for total CD11b<sup>+</sup>CD11c<sup>+</sup> myeloid cells (**Fig. 19G**). As non-hematopoietic cells can express CD44 as well (**Fig. 17D**), we assessed whether the iFB architecture was altered in the absence of CD44. Thus, I performed immunostaining on thin sections of the SI and colon of WT versus

CD44KO mice and observed a normal distribution and density of PDPN<sup>+</sup>CD34<sup>-</sup> and pericyptal PDPN<sup>+</sup>CD34<sup>+</sup> iFB in the distal SI and throughout the colon (**Fig. 19H**). Similarly,  $\alpha$ SMA<sup>+</sup> SMC and CD34<sup>+</sup> blood vessels and CD34<sup>+</sup> iFB appeared to be normal in density and localization in CD44ko intestines (**Fig. 19H**, and data not

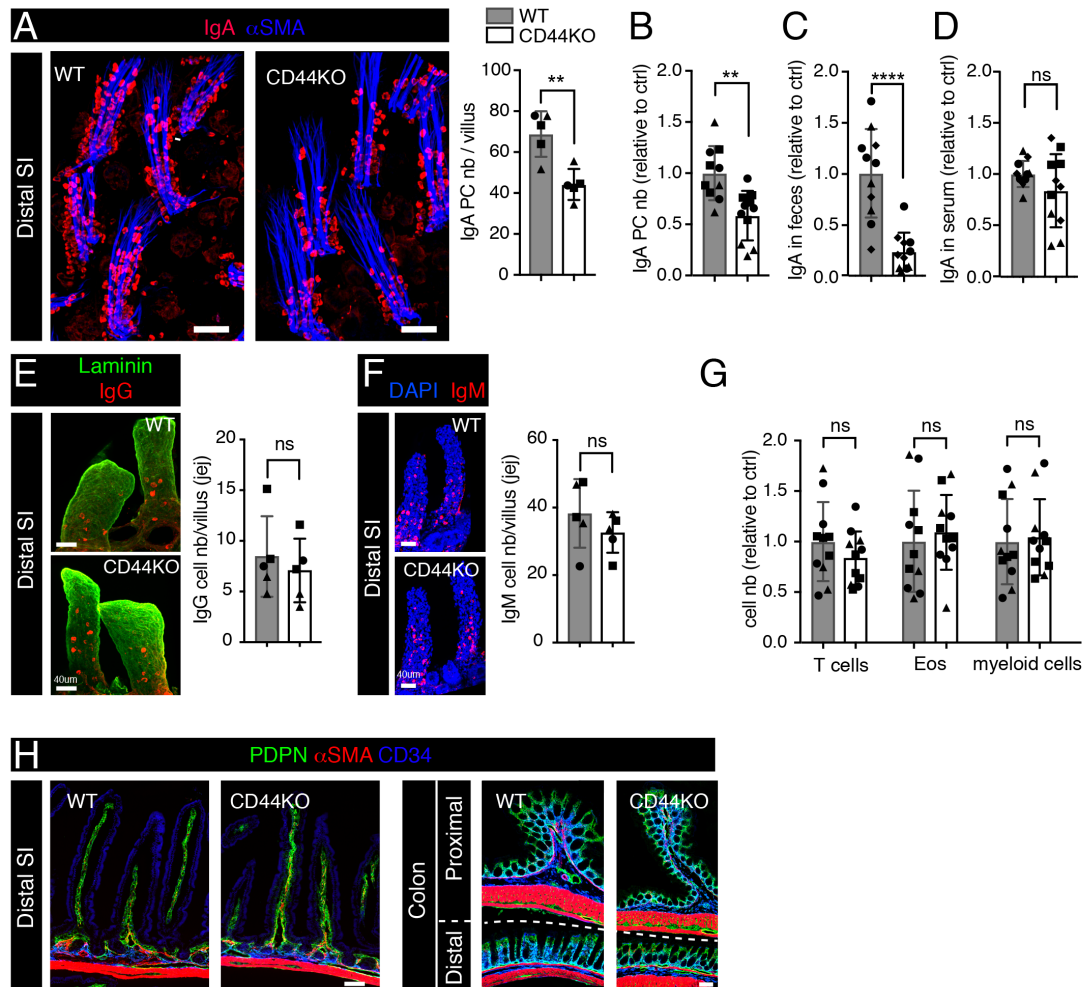


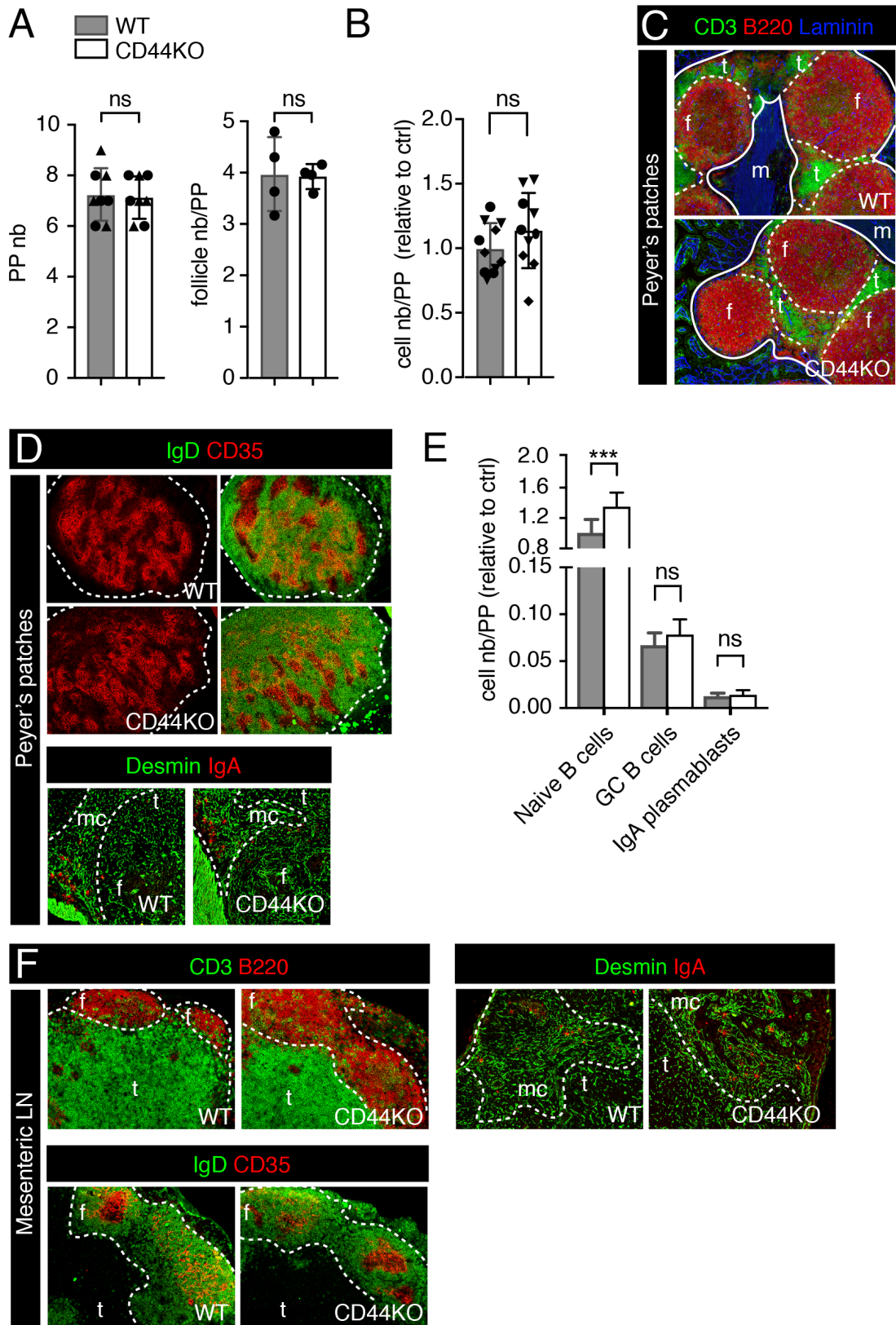
**Figure 19: The small intestine of CD44KO mice displays a reduction selectively in IgA<sup>+</sup> PC, and a marked decrease in secreted luminal IgA.** (A) Representative confocal microscope images of villi in jejunum of 4 weeks-cohoused WT versus CD44KO mice for IgA<sup>+</sup> PC (red) and  $\alpha$ SMA<sup>+</sup> smooth muscle cells (blue). The histogram on right side depicts the histological quantification of IgA PC numbers per villus. 5 mice with 4-6 villi per mouse were analyzed in three independent experiments (indicated by different symbols). (B) IgA<sup>+</sup> PC number per centimeter (cm) of jejunum was quantified by flow cytometry for WT versus CD44KO mice. n= 10-11 mice, pool of three independent experiments (indicated by different symbols). (C-D) IgA titers in feces (C) and serum (D) of WT versus CD44KO mice. (E-F) Left side: representative confocal microscopy images of PC subsets in villi of jejunum in WT versus CD44KO mice. Right side: histological quantification of the number of the indicated PC type per villus. (E) IgG<sup>+</sup> PC (in red) with laminin (in green). (F) As in E, but for IgM PC. 5 mice and 4-6 villi per mouse were analyzed in three independent experiments (shown with different symbols). (G) Relative cell number per cm of jejunum as analyzed by flow cytometry for: T cells (FSC<sup>lo</sup>CD3<sup>+</sup>), eosinophils (CD11b<sup>+</sup>CD11c<sup>lo</sup>SSC<sup>hi</sup>) and myeloid cells (F4/80<sup>+</sup>CD11b<sup>+</sup> CD11c<sup>+</sup>FSC<sup>hi</sup>). n= 10-11 mice, pool of three independent experiments (indicated by different symbols). (H) Histological staining for PDPN, CD34, and  $\alpha$ SMA of thin sections from the distal WT and CD44KO SI and colon (Proximal colon in upper row; distal colon in lower row). Scale bar: 50 $\mu$ m, A; 40 $\mu$ m, E & F; 80 $\mu$ m, H.

shown). These data demonstrate that CD44 has a selective role in regulating the homeostasis of IgA<sup>+</sup> PC within the SI, while being dispensable for many other LP cell types which typically express CD44 in WT mice.

The markedly reduced IgA<sup>+</sup> PC numbers in the SI of CD44KO mice could arise from defects in lymphocyte development within the bone marrow, defective homing to Peyer's patches (PP) or mLN, or alterations in their activation and/or differentiation within these organs. Therefore, I first evaluated the structure and composition of PP. The number of PP along the SI and their macroscopic follicular structures were identical in KO and WT mice (**Fig 20A**). Moreover, the number of cells isolated from digested PP was comparable in these two strains (**Fig. 20B**). Histological stainings of PP sections showed that B220<sup>+</sup> follicles and CD3 $\epsilon$ <sup>+</sup> T cells localize normally within PP with normal B220<sup>+</sup> follicle size and shape (**Fig. 20C**) indicating that there is no obvious deficiency in lymphocyte development and homing to the corresponding compartments within PP. Moreover, the PP follicles of CD44KO mice when compared to cohoused WT mice contained similar B220<sup>low</sup> germinal center (GC) areas with follicular T cells (**Fig. 20C**), along with a normal density and distribution of CD35<sup>+</sup> FDC and naïve IgD<sup>+</sup> B cells forming the follicular mantle. A comparable number of IgA<sup>+</sup> PB was observed (**Fig. 20D**). Flow cytometrical analysis of the B cell compartment revealed only a slight but significant increase in naïve B cells (B220<sup>+</sup>IgD<sup>+</sup>IgM<sup>low</sup>/GL7<sup>-</sup>) in PP of CD44KO relative to WT mice instead of the potential reduction expected (**Fig. 20E**, first column). However, neither GC B cells (IgD<sup>-</sup>GL7<sup>+</sup>) nor IgA<sup>+</sup> PB (IgD<sup>-</sup>IgM<sup>-</sup>CD19<sup>+</sup>IgA<sup>+</sup>FSC<sup>hi</sup>) numbers were altered in PP of CD44KO relative to WT mice indicating that the continuous B cell response to food and microbial antigens in SPF - like mice proceeds normally, at least regarding cell

---

**Figure 20: Peyer's patches and mesenteric lymph nodes of CD44KO mice do not show any obvious defect in composition or organization.** (A) Peyer's patch (PP) number along the SI (left graph; n=8) and number of follicles per PP (right graph; n=4) for 4 weeks-cohoused WT mice versus CD44KO mice as assessed by eye. (B) Total number of cells isolated from digested WT and CD44KO PP. n= 10-11 mice, 3 PP were pooled per mice, pool of three independent experiments (indicated by different symbols). (C) Histological analysis of PP structure (delimited by normal line) for the CD3<sup>+</sup> T cell zone (green, t) and B220<sup>+</sup> B cell follicles (red, f, surrounded by dashed line) in the two mouse strains. Laminin (blue) helps to distinguish between LP/or external muscle layers (m) and PP. Representative of three independent experiments and 5 mice in total. (D) Histological analysis of germinal centers (GC), as identified via CD35<sup>+</sup> follicular dendritic cells or FDC, IgD<sup>+</sup> naïve B cells, desmin+ iFB and IgA<sup>+</sup> plasmablasts in PP of WT versus CD44KO mice. B cell follicles are surrounded by a dashed line. Representative of three independent experiments and 5 mice per group. (E) Relative cell numbers of the three main B cell types present in PP as assessed by flow cytometry. n= 5-6 mice per group. (F) Similar analysis as in C & D but for mesenteric lymph nodes (mLN). mc: medullary cords. Representative of three independent experiments and three mice per group. 



numbers (**Fig. 20E**, second and third column). Histological stainings on mLN demonstrated that B and T zones appeared to be organized normally in CD44KO mice, with evidence for normal B cell responses as indicated by the similar presence of T cell containing germinal centers and IgA<sup>+</sup> PB/PC as in cohoused WT mice (**Fig. 20F**).

Altogether, our data from CD44KO mice revealed that these mice show a marked decrease in fecal IgA that correlates with a selective reduction of IgA<sup>+</sup> PC among immune cells of the SI LP. As secondary lymphoid organs draining the intestine, namely PP and mLN, appear to be normal in their composition, organization and ongoing T cell dependent B cell responses, these findings suggest that CD44 plays an important role either in PB homing from PP or mLN into the LP, or rather as our various lines of evidence indicate a critical role in the homeostasis of the IgA<sup>+</sup> PC pool within the LP.

## 6 Discussion

### 6.1 Intestinal fibroblasts

Beside immune hematopoietic populations, a complex network of mesenchymal stromal cells underlying the epithelium layer is attracting more attention since various studies highlighted their possible roles as regulators of the immune response, angiogenesis, and epithelial stem cell niche maintenance (Owens, 2015; Stzpourginski et al., 2017; Shoshkes-Carmel et al., 2018; Aoki et al., 2016; Thomson et al., 2018). In this study, we used a combination of PDPN and collagen1 $\alpha$ 1 promoter activity to identify and characterize the non-epithelial and non-endothelial stromal cell compartment.

#### 6.1.1 Intestinal fibroblast heterogeneity

High-magnification microscopic 3D analysis of col-GFP reporter mice revealed a unique and dense col-1 $\alpha$ 1<sup>+</sup> structural network throughout the LP of the SI and colon, from the epithelium monolayer to the bottom of the crypt and the submucosa, and describes with a new level of detail the intricate architecture of the fibroblastic network. Indeed, different iFB subsets were clearly observed based on their location and morphology but also on their marker profile (**Fig. 21**).

#### 6.1.2 Subepithelial iFB – telocytes

The morphologically most striking subset of iFB observed is the subepithelial iFB localizing, as its name indicates, just underneath the epithelium and its basement membrane. We showed that these cells display a flattened cell body and nucleus with a star-like shape due to their multiple pseudopodia contacting the adjacent subepithelial iFB. This highly interconnected layer seems to be the major cell type responsible for the maintenance of the basement membrane for epithelial cells as these iFB are embedded within this ERTR7<sup>+</sup> and Collagen IV<sup>+</sup> membrane. We also observed the subepithelial iFB in close contact with blood vessels and therefore they could play a role in BEC biology. The localization, the shape, and the cell-cell interconnection of the subepithelial cells observed in this study clearly indicate that they belong to the Foxl1<sup>+</sup> telocyte population observed in the Foxl1-Cre x Rosa26-

mTmG reporter mouse model (Aoki et al., 2016; Shoshkes-Carmel et al., 2018). Described for the first time in 2010, telocytes were defined by electron microscopy as cells displaying extremely long (ten to hundred micrometers) and thin (between 0.05 and 0.2 micrometers) cytoplasmic extensions called telopodes allowing various cell interactions and even cytoplasmic interconnections (Popescu and Faussone-Pellegrini, 2010; Radu et al., 2017; Cretoiu et al., 2012). Telocytes have been observed in close proximity to epithelial, endothelial, and neural cells in various organs such as the lung, heart and intestinal LP (Radu et al., 2017). Despite the ultrastructural description of the telocytes, specific markers have been missing in the telocyte field making the study of these cells challenging. PDGFR $\alpha$  and CD34 have been proposed early on for intestinal telocytes localizing to the pericryptal area (Vannucchi et al., 2013). It is only recently that Foxl1 promoter activity was used to identify subepithelial telocytes (Aoki et al., 2016; Shoshkes-Carmel et al., 2018), while CD34 expression was shown to subdivide telocytes into two spatially distinct subsets (Stzpeourginski et al., 2017; Shoshkes-Carmel et al., 2018). CD34 identifies only pericryptal telocytes in the vicinity of the Lgr5-expressing epithelial stem cells whereas subepithelial telocytes in the villi don't express CD34. Using 3D high-resolution imaging, I confirmed this CD34 distribution within the submucosa, with all col1 $\alpha$ 1-GFP<sup>+</sup> subepithelial mucosa iFB being CD34 positive localizing around the crypts. However, it is important to note that CD34 expression is not restricted to crypt-contacting subepithelial telocytes but, instead, stains the whole iFB compartment of the deep pericryptal mucosa and submucosa from the bottom of the crypts to the underlying muscle layers.

Surprisingly, different studies in the telocyte field aimed to separate fibroblasts and telocytes into two functionally and phenotypically distinct cell types using large spectrum gene expression comparisons of cultured fibroblasts versus telocytes from mouse lung highlighting more than one thousand genes being differently expressed between these two cell types, including differentially expressed microRNA (Zheng et al., 2013; Cismasiu et al., 2011). Interestingly, collagen IV expression was higher in telocytes compared to fibroblasts, which fits perfectly with our histological observations depicting a strong collagen IV accumulation around subepithelial iFB - telocytes and a weaker collagen IV labeling in the villus-internal area (Zheng et al., 2013). Furthermore, detailed analysis of the PDPN staining on our whole mount preparations suggested that subepithelial telocytes are PDPN<sup>lo</sup>, while internal iFB are clearly PDPN<sup>hi</sup> (data not shown, observation made by Jeremiah Latmani-Bernier and

myself). Based on the differences in their spatial distribution and microenvironment, it is not surprising that iFB and telocytes represent two functionally optimized cell

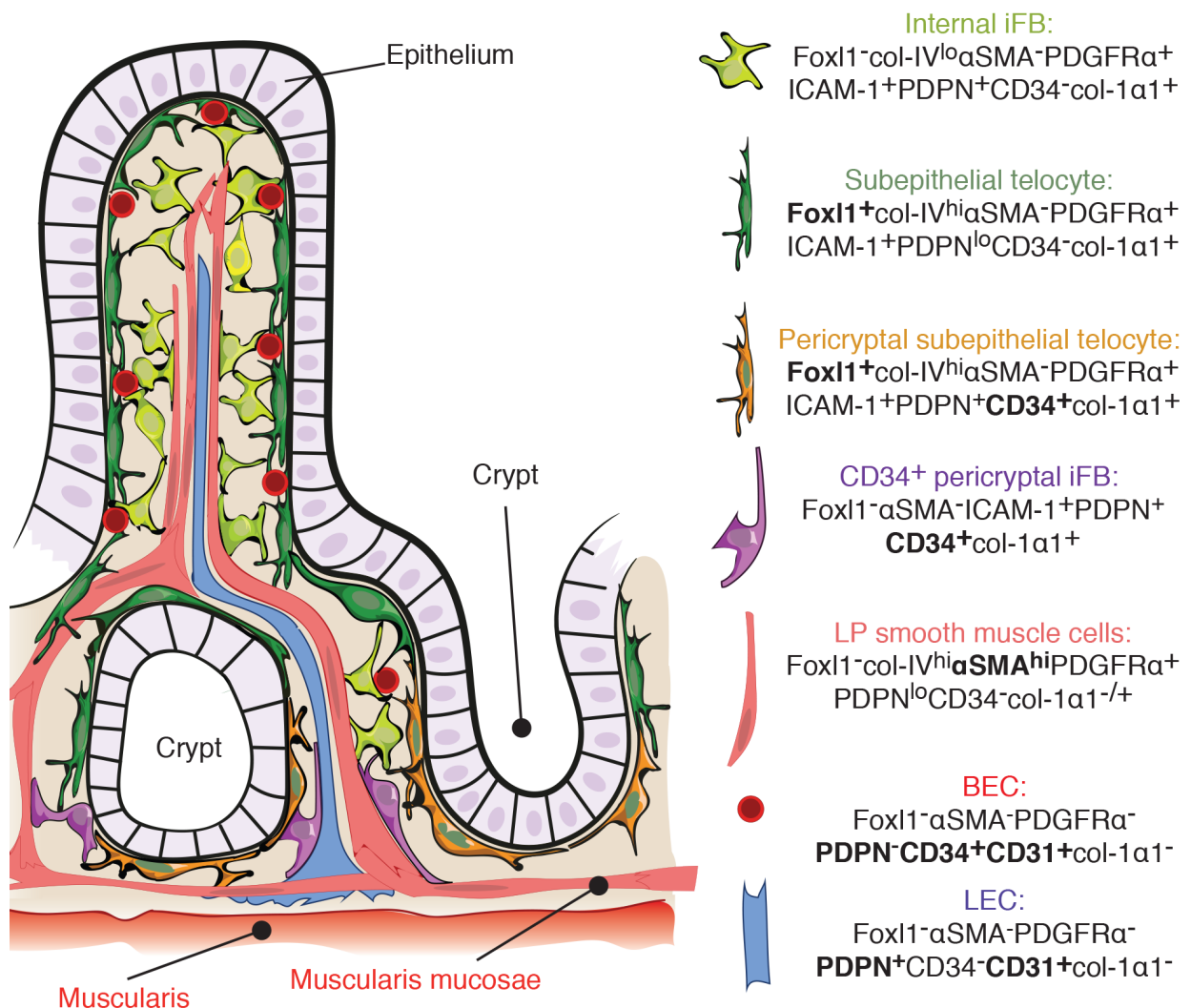


**Figure 21: Model for iFB subsets, distribution, and markers.** Model of the iFB organization based on previous studies as well as flow cytometrical and histological data generated in this work. Foxl-1 expressing Telocytes (dark green) form a highly interconnected network in the subepithelial zone. Telocytes localized near the crypt express CD34 (orange), while telocytes in the villus don't (dark green). Underneath this monolayer of telocytes, internal iFB are less branched, more roundish, and do not express Foxl-1 (light green). Internal iFB and telocytes embed BEC (red circles) and are interconnected together.  $\alpha$ SMA is highly expressed in the muscularis and in the smooth muscle cells (SMC) present in the LP (red), including the muscularis mucosae. LP SMC surround the lacteal (blue) and the crypts without being in direct contact with them. Notably, internal iFB connect physically subepithelial telocytes and the SMC. Finally, non-telocyte iFB expressing CD34 form an important network from the bottom of the crypts to the submucosa.

populations. But instead of suggesting that telocytes and iFB are two distinct cell types, I propose to group telocytes with underlying fibroblasts in the iFB family due to the many similarities between these cells. Fibroblasts are defined as reticular cells maintaining the structural framework that support the organs by secreting ECM components. Our histological and flow cytometrical investigation demonstrated that

internal iFB as well as subepithelial telocytes express collagen1 $\alpha$ 1, a major ECM component, PDGFR $\alpha$ , and ICAM-1, all well-known fibroblastic markers also used in the studies of LN and spleen FRC and BM FB. Telocytes and internal iFB may simply be in another activation or differentiation state but be derived from the same FB precursor. To gain more insight into this question, developmental studies as well as gene arrays on these two cell subsets isolated *ex vivo* from the SI could be performed to elucidate their potential common origin and their shared as well as distinct functions.

### 6.1.3 The lamina propria smooth muscle cells (SMC)

Historically,  $\alpha$ SMA expression was extensively used to identify intestinal fibroblasts/myofibroblasts and was often associated with subepithelial myofibroblasts contacting crypts in mice and humans (Mifflin et al. 2011, Pinchuk et al. 2010). However, recent studies (Bernier-Latmani et al., 2015), including our unpublished data, failed to reproduce the  $\alpha$ SMA expression staining on subepithelial cells of murine SI villi at steady-state using whole mount stainings. We observed  $\alpha$ SMA expression only in smooth muscle cells forming fibers around the lacteal (Bernier-Latmani et al., 2015). Instead, we demonstrated that subepithelial iFB are  $\alpha$ SMA<sup>-</sup> col1 $\alpha$ 1<sup>+</sup> iFB and belong to the telocyte subset as already mentioned above. Our observation is supported by findings of others on SI of Foxl1 reporter mice showing no overlap between Foxl1 and  $\alpha$ SMA (Aoki et al., 2016). However, I show, using high-magnification confocal 3D reconstruction, that  $\alpha$ SMA<sup>+</sup> cells form a continuous structure from from the pericryptal area - where they contact the muscularis mucosae - to the villus where they localize around the lacteal. However, I show that these  $\alpha$ SMA<sup>+</sup> cells are not in direct physical contact with the epithelial crypt cells as  $\alpha$ SMA<sup>-</sup> col1 $\alpha$ 1<sup>+</sup> telocytes form a cellular barrier between them. These findings reinforce the notion that there is no myofibroblast in the subepithelial zone of mice, at least in steady-state. In this work, flow cytometrical and histological analysis revealed that  $\alpha$ SMA<sup>hi</sup> cells express an intermediate level of PDPN and that 50-60% of them (as assessed by flow cytometry) have a low col1 $\alpha$ 1 promoter activity. Moreover, desmin is also expressed by  $\alpha$ SMA<sup>+</sup> SMC (Bernier-Latmani et al., 2015). Even though  $\alpha$ SMA<sup>hi</sup> cells and iFB shared several features, it is now clear that  $\alpha$ SMA<sup>hi</sup> cells of the LP constitute a SMC type responsible for the structural maintenance of the mucosa as well as the contraction of villi involved in food absorption, such as lipids (Choe et

---

al., 2015). Whether  $\alpha$ SMA<sup>+</sup> myofibroblasts (or subepithelial myofibroblasts) can arise from activated iFB under certain conditions such as infection, tissue damage, or IBD need to be further explored. Notably, the existence of subepithelial myofibroblasts in the pericryptal area of human SI and colon seems well-accepted even though higher-resolution microscopy could be performed to confirm this differential distribution of  $\alpha$ SMA expression between mice and humans. Of note, CD90, used as marker for myofibroblasts in humans, is not expressed by iFB nor SMC but only by nerves, lacteals and a subset of T cells. Finally, the observations and statements derived from cultured fibroblasts need to be interpreted with caution as  $\alpha$ SMA expression can be induced in FB due to culture on a plastic surface and/or the presence of fetal calf serum (FCS) making their faithful identification as myofibroblasts and their difficult functional analysis difficult (**Fig. 21**).

#### **6.1.4 Internal iFB**

Underneath the telocyte monolayer, another iFB subset forms a physical bridge between telocytes and central SMC. We showed that these internal iFBs display a more roundish cellular and nuclear morphology compared to telocytes or SMC. Although internal iFBs are less branched than telocytes, they still form a continuous network in the villus and pericryptal parenchyma, maintaining presumably the shape of the LP. In addition, internal iFBs are probably the iFB subset interacting the most with the different intestinal immune cell types, including IgA<sup>+</sup> PC, providing them a cellular scaffold for their proper homing and/or migration within the LP, as well as cytokines involved in immune regulation and cell survival. The characterization of the iFB subset function could constitute a fascinating research field in the future. Furthermore, in agreement with their distribution and the space that they occupy in the LP, internal iFBs represent most likely the main iFB subset, even though a direct quantification was not performed in this study.

#### **6.1.5 The size of the iFB population is underestimated by flow cytometric analysis**

The combination of the strong Col1-GFP expression in this reporter mouse and the whole mount staining technique optimized by Bernier-Latmani (Bernier-Latmani et al., 2015; Bernier-Latmani and Petrova, 2016) allowed us to highlight the important cell fraction that constitute iFB within SI *in vivo* reaching more than 40% of cells found

within the villi and probably even more in the pericryptal submucosa as most of the GFP<sup>+</sup>DAPI<sup>+</sup> cells localized also in the villi (data not shown). This high iFB frequency measured in col-GFP mice with my histological GFP and DAPI colocalization protocol ( $42.5 \pm 1.8$  %) and the iFB frequency I obtained after enzymatic digestion and flow cytometric analysis of the LP ( $8.2 \pm 0.6$  %) were obviously not consistent, demonstrating that stromal cell number and frequencies calculated with flow cytometry are underestimating more than five times the importance of the iFB compartment. Although I can only speculate about the reasons for this mismatch, inefficient cell isolation by tissue digests may be considered as the main confounding factor knowing that iFB (or stromal cells in general) form a compact, sessile, and interconnected network relying on multiple, if not continuous, firm adhesive interactions. These physical properties of iFB - iFB interactions are likely to make the iFB network resistant to complete extraction in the form of a single cell suspension. Moreover, beside their elongated morphology, the multiple and thin cellular extensions of iFBs make them, most likely, more sensitive to physical stress possibly leading to the death of many isolated iFB. Finally, the potentially incomplete ECM digestion, which is inherent to all isolation protocols, could represent an additional explanation. For example, it is difficult to imagine a healthy and complete extraction of the subepithelial telocytes considering their morphology, strong association with the basement membrane, and their localization in between basement membranes of the epithelial barrier and the blood vessels. Notably, upon digestion/extraction the survival of iFB as well as endothelial cells varied between 60% to 70% as measured by flow cytometry, and was always lower and less reproducible compared to the survival of isolated CD45<sup>+</sup> hematopoietic cells that often reached 95-98% survival. Similar observations were made upon isolation of pLN-derived stromal cells with a survival of 70% for FRC and 98-99% for CD45<sup>+</sup> hematopoietic cells (our unpublished observation). Gomariz and colleagues went even further in the quantification of CXCL12-expressing stromal cells in the BM by comparing frequencies and absolute numbers as measured by 3D microscopy (similar to our study) versus flow cytometry. While absolute numbers of Foxp3-expressing Treg were comparable between the two techniques, flow cytometric quantification neglected more than 95% of CXCL12-expressing cells and sinusoidal endothelial cells (Gomariz et al., 2018). Based on frequencies only, it seems that I lose less iFB than Gomariz and colleagues for CXCL12<sup>+</sup> BM stromal cells. This discrepancy may be explained by the use of different isolation protocols but most probably it stems from the different organs

---

investigated. Taken together, the observations for BM stroma by Gomariz and colleagues and our results for iFB raise fundamental questions about stroma quantification by flow cytometry. If isolation efficiency depends on isolation procedures but also cell location, cell attachments to ECM, and/or cell morphology, we can imagine that isolation of reticular cells, such as fibroblasts, telocytes, endothelial cells but also some myeloid cells, will lead to heterogeneous yields. I believe that stromal cell isolations are still relevant for the comparison between different cell types and conditions but should be interpreted with caution and confirmed by quantitative histology and the use of proper controls. In conclusion, stromal cell isolations clearly have their limitations for assessing relative proportions of cell types, and may even fail to isolate certain cell types.

### 6.1.6 Conclusions

To summarize, I provide the first high resolution histology analysis of the iFB compartment with them defined functionally by their  $col1\alpha1$  promoter activity. I report that the  $col1\alpha1$  promoter is highly and constitutively active in all iFB subsets described so far, including subepithelial telocytes of the villi,  $CD34^+$  pericryptal subepithelial telocytes,  $CD34^+$   $ACKR4^+$  submucosal iFB, and even some  $\alpha SMA^{hi}$  smooth muscle cells. The phenotypical characterization of the iFB subsets and other stromal cell types in the SI is summarized in the **Figure 21**, along with their distinct localization in the LP. In contrast, the  $col1\alpha1$  promoter activity was absent or very low in epithelial cells, the entire hematopoietic compartment, endothelial cells, and SMC from the two perpendicular muscle layers responsible for peristalsis. Importantly, I highlighted the limitation of isolation/flow cytometry in quantifying the stromal compartment. Col-GFP mice could be used in future for *ex vivo* and intravital iFB studies to look at their response to physical or chemical induced injury, or to investigate their interactions with other cells, such as hematopoietic cells, that may use the iFB network for their migration. ColGFP mice might also be used to compare fibroblasts from different sites and thereby compare their phenotype or function.

Indeed, fibroblasts are gaining more and more attention in many different tissues and they are thought to be morphologically and functionally optimized for every organ (Rinn et al., 2006). In addition, their high plasticity enables them to respond to various external stimuli, such as cytokines released during the immune response, chronic inflammation, or tissue injury. Future large-scale comparisons between iFB

subsets could underline distinct functions or different responses upon stimulation (immunization or disease model). New single-cell sequencing methods could also reveal unanticipated levels of phenotypical and functional heterogeneity, at steady state and under various stimulations, as it was shown for naive pLN-derived FRC (Rodda et al., 2018), lung (Xie et al., 2018), or skin (Philippeos et al., 2018). Finally, comparison between fibroblasts from different organs or tissues, such as iFBs, SLO-derived fibroblasts and skin fibroblasts, amongst others, could highlight the adaptation and plasticity of fibroblasts to their microenvironment and reveal functionally similar or distinct subsets.

### **6.2 iFB and myeloid cells as niche cells for IgA PC survival**

PC are not intrinsically long-lived and need specific survival factors from their microenvironment to survive. These survival factors are thought to be provided in geographically restricted areas of the body, called survival niches, as they can be found in the BM, in medullary cords of pLN, and most probably in the intestinal LP. In these specialized niches, different cells types provide adhesion and survival factors to PC. Non-hematopoietic and non-endothelial cells of the fibroblast lineage are a major component of these niches, contacting extensively PC in the BM and the medullary cords of pLN and being a potential source of chemoattractants and survival molecules, such as CXCL12, APRIL, BAFF, and IL-6. In addition, different myeloid cell subsets are thought to complete the niche and to provide APRIL, BAFF, and IL-6. In the intestine, different studies have shown that PC can survive during weeks or months (Hapfelmeier et al., 2010; Lemke et al., 2016; Landsverk et al., 2017). However, in contrast to BM and pLN niches, little is known about the niche composition and the survival factors involved within the SI.

In this study, I demonstrate that iFB represent a major cell type of the IgA<sup>+</sup> PC environment, constituting more than 40% of the cells. CD11b<sup>+</sup> myeloid cells and CD3ε<sup>+</sup> T cells are the other cells types localized in the IgA<sup>+</sup> PC neighborhood, although their respective number are lower than iFB. In addition, transcript analysis for plasma cell survival factors revealed that iFBs are a predominant source of *cxcl12* and *baff*, and could contribute to *april* production. In order to take all cell types into consideration and to facilitate the screening for cells promoting IgA<sup>+</sup> PC survival, I have set up an assay allowing to assess the role of all isolated iLPC as PC niche cells. On one hand, IgA<sup>+</sup> PC were only enriched for non-adhesive cells (with adhesive cells comprising mainly macrophages and iFB), and therefore contained all

---

other cell types in their natural ratio. On the other hand, the cells most frequently colocalizing with IgA<sup>+</sup> PC in situ were efficiently enriched by plastic adhesion allowing to test easily their capacity to promote PC survival. These cocultures revealed that only col1 $\alpha$ 1-GFP<sup>+</sup> PDPN<sup>+</sup> ICAM-1<sup>+</sup> VCAM-1<sup>+</sup> iFB and CD103<sup>-</sup> CD11b<sup>+</sup> CD11c<sup>+</sup> F4/80<sup>+</sup> M $\phi$  cultured for 5 days can promote IgA<sup>+</sup> PC survival and function and did so in an exclusively contact-dependent manner.

### **6.2.1 Synergistic PC survival effect by iFB and M $\phi$**

When combining iFB and M $\phi$ , I have observed a synergistic effect on PC survival and function. The nature of this functional interaction between iFB and M $\phi$  is still unknown and could be an interesting avenue for future research. Such iFB and myeloid cell interactions have been previously reported by our lab for the PB/PC survival niche in the pLN. Indeed, isolated FRC from the medullary cords, namely MedRC, and myeloid cells showed synergistic behavior in promoting purified PC survival through IL-6 production (Huang et al. 2018). In contrast to pLN-derived PB/PC survival which was independent of cell contact, proximity between IgA<sup>+</sup> PC and intestinal AC was crucial for PC survival and reduced by more than 60% upon neutralization of the surface receptor CD44. We can hypothesize that iFB - M $\phi$  cocultures induce an upregulation of CD44 or CD44 ligands on either one or both of the cells, or they trigger the expression of additional survival factors that act in synergy with CD44, for example by amplifying the CD44 prosurvival signaling pathway. To test these hypothesis, CD44 MFI on iFB and M $\phi$  could be first measured by flow cytometry when cultured alone and together in the AC mix to check whether CD44 is upregulated. Similar analysis should be performed for IgA<sup>+</sup> PC from the different culture conditions. Alternatively, HA synthase and or hyaluronidase transcripts could be quantified in iFB or M $\phi$  cultured alone or in the mix of both cell types. To gain insights into the differential expression of factors, such as upregulated prosurvival molecules or downregulated pro-apoptosis molecules, RNA sequencing could be performed on lysates of iFB, M $\phi$  or AC. In conclusion, iFB and M $\phi$  alone promote IgA<sup>+</sup> PC survival and function, while the mix of iFB/ M $\phi$  (AC) promote it much more strongly. The prosurvival effect of iFB and M $\phi$  on IgA<sup>+</sup> PC is to a large extent, but not entirely, dependent on CD44 engagement. Importantly, I was not able to culture efficiently CD31<sup>+</sup> endothelial cells or EpCAM<sup>+</sup> epithelial cells with this protocol.

Therefore, future investigations may establish the right culture conditions to test these cells further as potential niche cells for PC.

### 6.2.2 Role for epithelial cells in IgA<sup>+</sup> PC survival?

In my hands, coculture of IgA<sup>+</sup> PC and epithelial cells failed as all epithelial cells died before providing any potential survival stimuli to PC, thus implying that my co-culture setting cannot give insight into epithelial cell involvement in the PC niche. In contrast to other iLPC that share the same microenvironment than IgA<sup>+</sup> PC, I and others showed that the epithelium layer is physically separated from IgA<sup>+</sup> PC *in situ* by a dense basement membrane, a subepithelial telocyte network, and blood vessels. This indicates that potential pro-survival factors provided by the epithelium need to be soluble, not adhesive to basement membrane proteins and able to reach the underlying PC niche in a sufficient concentration. In line with this observation, epithelial cells have been described to produce APRIL as based on histological stainings of APRIL protein in intestines from mice and humans (Chu et al., 2014; Lemke et al., 2016; He et al., 2007; Wang et al., 2017b). Indeed, our RT-qPCR quantification on various sorted iLPC showed that epithelial cells constitute an important source of *april* transcripts *in vivo*, but also emphasizes that iFB and EC express a similar relative level of *april* transcripts as epithelial cells. However, this transcript expression in the LP was not confirmed by APRIL protein staining on thin sections as reported by others (Chu et al., 2014; Lemke et al., 2016). This mismatch between histological APRIL protein staining and our RT-qPCR data could be partially explained by the greater ease to visualize epithelial cells compared to iFB. Moreover, we observed that epithelial cells display very high auto-florescence relative to the underlying mucosa besides their propensity to nonspecifically bind antibodies in histology making the interpretation of some detected signals challenging. For example, PDGFR $\alpha$  staining of intestinal thin sections has shown that epithelial cells are positive for this receptor, while flow cytometrical analysis demonstrated clearly that this is not the case. For the particular case of APRIL, the antibody used by Chu and colleagues to highlight the APRIL expression by eosinophils and epithelial cells has been previously shown to give a similar signal in WT and APRIL-KO mice (Belnoue et al., 2012). However, western-blot analysis performed on murine epithelial cell lysate confirmed their APRIL expression, but this study did not compare APRIL production by epithelial versus other cell types (Wang et al., 2017b). Finally, we

---

cannot exclude that mRNA level is not always translated by similar protein expression level, due to differential mRNA translation control or mRNA stabilization during the cell sorting. Despite these technical difficulties to study the APRIL source at the protein level, epithelial cells contributions to IgA<sup>+</sup> PC homeostasis need to be further explored *in vitro* and potentially *in vivo*. *In vitro* organoid cultures could be an option worth trying to investigate this question. Although villin-cre or villin-CreERT2 could be used to target intestinal epithelial cells (el Marjou et al., 2004), APRIL<sup>flox/flox</sup> mice have not yet been reported making the *in vivo* investigation of the epithelial APRIL involvement in the PC niche impossible for the moment.

### 6.2.3 Role for endothelial cells in IgA<sup>+</sup> PC survival?

Our 3D histological analysis showed that blood vessels and IgA<sup>+</sup> PC do not contact each other due to iFB and basement membranes often enwrapping these vessels. LEC are also separated from IgA<sup>+</sup> PC by a basement membrane and  $\alpha$ SMA<sup>hi</sup> smooth muscle cells that form a sort of a cage around the lacteal. These observations indicate that endothelial cells could only interfere with PC survival through the secretion of soluble factors similar to epithelial cells. By RT-qPCR, we showed that BEC and LEC may be a potent source of APRIL and BAFF, respectively (**Fig. 8H**). CD31<sup>+</sup> endothelial cells can be efficiently isolated from the LP (**Fig. 8C**) but they adhere only poorly to plastic and are rapidly overgrown by proliferating iFB, so that I have not tested their capacity to help in PC survival. In future, iFB and myeloid cells could be removed by MACS before plating endothelial cells in the appropriate medium allowing their survival or growth. Similar to epithelial cells, the involvement of endothelial cells as part of the PC survival niche needs to be further explored. However, we show here that the endothelial compartment is relatively small compared to iFB in the IgA<sup>+</sup> PC niche, besides being often shielded off by iFB and SMC, suggesting that iFB and immune cells should play a bigger role in this process.

### 6.2.4 Role for eosinophils in IgA<sup>+</sup> PC survival?

While my coculture assay lacked epithelial and endothelial cells, live eosinophils were well represented (about 5%), suggesting that they could fulfill their potential PC pro-survival effect. While Chu and colleagues reported a crucial role of eosinophils in promoting IgA<sup>+</sup> PC survival via APRIL and IL-6 production, Jung et al. generated

contradictory results indicating that eosinophils are not essential, not only in PC survival *in vitro*, but also as APRIL and IL-6 source (Chu et al., 2014; Jung et al., 2015). The findings by Jung and colleagues were partially confirmed by our results. Indeed, the presence of eosinophils in the AC-depleted iLPC does not seem to promote efficiently PC survival as only rare PC survived in absence of AC. In addition, sorted eosinophils did not reinforce the prosurvival effect by AC on sorted IgA<sup>+</sup> PC. Of note no survival factors were added in order to promote efficient eosinophil survival (such as IL-5 or GM-CSF), like in the two previous studies (Chu et al., 2014; Jung et al., 2015). But in the two settings described above, eosinophils are still present in the culture after 24h (approx. 5% of AC-depleted iLPC, and 30% of the sorted eosinophil/IgA<sup>+</sup> PC cocultures). Moreover, Chu et al reported extended contacts between IgA<sup>+</sup> PC and major basic protein (MBP)<sup>+</sup> eosinophils which was not confirmed by us using 3D reconstruction of the niche wherein only 20% of IgA<sup>+</sup> PC contacted Siglec-F<sup>+</sup> cells. Furthermore, weak survival factor expression by eosinophils reported by Jung and colleagues was confirmed by our RT-qPCR data performed on a sorted myeloid cell pool, which included 30-35% of eosinophils, displaying a poor *april*, *baff*, and *cxcl12* transcript expression level compared to iFBs. Interestingly, the eosinophil dependency described for BM PC survival - notably by the same lab proposing the eosinophil dependency for SI PC survival - was also recently questioned following the publication of two studies demonstrating that the BM PC pool is normal in eosinophil-deficient mice at steady state and upon immunization (Haberland et al., 2018; Bortnick et al., 2018). The authors of these papers explained these unexpected results by the lack of proper co-housing in the study by Chu and colleagues. Indeed, the authors observed that PC numbers strongly vary in mice derived from different facilities, indicating that cohousing is indispensable for ensuring a comparable microbiome. Taken together, our *in vitro* data along with the Jung study suggest that eosinophils are not essential for providing IgA<sup>+</sup> PC survival factors. However, several lines of evidence point to a role of these cells in gut PC responses due to their function in PP development and IgA class switch recombination. Moreover, I would like to emphasize that eosinophils show a high turnover rate *in vivo* with a half-life of approximately 6 days in the SI LP which is considerably longer than in the lung or blood (Carlens et al., 2009). This short life span is harder to reconcile with the concept of a robust and constitutive survival niche such as the one that could be provided by the resident iFB and non-migratory M $\phi$  with presumably longer half-lives. Indeed, in a preliminary EdU

---

experiment, I observed that less than 0.5% of iFB were EdU<sup>+</sup> after 12 days of EdU treatment (in drinking water). However, we cannot exclude that eosinophils are constantly replaced and contribute to the niche possibly by adding another level of regulation to PC homeostasis. Altogether, however, most evidence points to a non-essential role of eosinophils in IgA<sup>+</sup> PC survival.

### **6.3 Is the survival of IgA<sup>+</sup> PC really independent of IL-6, BAFF or APRIL?**

Despite the apparent absent role for a soluble factor in my PC survival assay as suggested by my transwell and supernatant experiments, we and others have made observations that hint to a contribution of cytokines likes IL-6, April and BAFF, *in vitro* and *in vivo*.

#### **6.3.1 Role of IL-6**

As already mentioned in the introduction, the role of IL-6 for PC survival is still not clear *in vivo*. Although it seems important for the maintenance of short-lived PC in the medullary cords of pLN (Huang et al. 2018), its function in promoting PC survival seems more limited in the BM. However, the number of IgA<sup>+</sup> PC was dramatically reduced in IL-6KO LP at steady state and after mucosal challenges with either OVA or vaccinia virus (Ramsay et al. 1994). In my hands, IL-6KO and WT mice showed similar IgA<sup>+</sup> PC numbers at steady-state when mice were sex-matched and cohoused for four weeks (**Fig. 14E**). Unfortunately, the data for IgA secretion are missing for these experiments. However, we obtained *in vitro* evidence for a role of IL-6 in the maintenance of antibody production. The cocultures of PC with WT or IL-6 KO AC led to the same number of surviving IgA<sup>+</sup> PC (**Fig. 14A**) but to a slightly reduced IgA production (**Fig. 14B**) and reduced MFI for the surface IgA (**Fig. 14C**), while AC from both WT and IL-6KO seemed similar in terms of morphology and proliferative features (**Fig. 14D** and data not shown). However, I couldn't confirm the IgA secretion phenotype using neutralizing anti-IL-6 antibodies *in vitro*, suggesting that other parameters may be affected in IL-6KO AC. All together these data suggest that IL-6 is not involved in the IgA<sup>+</sup> PC survival at steady state.

### 6.3.2 Role of APRIL

APRIL has been shown to be expressed in the LP of the SI and colon in mice (Barone et al., 2009) and humans (Gustafson et al., 2014). The direct role of BAFF and APRIL on IgA<sup>+</sup> PC survival has not been clearly demonstrated *in vivo* as these two cytokines are also involved in the IgA CSR (Litinskiy et al., 2002; Castigli et al., 2005). However, *in vitro* studies showed that soluble oligomerized APRIL can boost the survival of purified tonsillar PC (Huard et al., 2008). In addition, BCMA blockage decreases while recombinant APRIL increases IgA secretion from cultured human intestinal biopsies (Mesin et al., 2011). To date, intestinal epithelial cells are the most frequently reported cellular source for APRIL in the LP (Lemke et al., 2016; He et al., 2007; Barone et al., 2009; Wang et al., 2017b).

In this study, *April* mRNA was detected in 5 days cultured AC and in our iFB cell line (that I have described in my master thesis) at the same level as isolated iFB suggesting that AC keep APRIL expression *in vitro*. But neither TACI-fc as soluble APRIL receptor nor AC-conditioned SN showed any effect on IgA<sup>+</sup> PC numbers or function. Prosurvival effects of APRIL, but not BAFF, have been shown to depend on its ability to bind heparin sulfate proteoglycans (HSPG) which are covalently attached to the protein core of the CD138 molecule (also called Syndecan-1) abundantly expressed by PC (Ingold et al., 2005; Belnoue et al., 2008). While CD138 is preserved on the surface of LN after cell isolation by meshing it is lost after collagenase digestion as used in the experiments described here (data not shown). Even though CD138 is re-expressed on all IgA<sup>+</sup> PC after 24 hours of coculture, HSPG attached to CD138 cannot accumulate APRIL on the PC at the beginning of the coculture. In fact, APRIL needs a moiety promoting its oligomerization as shown using APRIL-collagen-fusion proteins or APRIL binding to HSPG-coated plastic to observe the prosurvival effect on purified PC (Huard et al., 2008). APRIL mutants unable to bind HSPG are unable to promote PC survival (Huard et al., 2008). Thus, even though APRIL may be secreted by AC and be present in AC-conditioned SN, it possibly cannot oligomerize and bind efficiently to the BCMA receptor on IgA<sup>+</sup> PC to enhance their survival in my *in vitro* cocultures, which could explain the undetectable effect of TACI-fc. In order to address the potential role of APRIL secreted by iFB and/or M $\phi$ , recombinant TACI-fc could be added a couple of hours after the beginning of the coculture when CD138 is re-expressed on IgA<sup>+</sup> PC. Alternatively, APRIL could be added to HSPG-coated wells in order to address whether APRIL has a role for intestinal IgA<sup>+</sup> PC survival at all *in vitro*.

---

### 6.3.3 Role of BAFF

In contrast to *april* transcripts, *baff* expression is dramatically reduced in 5 days cultured AC and iFB cell line, similar to cultured pLN FRC (Huang et al. 2018) which indicates that the BAFF function cannot be assessed using the current assay. Moreover, PC cocultured with WT or BAFF-KO AC gave rise to comparable PC survival and IgA secretion (**Table 1**). Attempts to compensate the loss of BAFF expression by adding 60-mer BAFF molecules on top of AC - IgA<sup>+</sup> PC cocultures did not show any benefit for PC survival (data not shown).

Importantly, the activity of the BAFF 60-mer as well as other molecules tested *in vitro* were not controlled systematically, although they were obtained from collaborators or from typically reliable sources. Of note, the recombinant IL-6 and anti-IL-6 antibody used in the cultures was validated in our lab (Huang et al. 2018), while the TACI-fc used in my cocultures showed the expected effects *in vivo*, namely a reduction of B cells in the spleen and of IgA<sup>+</sup> PC in the SI (our unpublished observations). However, it is important to underline the need of further studies to address the role of BAFF and APRIL in the intestinal PC survival process.

Finally, it should be emphasized that all intestinal cells used in these assays were isolated from “naïve” SPF adult mice and we can speculate on the changes occurring in the PC niche upon an intestinal pathogen infection, toxin administration or oral vaccination. Future investigations should test whether the survival factor expression and IgA<sup>+</sup> PC survival changes when AC and IgA<sup>+</sup> PC are isolated from “stimulated” or more inflamed SI. As all the data were generated with SI-derived cells, we can speculate on the similarities and differences of the PC niche in the SI and the colon.

### 6.3.4 Is there an iFB subset functionally dedicated to PC survival?

In the first half of my thesis, I have reported the presence of various col1 $\alpha$ 1<sup>+</sup>PDPN<sup>+</sup> iFB subsets observed in homeostatic SI. In the second half of my thesis work I followed up on this phenotypic iFB characterization with the identification of an important function of iFB in IgA<sup>+</sup> PC maintenance and function that was mediated via cell contact and CD44. In this PC survival assay I have not investigated single iFB subsets. Flow cytometrical and histological analysis performed on 5d-cultured iFB

showed that about 40% express  $\alpha$ SMA and about 60% CD34 (data not shown), comparable to the proportions measured *ex vivo*. However, the frequency of  $\alpha$ SMA<sup>+</sup> cells expressing CD34 was assessed only twice and varies greatly. The high frequency of  $\alpha$ SMA<sup>+</sup> cells after 5 days of culture compared to *ex vivo* (6-8% of the non-endothelial stromal cells or 0.5-0.7% of total live cells) might be explained by iFB activation, as mentioned before, giving rise to myofibroblasts. These observations show that the iFB heterogeneity is maintained upon short-term culture but makes their functional distinction impossible in the context of PC survival. By histology, I observed that IgA<sup>+</sup> PC often cluster in the middle of the villus clearly separated from the CD34<sup>+</sup> iFB of the submucosa, but almost always contacting CD34<sup>-</sup> iFB internal to the villus and not lining the epithelial layer. Notably, sorted CD34<sup>-</sup> iFB did not show enrichment for *cxcl12*, *baff* or *april* compared to CD34<sup>+</sup> submucosal iFB (data not shown), indicating that the preferential homing of IgA<sup>+</sup> PC into the CD34<sup>-</sup> iFB network is probably not based solely on these factors. Therefore, the basis of this PC segregation *in vivo* is still unclear and remains to be defined in the future. As a first step, coculture of IgA<sup>+</sup> PC with CD34<sup>+</sup> versus CD34<sup>-</sup> iFB constitute an interesting experiment. In the future, RNA sequencing performed on the different iFB subsets identified or single cell sequencing of stromal cells should give interesting insight, not only for PC survival molecules, but also for other functions of iFB that remain to be investigated, as mentioned above. As there is no surface marker to identify SMC and that they represent only 0.5-0.7% of live cells in a cell suspension, it is quite challenging to purify and study the role of these cells *in vitro* and *in vivo* in the context of PC survival.  $\alpha$ SMA-Cre mouse could be used to identify SMC *in vivo* and to study them *in vitro* without having to stain them intracellularly (LeBleu et al., 2013). The single cell sequencing of non-endothelial stromal cells may also be the way to characterize better the  $\alpha$ SMA<sup>+</sup> SMC similar to iFB described above. Nevertheless, our histological data clearly indicate that  $\alpha$ SMA<sup>lo</sup> iFB contact IgA<sup>+</sup> PC more frequently than the  $\alpha$ SMA<sup>hi</sup> SMC making them better candidates as niche cells for PC (**Fig. 16A and B**).

---

## **6.4 PC survival promoted by adherent cells is mediated by CD44 interactions *in vitro***

### **6.4.1 PC survival is mediated by CD44 *in vitro***

CD44 represents a type I transmembrane glycoprotein that exists in different forms, one called standard CD44 (the main molecule expressed under physiological conditions) and at least five variant CD44 molecules, all derived from a single gene but from six alternatively spliced transcripts (Ponta et al., 2003). Further heterogeneity is introduced by extensive post-translational modifications including *N*- and *O*-linked glycosylations (Camp et al., 1991; English et al., 1998). CD44 is ubiquitously expressed in many normal adult and fetal tissues and is found on virtually all hematopoietic cells. Its function has been mostly studied in cancer progression (Senbanjo and Chellaiah, 2017) and in T cells. CD44 is considered as a marker for Ag-experienced, effector, and memory T cells as they express it at higher levels than naive T cells (Baaten et al., 2012). On T cells and cancer cells, CD44 has been described as a critical regulator of cell rolling and adhesion to the activated endothelium at the site of inflammation (Ponta et al., 2003), transmigration (Ley et al., 2007), and cell migration in general including cancer cell metastasis, involving both cell-cell and cell-ECM interactions (Alon et al., 1995; Siegelman et al., 2000). Importantly, the affinity of CD44 for its ligands is dependent on the post-translational modifications of CD44 (Skelton et al., 1998). CD44 is known to bind numerous ligands found in the extracellular space, including hyaluronic acid (HA), osteopontin, collagen, fibronectin, laminin, and matrix metalloproteinases (Goodison et al., 1999; Ponta et al., 2003; Misra et al., 2015). Besides its role in cell migration and adhesion, CD44 can promote cell survival by inducing intracellular signals directly through its intracellular domain (CD44-ICD) that bind kinases (Okamoto et al., 2001; Thorne et al., 2004) or through interaction with co-receptors such as the integrin VLA-4 (Marhaba et al., 2006; Lefebvre et al., 2010). Indeed, primary T cell and memory Th1 cell survival has been shown to depend on CD44 mediated activation of the Akt/PI3K pathway (Marhaba et al., 2006; Baaten et al., 2012). Moreover, CD44-ICD can be cleaved by metalloproteases and act as transcription factor binding to a DNA consensus sequence and regulating cell survival during stress, inflammation, oxidative glycolysis, or tumor invasion (Okamoto et al., 2001). The role of CD44 in cell survival seems to be highly cell- and context-dependent. For example, CD44

expression on activated T cells has been associated with both resistance (Marhaba et al., 2006; Naor et al., 2007; Wittig et al., 2000; Baaten et al., 2012) and susceptibility (McKallip et al., 2002; Nakano et al., 2007) to apoptosis. In the context of PC survival, only *in vitro* CD44 neutralization experiments have been performed using different Ab clones leading to conflicting results. Indeed, targeting of CD44 has been reported to promote BM PC survival *in vitro* using neutralizing Ab (IM7) and agonist Ab (IRAWB) clones (Cassese et al., 2003) or to have no effect when CD44-HA neutralizing KM81 clone was used (Minges Wols et al., 2002). Importantly, the IM7 clone has been shown to be poorly efficient in abolishing CD44-HA binding, to induce intracellular signaling and CD44 shedding (Ishiwatari-Hayasaka et al., 1999), indicating that the effects of this clone are difficult to interpret. Interestingly, neutralization of various CD44 isoforms leads to the inhibition of binding between immortalized PC lines and BM-derived stromal cells (Van Driel et al., 2002). In my work, neutralization assays showed that CD44 explained a major part of the prosurvival effect AC had on IgA<sup>+</sup> PC *in vitro*, reducing the survival about 75% relative to PC cultured alone. Notably, I used the KM201 clone of the anti-CD44 antibody. KM201 inhibits efficiently CD44-HA binding (Zheng et al., 1995; Ishiwatari-Hayasaka et al., 1999) without inducing CD44 mediated intracellular signaling or CD44 shedding, in contrast to IM7 (Ishiwatari-Hayasaka et al., 1999). I have confirmed the role of CD44 in PC maintenance by using CD44-deficient PC which were more sensitive to death compared to WT IgA<sup>+</sup> PC. Interestingly, CD44 deficient AC were also less efficient as niche cells for WT and CD44KO IgA<sup>+</sup> PC suggesting an important role for CD44 both on the niche cells and on IgA<sup>+</sup> PC. Interestingly, dermal CD44KO fibroblasts seem to have an impaired ECM production, strength of cell adhesion, contact inhibition, and survival *in vitro* (Tsuneki and Madri, 2016). Even though CD44KO and WT AC proliferated similarly, CD44KO AC might display similar defects as dermal CD44KO fibroblasts or have other alterations leading to an impaired PC survival which is only indirectly linked to CD44 deficiency in AC. For example, I could imagine that CD44-deficient AC produce less HA, which leads to a reduced stimulation of CD44 on PC. Alternatively, HA or another CD44 ligand that is produced by the iFB or macrophages could be captured by the CD44 expressed at the surface of the AC with another site of the repetitive ligand being recognized by the CD44 on the neighboring PC surface leading both to cell adhesion and cell survival signaling in PC.

---

In addition to CD44,  $\alpha_4$  neutralization led to a small but reproducible reduction of PC survival *in vitro*. The existence of a shared survival pathway between CD44 and  $\alpha_4$  need further investigations. Coblockage of CD44 and  $\alpha_4$  was performed three times. In each experiment, I observed a trend in line with an additional effect suggesting that they act together, but only one experiment gave a statistically significant difference. Moreover, the  $\alpha_4$  effect was reproducible only when a very high concentration of antibody was added (30 $\mu$ g/ml instead of 10 $\mu$ g/ml used for KM201), suggesting that its contribution may be minor compared to CD44, at least for IgA<sup>+</sup> PC survival. As mentioned previously, CD44 can bind to coreceptor like LFA-1 ( $\alpha_L\beta_2$ ) or VLA-4 ( $\alpha_4\beta_1$ ) integrins through its transmembrane domain leading to kinase activation and subsequent intracellular signaling. CD44 has been shown to bind  $\alpha_4$  on lymphocytes that can lead to the formation of a molecular platform for kinase activation (Nandi et al., 2004; Estess et al., 1998; Marhaba et al., 2006). Therefore I can hypothesize that CD44 binds  $\alpha_4$ , either  $\alpha_4\beta_1$  (VLA-4) or  $\alpha_4\beta_7$  (LPAM), which strengthen the CD44 prosurvival signal. Due to the weak effect of  $\alpha_4$  neutralization, the CD44 prosurvival pathway is likely to be only moderately enhanced by  $\alpha_4$ -mediated kinase activation.

CD44 neutralization using the KM201 Ab has never completely abolished the PC survival mediated by AC or iFB. Indeed, approx. 20% of AC-mediated effect was still there in all experiments performed with 10 $\mu$ g/ml of KM201. Moreover, the KM201 treatment reached a plateau at a concentration of more than 20  $\mu$ g/ml, leaving an unknown prosurvival effect of AC in the culture (data not shown). In line with this, CD44KO PC cocultured with CD44KO AC survived better than CD44KO PC alone indicating that without CD44 at all, AC can still promote PC survival using other mechanisms. I speculate that  $\alpha_4$  can contribute as alternative adhesion molecule with the capacity to signal or that re-expression of CD138 may allow an APRIL effect in a later stage of the culture.

#### **6.4.2 HA as the main CD44 ligand for IgA<sup>+</sup> PC survival?**

Having identified CD44 as the key prosurvival molecule I also investigated what the major ligand of CD44 involved in PC survival could be. HA is the most studied CD44 ligand, represents a ubiquitous and major component of the ECM, and is present in large amounts in virtually all organs. HA is a non-sulphated glycosaminoglycan (GAG) and is composed of repeating polymeric disaccharides of D-glucuronic acid

and N-acetyl-D-glucosamine linked by a glucuronic  $\beta$  (1 $\rightarrow$ 3) bond (Weissmann et al., 1954). Unlike other GAG, HA is not covalently attached to a protein moiety. HA turnover is highly regulated by its synthesis and degradation and its half-life varies between 3-5min in the blood and a couple of weeks in cartilage (Laurent et al., 1991). Cellular HA synthase (HAS1-3) and hyaluronidases (Hyal 1-3) mediate the production and degradation of HA, respectively (Itano, 2008; Itano and Kimata, 2008; Itano et al., 2008). Notably, CD44 seems to mediate HA uptake leading to HA catabolism in the lysosome by Hyal-1 (Harada and Takahashi, 2007; Stern et al., 2007). I have attempted to neutralize HA using Pep-1 which resulted in a small but significant reduction of the IgA<sup>+</sup> PC survival *in vitro*. The magnitude of the IgA<sup>+</sup> PC reduction induced by pep-1 was not comparable to the anti-CD44/KM201 effect, indicating that another CD44 ligand could play a role in this process. Alternatively, the highly repetitive structure of HA can make its complete neutralization difficult. Moreover, high concentrations of pep-1 in the culture medium led to AC detachment inducing the complete disorganization of the coculture (data not shown). *In vivo* Pep-1 administration leads to a marked decrease of the SI and colon length, villus height in the SI, crypt depth and epithelial proliferation (Riehl et al., 2012a). Interestingly exogenous HA injection gave rise to the exact opposite phenotype indicating that HA contributes to the regulation of normal SI and colon growth and structure (Riehl et al., 2012a). HA deposition is also increased in IBD and upon radiation injury (Riehl et al., 2012b; Wolfs et al., 2010; Zheng et al., 2009). Notably, the function of intestinal HA on crypt and Lgr5<sup>+</sup> stem cell proliferation is mediated via its binding to CD44 but also to Toll-like receptors (Riehl et al., 2012a; Riehl et al., 2015).

Interestingly, the size and branching of HA correlate with the inflammatory state of a particular tissue. Long-sized HA (>1000kDa) is found in healthy tissue whereas short HA fragments (<500kDa) are generated upon infection or tissue damage. Long-sized HA fragmentation can result from degradation by reactive oxygen species (ROS) produced in myeloid cells (Agren et al., 1997; Moseley et al., 1997) or altered expression of Hyal enzymes (Stern, 2004). Alternatively, changed HA synthase activity can result in production of shorter HA chains (Cheng et al., 2011; Bracke et al., 2010; Cheng et al. 2011; Bracke et al. 2010). In this study, cleavage of HA produced by AC in culture increased IgA<sup>+</sup> PC survival *in vitro*. Indeed hyaluronidase (hyal) digestion of HA induced a significantly higher PC survival than the synergistic iFB - M $\phi$  coculture and showed a dose dependence (**Fig. 18A**). In this setting, AC morphology and adhesion were not changed upon HA digestion by hyal (**Fig. 18B**).

---

This interesting finding suggest that the LP PC niche can be modulated by the HA composition in the extracellular compartment that may change subsequent to infection or tissue damage. Moreover, this indicates that CD44 is important not only for PC homeostasis at steady state but possibly also in inflammatory conditions. Further investigations into the HA biology in IgA<sup>+</sup> PC survival should represent an interesting avenue for future research. However, my attempts to boost IgA<sup>+</sup> PC survival by adding commercially available high molecular weight HA resulted in only a small prosurvival effect (data not shown) suggesting that the biology of this process may be complex. For example, AC or iFB are maybe necessary to provide a support to organized HA molecules properly around cocultured PC in the well and that floating HA is not able to form the structural conformation responsible for the prosurvival effect.

#### **6.4.3 Alternative ligands for CD44?**

CD44 can bind various ECM components other than HA which all represent candidates as promoters of PC survival. When AC or iFB alone were removed using EDTA or triton in order to check the effect of AC-derived ECM on IgA<sup>+</sup> PC survival, no positive effect was observed on PC survival and IgA secretion (**Table 3**). However, I did not check for the actual presence of ECM in the EDTA/triton treated wells. In addition, ECM staining on 5 days-cultured AC revealed that ECM components (including Collagen IV, laminin, and fibronectin) do not form a clear extracellular network but seem instead to be restricted to the AC cell body (data not shown). This preliminary result suggests that ECM components are either not secreted, or more likely that they are strongly associated with AC, which then may mean that the ECM is removed with the AC. Therefore I have added commercially available collagen-I or fibronectin but they did not rescue IgA<sup>+</sup> PC on their own, indicating that they are not sufficient for PC survival (**Table 3**). Interestingly, culture of AC in fibronectin-coated wells induced a decrease of PDPN expression by iFB, either by selecting a PDPN<sup>lo</sup> iFB subset or by reducing the PDPN expression of iFB, and a decrease in IgA<sup>+</sup> PC survival (**Table 3**). Depending on what aspect of the AC culture fibronectin acts on, we can speculate that the PDPN<sup>lo</sup> iFB subset is more limited in promoting PC survival. Alternatively, fibronectin could have an impact on AC biology reducing, for example, the expression of PC survival factors such CD44 ligand or others.

## 6.5 IgA<sup>+</sup> PC homeostasis is impaired in CD44KO mice

CD44 is highly expressed during embryogenesis suggesting an important role of CD44 in early development. However, CD44KO are viable and fertile and do not exhibit any obvious phenotype. Although the development of the lymphoid system is not affected, CD44KO lymphoid cells exhibit an impaired homing to the thymus and pLN (Protin et al., 1999). Interestingly, the IgA response in the intestine of CD44KO mice has to the best of my knowledge not yet been studied. Despite the wide CD44 expression in the LP, I found a selective deficiency in IgA<sup>+</sup> PC numbers, but not in other immune cell types, with a reduction of about 40% as quantified by flow cytometry and histology in CD44KO relative to co-housed, sex/age-matched WT mice. The reduction in IgA<sup>+</sup> PC numbers was confirmed by a dramatic reduction of IgA in the feces. These findings suggest that CD44 is not essential as general homing molecule for LP cells coming from the blood, but that it may be having a limiting role particularly for IgA<sup>+</sup> PC homeostasis. Interestingly, IgG- and IgM-expressing PC numbers were unchanged in CD44KO SI, suggesting that neither their homing nor maintenance *in vivo* does require CD44. Consistent with those results, free IgG was unchanged in the gut lumen of CD44KO mice (data not shown). Unfortunately, the ELISA data for fecal IgM were unclear because they gave a surprisingly high background despite the use of two different strategies, not allowing me to correlate the IgM<sup>+</sup> PC number with the secreted IgM levels. As IgG<sup>+</sup> PC home preferentially to the BM, I also checked total IgG titers in the serum of CD44KO as a readout for the BM PC niche. Notably, IgG titers were normal in the CD44KO mouse serum at steady state, suggesting that IgG<sup>+</sup> PC have different requirement to survive, certainly in the LP, but presumably also in the BM (data not shown). In contrast to fecal free IgA, IgA titer in the serum of CD44KO mice was normal, similarly to IgG.

The reasons beyond this different sensibility to the lack of CD44 between IgA<sup>+</sup> PC and IgM/IgG<sup>+</sup> PC in SI are unknown as they all express CD44 on their surface (only LEC were CD44 negative in the LP). Although the precise CD44 MFI on IgM/IgG<sup>+</sup> PC was not assessed in this study, it appears that the CD44 expression level is not related to the phenotype observed in CD44KO mice. Indeed, myeloid cells, in particular eosinophils, display a higher CD44 MFI than IgA<sup>+</sup> PC (**Fig. 17D**), without being affected number wise in CD44KO SI. An alternative hypothesis could postulate that IgM/IgG<sup>+</sup> PC survival/retention or migration in the LP is actually CD44 independent and that their presence/maintenance in the SI is mainly mediated by

---

other unknown factors. This different need could translate into different regulations and functions for IgA<sup>+</sup> or IgM/IgG<sup>+</sup> PC in SI. In agreement with the concept of an alternative survival factor that allows IgG<sup>+</sup>/IgM<sup>+</sup> PC to survive despite the lack of CD44, Fedorchenko and colleague demonstrated that CD44 deficiency in murine B cell leukemia impaired the BCR kinase response (Fedorchenko et al., 2013). This finding is highly relevant for IgA<sup>+</sup> PC as they have been shown to maintain a functional IgA BCR on their surface in contrast to IgG<sup>+</sup> PC (Kamata et al., 2000; Pinto et al., 2013). Moreover, the survival of *ex vivo* IgA<sup>+</sup> PC isolated from human colon was increased followed by BCR stimulation *in vitro*, which was not the case of IgM<sup>+</sup> cells (even though they have a functional BCR as well) and for IgG<sup>+</sup> PC (Pinto et al., 2013). Therefore, it is tempting to speculate on the role of surface IgA BCR signaling in the differential maintenance of IgA<sup>+</sup> PC and IgG<sup>+</sup>/IgM<sup>+</sup> PC in the LP of WT and CD44KO mice. The CD44 independence of IgG<sup>+</sup>/IgM<sup>+</sup> PC could be assessed by KM201 treatment or by comparing survival of CD44KO and WT cells in our *in vitro* coculture assay.

As previously mentioned, IgA and IgG titers were found to be normal in the serum. This finding is particularly interesting knowing that a large proportion of BM PC are actually IgA<sup>+</sup> PC (Lemke et al., 2016; Mei et al., 2009; Youngman et al., 2002). These data suggest that the fecal and serum IgA source is physically separated in the LP and the BM, respectively, and that CD44 may not be essential for PC maintenance in the BM, independent of the isotype. This unanticipated geographical restriction of the CD44 sensitivity of IgA<sup>+</sup> PC adds another level of complexity to the biology of PC niches. These observations suggest that not only PC have differential needs for their survival, as discussed above, but also that the niches themselves provide different environments in the LP versus the BM. It remains to be seen how immunization-induced PC niches in the spleen and LN are affected by CD44 deficiency. However, it is important to mention that, so far, I have not investigated BM PC nor BM fibroblasts in detail. Therefore, further experiments are needed to confirm this potential difference in CD44 requirement between the LP and BM PC survival niche. Interestingly, a recent paper showed that gut-derived fibroblasts are better than splenic and BM-derived in inducing IgA<sup>+</sup> differentiation from BM derived B cells indicating that gut-derived fibroblasts are optimized in shaping the IgA response (Cen et al., 2018).

Unfortunately, we haven't been able to generate any evidence for a direct prosurvival role of CD44 *in vivo* and we cannot formally exclude that the reduction in IgA<sup>+</sup> PC in

the LP of the SI is due to an impaired IgA<sup>+</sup> PB/PC trafficking, migration or retention within the LP. To assess the prosurvival effect of a molecule or process, flow cytometric quantification of anti-apoptotic proteins such as MCL-1, AP-1, or Bcl2 is often used. However, we failed to generate such data for LN PC in settings of reduced niche numbers or reduced survival factors (Huang et al. 2018 unpublished data). Interestingly in chronic B lymphoid cell leukemia (CCL), IM7 treatment reduced CLL cell survival and MCL1 expression as measured by flow cytometry and western blot, respectively (Fedorchenko et al., 2013). The convincing data generated by western blot for the MCL-1 expression by Fedorchenko and colleagues suggests that similar experiment could be carried out on IgA<sup>+</sup> PC isolated and sorted from WT and CD44KO SI (Fedorchenko et al., 2013). Reduced MCL-1 expression in CD44KO IgA<sup>+</sup> PC would be consistent with an implication of CD44 in the survival of PC. Alternatively, to show directly an impairment of survival, I could examine the homing of IgA<sup>+</sup> PC. If we reason that B cell development and response are not impaired, as B cell subset analysis from PP suggest, one could imagine that IgA<sup>+</sup> PC will accumulate in other niches such as the BM if CD44 deficiency impacts their LP homing. Therefore, IgA<sup>+</sup> PC number and frequencies could be assessed in the BM, blood or spleen.

In the future, it may be worthwhile investigating the IgA<sup>+</sup> PC niche composition upon oral immunization or SI injury, and its dependence on CD44. Indeed, strong IgA responses as induced by administration of oral Ag, such as CT-OVA immunization (Lemke et al., 2016), could have an effect on the PC niche composition and the CD44 involvement as well as the intrinsic features of Ag-specific IgA<sup>+</sup> PC. Moreover, the role of APRIL and BAFF could be also further investigated *in vivo* at steady state and upon immunization, by using neutralizing antibodies to circumvent developmental effects. Indeed, CD44 deficiency led only to a 40% reduction of IgA<sup>+</sup> PC reduction *in vivo*, indicating that additional factors are involved. Furthermore, *April* and *baff* transcripts were enriched in iFB, BEC, and epithelial cells and could enhance the CD44 prosurvival effect. In agreement with these results, the density of the iFB network and their vicinity to IgA<sup>+</sup> PC, potentially through HA-CD44 interactions, as well as their strong production of various soluble PC factors make iFB an important component of the IgA<sup>+</sup> PC niche (**Fig. 22**).

## 6.6 General conclusions

In this study, we highlight the unique structural organization of iFB as well as their phenotypical and morphological heterogeneity using a collagen1 $\alpha$ 1-GFP reporter mice. We showed that iFB participate in the production of well-known PC survival factors such *april*, *baff*, and *cxcl12* *in vivo*. I found that iFB and M $\phi$  promote IgA<sup>+</sup> PC survival and function in a contact dependent manner requiring CD44 and most likely HA. The role of CD44 in the maintenance of IgA<sup>+</sup> PC homeostasis was further confirmed *in vivo* after characterization of CD44KO mice as compared with WT. These results leads to the identification of a new player in intestinal PC homeostasis that accumulate all the features of a PC survival niche cell, namely stability, abundance, direct and extensive physical contact, and source of major PC survival factors. Here, I propose a model of the IgA<sup>+</sup> PC niche present in the LP of the SI that combines my findings and current literature. In this niche, IgA<sup>+</sup> PC survival is mediated by the extensive contact between iFB and IgA<sup>+</sup> PC through CD44 and its ligands that include HA. CD44 binding to its ligand triggers intracellular signaling pathway within the PC regulating their survival. CD44 expression on iFB participate to this process indirectly maybe be by ensuring the close proximity between iFB and IgA<sup>+</sup> PC and/or by regulating the ligand conformation. Notably,  $\alpha_4$  might participate to the PC survival. Removal of the CD44 from this system results in a 40% reduction of the IgA<sup>+</sup> PC in SI, which suggests that other factors can participate in the niche formation or take over. Indeed, CXCL12 seems to be provided almost exclusively by iFB and is probably responsible for the PC migration and retention within the niche, which allow the CD44 engagement. iFB seem to be a major source of APRIL and BAFF as well. Combined with their proximity with IgA<sup>+</sup> PC, iFB could be a major player in the formation of the microenvironment rich in soluble PC survival factors. As previously known from the literature, epithelial cells constitute a rich source of APRIL and their omnipresence all around the villus help probably to concentrate a sufficient amount of this molecule at the edge of the niche. Finally BEC and LEC could complete this picture as they display an important expression of *april* and *baff* transcripts. In contrast to the dogma derived from other PC survival niche, myeloid cells do not seem to be a major source of soluble factors *in vivo* but rather act on IgA<sup>+</sup> PC through direct interaction. It is finally interesting to mention that this intestinal niche could react to its environment, which is most probably more dynamic than in

other niche such as the one in the BM or pLN, as the microbiota delivers constant stimulations.

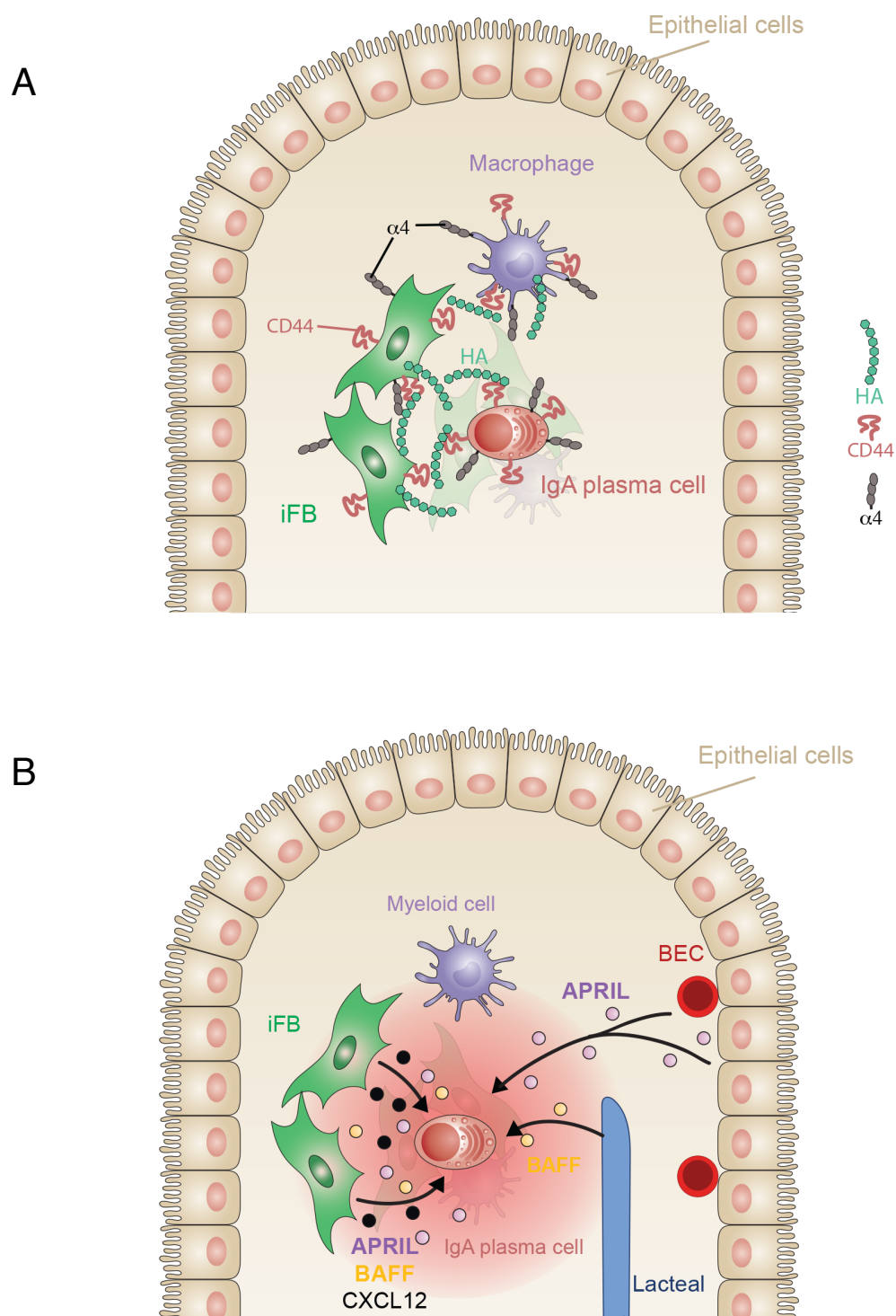


**Figure 22: IgA<sup>+</sup> PC survival niche model.** (A) iFB and macrophages are in contact with IgA<sup>+</sup> PC in the LP and promote their survival through a CD44-HA dependent manner. In this model iFB and macrophages are secreting HA.  $\alpha_4$  could complete this picture by strengthening the iFB - IgA<sup>+</sup> PC interaction and the CD44 intracellular signaling. (B) CD44 neutralization or CD44 deficiency does not abolish completely the PC survival indicating that additional factors are part of this niche. iFB could secrete also CXCL12, APRIL and BAFF, which attract and retain IgA<sup>+</sup> PC in the niche as well as promoting their survival. Epithelial cells contribute also to the APRIL secretion and participate to the formation of the PC niche rich in PC survival factors. BEC and LEC could also contribute to the formation of this survival niche by expressing APRIL and BAFF, respectively.

## 6.7 Contributions by others

**Jeremiah Latmani-Bernier (Petrova's lab)** collected, treated, and stained the SI and colon whole mount.

**Chen-Hing Yang** performed preliminary experiments on iLPC isolation and significantly optimized the debris/dead cell exclusion by flow cytometry from iLPC isolation. She performed half of the cell sorting for the transcript quantification of PC survival factor.

**Stefanie Siegert** introduced the Swiss role technique in the lab, performed PDPN staining shown in **Annex 1C**. She established several stainings in gut thin sections and whole mounts, including ICAM-1, colGFP, CD34, IgA, etc, stainings.

**Leonardo Scarpellino:** performed the RNA extraction and RT-qPCR for the PC survival factors. He performed the staining and the image acquisition of WT and CD44KO Peyer's patches and mLN.



## 7 Material and methods

**Mice.** WT C57BL/6 (B6) mice were obtained from Harlan Olac (Netherlands) and in part bred locally. Other B6 mice used in this thesis were bred locally and include Col.1 $\alpha$ 1-GFP transgenic mice (Yata et al., 2003), IL-6KO mice (Kopf et al., 1998), and CD44KO mice (Protin et al. 1999). All mice were maintained in specific pathogen free (SPF) conditions. Mice were used between 8 and 16 weeks old. For WT and CD44KO comparison, mice were co-housed for 3-4 weeks prior to analysis

**Intestinal cell isolation.** To isolate LP cells the second half of the small intestine (SI) corresponding to the second half of jejunum and the complete ileum was collected and flushed with cold PBS to remove feces and microbiota. PP as well as mesenteric fat tissues were removed and the SI was cut longitudinally, followed by cold PBS wash steps. The SI was then cut into 0.5-1cm pieces and incubated for 20min in 30ml DMEM medium (Gibco) containing 10 mM EDTA with gentle stirring at 37°C. Every 10min, the tubes were vigorously shaken to help remove epithelial cells and intraepithelial lymphocytes besides removing the remaining mucus and microbiota. Tissues were washed four times with cold PBS by vortexing and then keeping them on ice in complete DMEM containing 10%FCS, 1%HEPES, 1% Penicillin/Streptavidin and 1% Gentamicin (antibiotics) before the next step. Afterwards, the tissues were cut into approximately 1mm fine pieces and incubated for 20 min in digestion buffer containing DMEM, 2% FCS, Liberase TL (0.2mg/ml; Roche), DNase I (1 U/mL; Invitrogen), and 1% Gentamicin at 37°C with gentle stirring. In order to help the tissue dissociation, the pieces of intestine were mixed by pipetting up/down several times after 10 and 20min. Isolated cells in the supernatant were harvested and kept on ice with a 1/1 volume of complete DMEM until the end of the digestion process while 5ml of fresh digestion buffer were added on remaining tissue pieces. In total, three identical digestions were performed for the complete dissociation of the intestine. The obtained cell suspension was passed through a 40  $\mu$ m cell strainer, centrifuged for 6 min at 150g (at 4°C) before resuspending the cell pellet in complete DMEM medium for subsequent cell culture or in FACS buffer (PBS, 2% FCS, 2mM EDTA, 0.02% NaN<sub>3</sub>; for cell sorting experiments, we used a FACS buffer without NaN<sub>3</sub>) for flow cytometry analysis.

For the isolation of epithelium and intraepithelial lymphocytes, the second half of the SI was collected and flushed with cold PBS to remove feces. The small intestine was

then cut longitudinally, followed by cold PBS wash steps. Intestines were then cut into 1cm pieces and directly digested three times with the Liberase TL digestion mix as described above but without any prior EDTA treatment. The obtained cell suspension was passed through a 40  $\mu$ m cell strainer, spun down for 6 min at 150g at 4°C before resuspending the cell pellet in complete DMEM medium or FACS buffer.

For Peyer's patch (PP) cell isolation, three or four PP were collected from jejunum and ileum of the small intestine followed by cold PBS washing. PP were stretched out with needles to facilitate enzymatic dissociation. PP were then digested for 30 min in digestion buffer (Liberase TL mix as above) at 37°C with gentle stirring and pipetting every 10 min. Isolated cells were filtered through a 40  $\mu$ m cell strainer, spun down and resuspended in FACS buffer as described above

**Flow Cytometry and Cell Sorting.** Cells were incubated with Fc-block (anti-CD16/32) for 20min on ice and then stained with conjugated antibodies (listed in this table 5) in FACS buffer for 30min. Biotin-conjugated primary antibodies were detected with fluorochrome-coupled streptavidin (table 5). Dead cells were excluded using DAPI (Invitrogen) or Zombie Aqua kit (BioLegend). If needed, cells were fixed with 1% PFA for 1h or with BD Cytofix/Cytoperm kit for intracellular staining (BD Bioscience). Data were acquired on a LSRII (BD Biosystems) flow cytometer and analyzed with FlowJo (TreeStar) software. Cells were sorted with a FACSAria Ib flow cytometer, and collected directly in lysis buffer (RNeasy micro kit, Qiagen) for RNA isolation, or in complete DMEM for cell culture.

**iFB cell line generation.**  $2 \times 10^6$  isolated iLPC from the second half of the SI of a col-1 $\alpha$ 1-GFP mouse were cultured in 24 well plate in complete DMEM (Gibco/Invitrogen) completed with 10% FCS, 1%HEPES, 1% penicillin/streptavidin, and 1% gentamicin. Non-AC cells were removed 6 h later and remaining AC were cultured, in the same well, until they reached confluency (within 3-5 days). At this point, cells were detached using 2mM EDTA in PBS and replated in a new well (1/2). After 5-6 passages, no more myeloid cells were observed by microscopy or detected by flow cytometry leaving only purified proliferating iFB. The GFP-expressing iFB line was used at passage 15 for PC coculture or mRNA isolation.

---

**MACS Purification of AC and Plasma Cell purification.** For primary culture of ex vivo iFB, hematopoietic cells were depleted from isolated iLPC using  $\alpha$ CD45-coupled beads (Mojosort, Biolegend) while, for M $\phi$  primary culture, myeloid cells were enriched using biotinylated CD11b/CD11c antibodies followed by streptavidin-beads (Mojosort) labeling. Labeled iLPC were then passed through magnetic-activated cell sorting (MACS) columns for cell enrichment.  $1.5 \times 10^5$  CD45<sup>-</sup>iFB and CD11b<sup>+</sup>CD11c<sup>+</sup> myeloid cells obtained were cultured 5 days in complete DMEM in a 96 well plate. In the case of mixed adherent cells (AC) either  $6 \times 10^4$  purified iFB and  $8 \times 10^4$  CD11b<sup>+</sup>CD11c<sup>+</sup> myeloid cells were mixed before plating, or total isolated iLPC were cultured for 2h before washing out the non-AC.

Three different strategies were used to enrich or purify IgA plasma cells:

1. iLPC were depleted of AC by culturing them for 2 h in 10 cm dishes. Next, non-AC including IgA PC were collected by washing the culture dish and then either directly co-cultured with AC or (2).
2. In addition to strategy 1, CD19<sup>+</sup> naïve B cells were depleted from the non-AC mix using biotinylated  $\alpha$ CD19 antibody followed by streptavidin-beads and MACS depletion prior to co-culture.
3. IgA<sup>+</sup> PC were purified by FACS sorting using a gating strategy for live CD45<sup>+</sup>CD3 $\epsilon$ <sup>-</sup>CD19<sup>-</sup>CD11b<sup>lo</sup>CD11c<sup>lo</sup>IgA<sup>+</sup>FSC<sup>hi</sup> cells.

**IgA plasma cell co-culture.** Adherent feeder cells isolated from the SI LP, such as iFB, M $\phi$ , and/or AC, were cultured in a monolayer for 5 days to confluency before adding on top 10'000-20'000 enriched PC or 10'000 FACS-sorted PC. Note that the AC culture medium was not replaced for at least the two days before adding PC allowing potential AC-derived soluble factors to accumulate in the medium. For experiments involving neutralizing Ab treatments to target stromal molecules such as ICAM-1 (YN1/1.7.4, in house), VCAM-1 (M/K2.7, in house) or MadCAM-1 (Meca-367, BioXcell), AC were pretreated for 1h before adding PC, usually 10 $\mu$ g/ml if not indicated otherwise. For experiments neutralizing PC-derived molecules such as  $\alpha_L$  (M17/4, in house),  $\alpha_4$  (PS/2, in house) or CD44 (KM201, abcam), enriched PC were pretreated 1h at 4°C with these antibodies before adding them to the feeder cells. For experiments using recombinant proteins: these cytokines were added (10pg/ml) at the same time as PC. Co-cultures were performed during 24h. Surviving cells were harvested by gentle pipetting the cell layer after a 1mM EDTA treatment for 2min, stained using antibodies (table 5) and analyzed by flow cytometry. For IgA secretion

in the SN, the medium was gently collected before cell detachment and stored at -20°C for ulterior analysis.

**ELISA.** For quantification of IgA concentrations in the culture supernatant, feces or blood serum, flat-bottom 96-well MaxiSorp plates (Nunc) were coated with anti-IgA following the kit's instructions (Invitrogen). The following steps were performed according to manufacturer's protocols. For IgG and IgM ELISA, plates were coated with 0.2  $\mu\text{g}/\text{mL}$  of goat-anti mouse IgG1/2a/2b/3 or rat-anti-mouse IgM antibodies. Serial dilutions of samples were added for 2 h and bound antibody was detected with biotinylated goat anti-mouse IgM or IgG (Invitrogen) followed by HRP-conjugated streptavidin (Jackson). Color development using 3,3',5,5'-tetramethylbenzidine solution (Sigma) was measured at 450 nm with correction set at 550 nm.

**RT-qPCR.** RNA was isolated using the QIAGEN RNeasy Plus Micro Kit. First-strand cDNA synthesis, quantitative real-time PCR using Sybr-green, primers, and normalization using the housekeeping gene *hprt* were performed as described previously (Link A. et al. 2007) or shown in table 4.

**Immunofluorescence (IF) staining and imaging of thin sections.** Cryostat sections (8-10 $\mu\text{m}$ ) of OCT (Tissue-Tek, Sakura)-embedded intestine, PP, or mLN were collected on Superfrost/Plus glass slides (Fisher), then air dried overnight, fixed using ice-cold acetone for 10 min and rehydrated in PBS. Sections were quenched using 0.3%  $\text{H}_2\text{O}_2$  in PBS, blocked using 0.1% BSA and 1-4% animal serum in PBS. Staining was performed for 60 min at room temperature using antibodies listed in Table 6. Primary antibodies, if needed, were detected and visualized with secondary antibodies coupled to fluorochromes (Table 6). Images were acquired on a Zeiss Axio Imager ZL and treated with photoshop software (Adobe)

**Whole-mount staining and image acquisition.** Tissues from SI and colon were processed as previously described (Bernier-Latmani J. et al. 2015; Bernier-Latmani and Petrova 2016). Briefly, mice were perfused with 4% paraformaldehyde (PFA) by cardiac puncture. The small intestine was then quickly dissected in ice-cold PBS, cleaned, cut longitudinally, and pinned on silicon plates. Intestines were then fixed overnight at 4°C in 15% picric acid, 0.5% PFA, and 0.1 M sodium phosphate. Samples were washed 3 times in ice-cold PBS for 5 minutes and subsequently

---

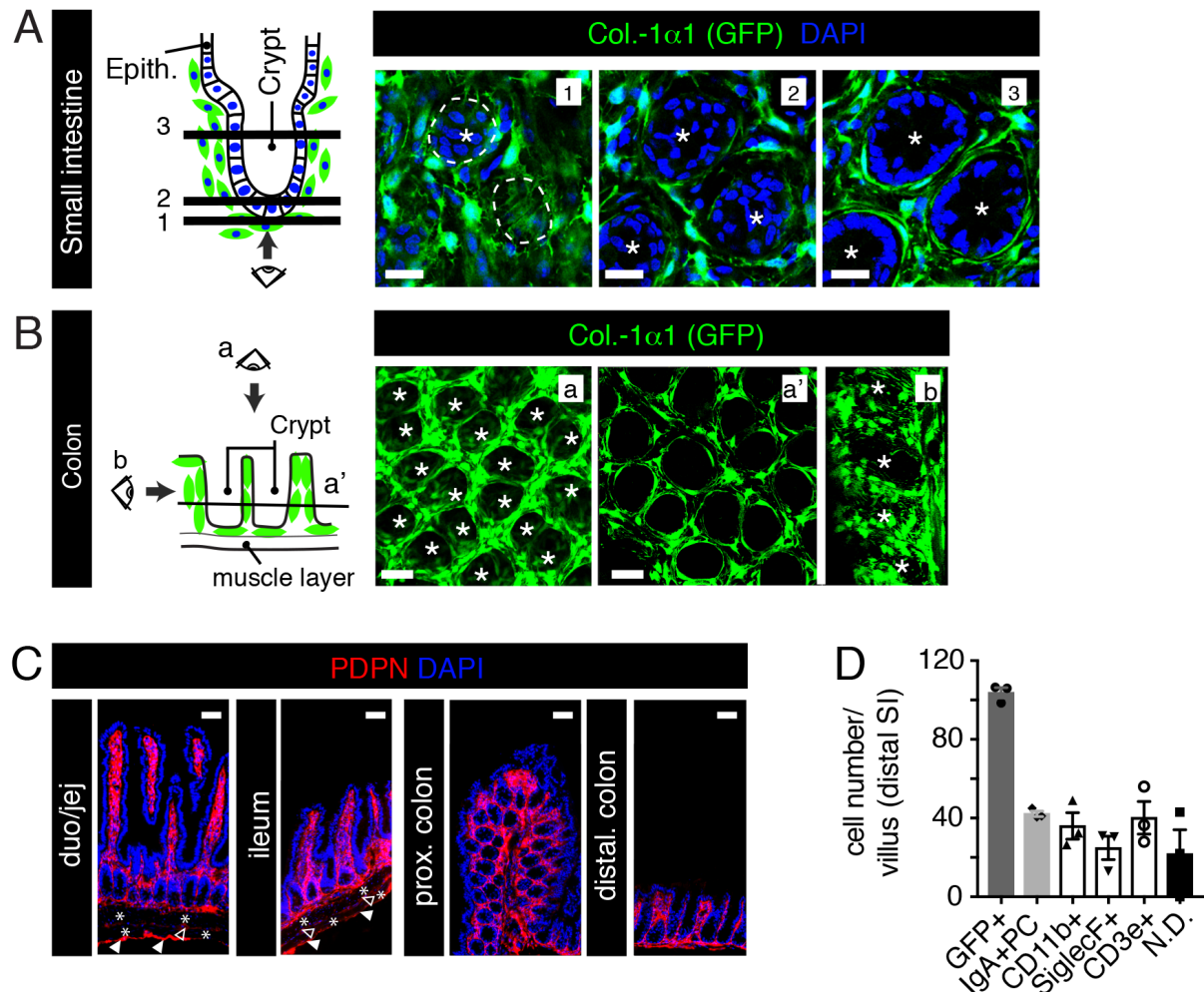
incubated for 3 hours with 10% sucrose in PBS and overnight in 20% sucrose along with 10% glycerol in PBS. Following the last wash step, samples were stored in 0.1% sodium azide in PBS. Epithelial cells were removed physically for whole mount immunostaining using a small stick. Confocal images were obtained using a Zeiss lsm 880 airyscan and analysed with Imaris (Bitplane), ImageJ, and photoshop (Adobe) software.

**Contact and cell number quantification on three-dimensional (3D) images from labeled whole mount samples.** Using high magnification 3D images of villi the contact of IgA plasma cells with neighboring cells was assessed by eye (Imaris and ImageJ). In some experiments, the colocalization tool of Imaris (Bitplane) was used to confirm iFB – PC contacts. DAPI staining was used to define the number of niche cells (neighbors) for a given PC. For cell number quantification, only cells within a villus were taken into account while pericryptal areas were excluded. The spot Imaris plugin was used to count automatically hematopoietic cells (IgA<sup>+</sup> PC, T cells, eosinophils, CD11b<sup>hi</sup> cells). The same technique was used for counting the number of nucleated DAPI<sup>+</sup> cells. For iFB quantification, colocalization of col-1 $\alpha$ 1-GFP with DAPI signals was investigated in order to identify fibroblast nuclei followed by the spot plugin to count them.

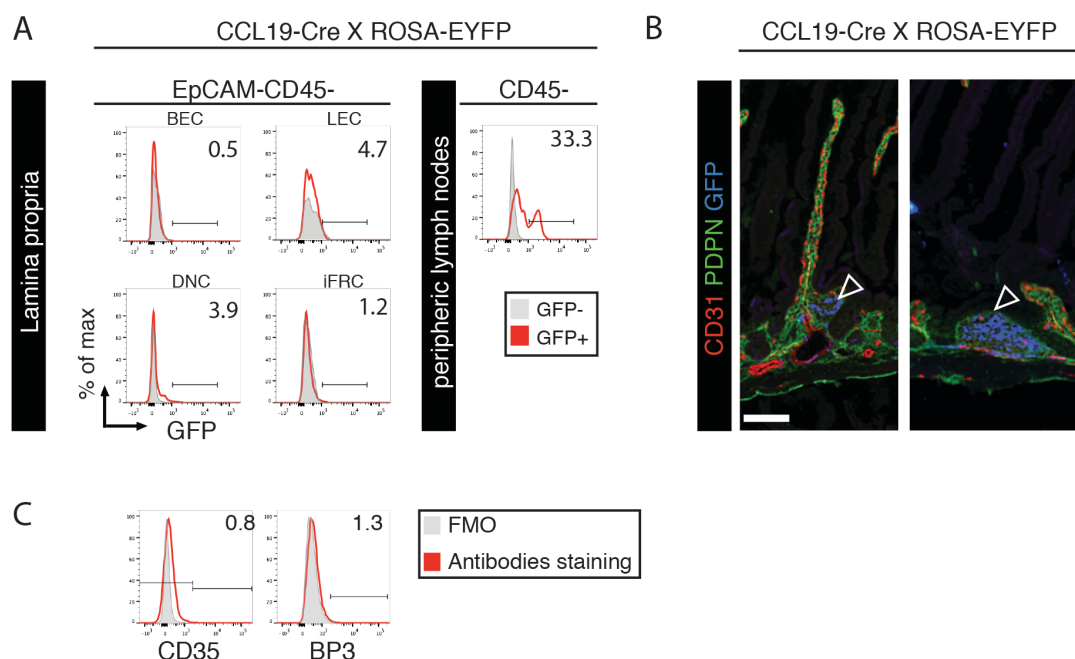
**Statistical analysis.** Two-tailed unpaired Student's t test or 1-way ANOVA tests were performed to determine statistical significance by calculating the probability of difference between two means, with a Bonferroni correction performed to account for multiple testing or Welch's correction to account for differences in variance where noted. P values are indicated as \* /# for  $p < 0.05$ , \*\* /## for  $p < 0.01$ , \*\*\* /### for  $p < 0.001$ , \*\*\*\* /#### for  $p < 0.0001$ , and ns for "statistically not significant.



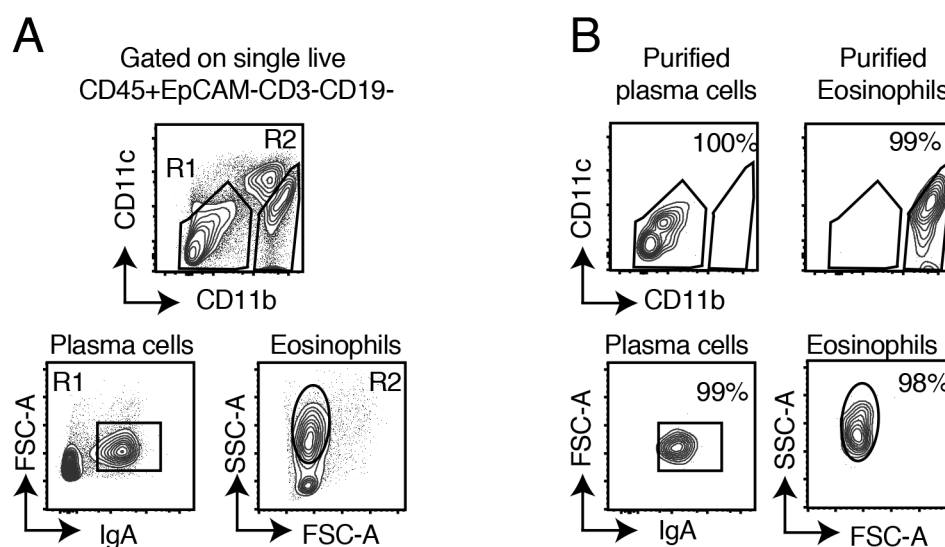
## 8 Annexes



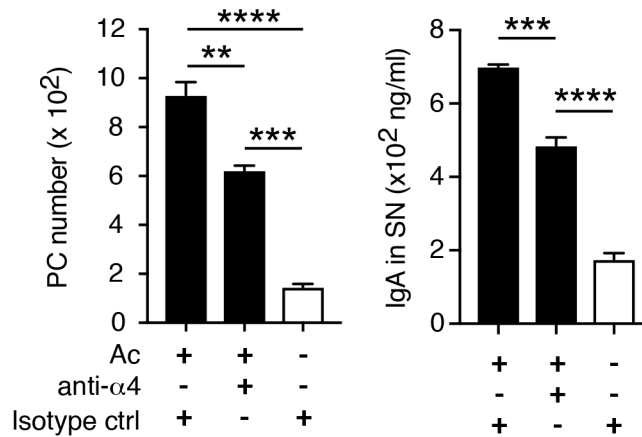
**Annex 1: iFB are present in villi and crypts of both the small intestine and colon, express pdpn and represent the most frequent cell type in the LP of the small intestine.** (A and B) Representative confocal microscope images of the intestine from adult collagen1 $\alpha$ 1-GFP (col-GFP) transgenic mice after epithelial layer elimination and whole-mount immunostaining. Drawings on left side indicate the point of view (eye) and the level of confocal imaging (black lines in A) relative to the intestinal structures with microscopic images shown on right side. (A) One villus in the SI imaged at three different depths of the pericryptal mucosa. Note that epithelial cells (DAPI<sup>+</sup>GFP<sup>+</sup>) were not successfully removed in the crypt due to their localization that protects them from physical stress. (B) Mucosa of the large intestine in top view of a 3D reconstruction of the whole large intestine wall (a) or a single optical section (a'); or in side view of a single optical section (b). Stars mark crypts. (C) PDPN (red) expression in the different parts of the gut, namely duodenum (duo)/ jejunum (jej), ileum, proximal and distal colon. Stars show the muscle layers of the muscularis, filled arrowheads point to the PDPN<sup>+</sup> external layer of the SI, probably the serosa, and empty arrowheads point the thin PDPN<sup>0</sup> space in between the two sublayers of the muscularis. (D) Absolute number of indicated cell types in the distal SI. N.D = identity of the cell (DAPI<sup>+</sup> nucleus) is unknown. This number was obtained after deduction of the known DAPI<sup>+</sup> cells. Thus total DAPI<sup>+</sup> - CD11b<sup>+</sup>/IgA<sup>+</sup>GFP<sup>+</sup> cells - CD3e<sup>+</sup> cells = N.D. cells. Images are representative for results observed in tissues from 3 mice (A, B) or 5 mice (C).



**Annex 2: iFB are distinct from pLN FRC in terms of CCL19-cre expression and certain fibroblast markers.** (A) Flow cytometric analysis of EYFP expression in stromal cell subsets from digested iLP of the SI or digested pLN isolated from a CCL19-Cre X ROSA-EYFP mouse. Intestinal cells were obtained after iLP digestion whereas FRC come from meshed pLN. Data of intestine are representative of one experiment, and pLN of several experiments. (B) Histological staining of EYFP, CD31 and pdpn in the SI of CCL19-Cre X ROSA-EYFP mice. Data are representative of two experiments from a single mouse. Scale bar: 50 $\mu$ m. (C) CD35 and BP3 expression on CD31<sup>+</sup>PDPN<sup>+</sup> iFB from the digested iLP of the SI. n=2



**Annex 3: Sorting of IgA<sup>+</sup> PC and eosinophils.** (A) Gating strategy used for flow cytometry sorting of intestinal PC and eosinophils. Single DAPI<sup>-</sup>CD45<sup>+</sup>EpCAM<sup>+</sup>CD3<sup>-</sup>CD19<sup>-</sup> cells were further subdivided according their CD11b and CD11c profile. All IgA<sup>+</sup> PC were found in the CD11b<sup>c<sup>-</sup>low</sup> gate (R1). The surface IgA and FSC-A<sup>hi</sup> phenotype (as compared to T cells) was then used to identify intestinal PC within the R1 gated population. Eosinophils display a CD11b<sup>+</sup>CD11c<sup>lo</sup> phenotype (R2) and show a unique SSC-A<sup>hi</sup> phenotype within the R2 gated population. The % indicates the level of purity. Preliminary experiments demonstrated that 99% of the cells identified by this eosinophil gating strategy are Siglec-F<sup>hi</sup> (not shown). (B) PC and eosinophil sorting efficiencies were checked by flow cytometry and reached at least 97% purity.



**Annex 4: The integrin  $\alpha_4$ -chain participates in the promotion of IgA<sup>+</sup> PC by iFB/monocytes *in vitro*.** Same protocol as used in fig. 17, culturing iLPC on top of Ac for 24h. iLPC were treated with isotype control (ctrl) Ab or 30  $\mu$ g/ml of anti- $\alpha_4$  Ab. IgA<sup>+</sup> PC survival and secreted levels of IgA were assessed by flow cytometry and ELISA, respectively. Data are representative of at least three independent experiments. n=3 mice.

**Annex - table 4: Primers used for RT-qPCR**

| Target        | Forward               | Reverse                 |
|---------------|-----------------------|-------------------------|
| <i>april</i>  | GGTGGTATCTCGGGAAGGAC  | CCCCTTGATGTAAATGAAAGACA |
| <i>baff</i>   | AGACGCGCTTCCAGGGACC   | TAGTCGGCGTGTGCGCTGTCTG  |
| <i>cxcl12</i> | TGCATCAGTGACGCTAAACCA | TTCTTCAGCCGTGCAACAATC   |

**Annex - table 5: Flow cytometry and MACS antibody list**

| Target         | Species      | Clone    | Conjugate    | Vendor      |
|----------------|--------------|----------|--------------|-------------|
| CD11b          | Rat          | M1/70    | Alexa 700    | eBioscience |
| CD11b          | Rat          | M1/70    | Biotin       | BioLegend   |
| CD11c          | Arm. Hamster | N418     | Biotin       | Home-made   |
| CD11c          | Arm. Hamster | N418     | PE-Cy5.5     | eBioscience |
| CD19           | Rat          | ID3      | Biotin       | Home-made   |
| CD19           | Rat          | ID3      | BV605        | BD Horizon  |
| CD3 $\epsilon$ | Arm. Hamster | 145-2C11 | Biotin       | eBioscience |
| CD3 $\epsilon$ | Arm. Hamster | 145-2C11 | FITC         | Home-made   |
| CD31 (PECAM-1) | Rat          | 390      | Pacific blue | BioLegend   |
| CD31 (PECAM-1) | Rat          | 390      | PE-Cy7       | BioLegend   |
| CD35 (CR1)     | Rat          | 8D9      | PE           | eBioscience |
| CD44           | Rat          | IM7      | FITC         | Home-made   |
| CD45pan        | Rat          | 30-F11   | APC-Cy7      | BioLegend   |

## Annexes

---

|                       |              |              |            |                  |
|-----------------------|--------------|--------------|------------|------------------|
| CD45pan               | Rat          | 30-F11       | PE-Cy7     | BioLegend        |
| B220 (CD45R)          | Rat          | RA3-6B2      | Alexa 700  | BioLegend        |
| EpCAM (CD326)         | Rat          | G8.8         | eFluor 450 | eBioscience      |
| ICAM-1 (CD54)         | Rat          | YN1/1.7.4    | Biotin     | Home-made        |
| IgA                   | Rat          | 11.44.2      | Biotin     | Southern Biotech |
| IgA                   | Rat          | 11.44.2      | FITC       | Southern Biotech |
| IgA                   | Rat          | 11.44.2      | PE         | Southern Biotech |
| IgD                   | Rat          | 11-26c       | FITC       | eBioscience      |
| IgM                   | Rat          | RMM-1        | APC        | BioLegend        |
| IgM                   | Rat          | RMM-1        | APC-Cy7    | BioLegend        |
| MadCAM-1              | Rat          | Meca-89      | Biotin     | eBioscience      |
| MHCII (I-A/I-E)       | Rat          | M5/114.1.5.2 | Alexa 647  | Home-made        |
| Podoplanin (gp38)     | Syr. Hamster | 8.1.1        | Alexa 647  | Home-made        |
| Podoplanin (gp38)     | Syr. Hamster | 8.1.1        | PE         | BioLegend        |
| Streptavidin          |              |              | Alexa 700  | Invitrogen       |
| Streptavidin          |              |              | APC        | BioLegend        |
| Streptavidin          |              |              | PE         | eBioscience      |
| Syndecan-1<br>(CD138) | Rat          | 281-2        | Biotin     | BD-Pharmingen    |
| TCR $\beta$           | Arm. Hamster | H57          | FITC       | Home-made        |
| Ter119                | Rat          | TER119       | BV650      | Biolegend        |
| VCAM-1(CD106)         | Rat          | M/K2.7       | Biotin     | eBioscience      |

---

---

**Annex - table 6: Histology antibody list**

| Target            | Species      | Clone or source | Conjugate | Vendor                    |
|-------------------|--------------|-----------------|-----------|---------------------------|
| $\alpha$ SMA      | Mouse        | 1A4             | Cy3       | Sigma                     |
| CD11b             | Rat          | M1/70           | None      | Home-made                 |
| CD3 $\epsilon$    | Arm. Hamster | 145-2C11        | None      | Home-made                 |
| CD31 (PECAM-1)    | Rat          | GC-51           | None      | Hybridoma                 |
| CD34              | Rat          | RAM34           | None      | eBioscience               |
| hCollagen I       | Goat         | Polyclonal      | None      | Southern Biotech          |
| ERTR7             | Rat          | ERTR7           | None      | BioXCell                  |
| GFP               | Rabbit       | Polyclonal      | None      | Invitrogen                |
| IgA               | Goat         | Polyclonal      | None      | Southern Biotech          |
| IgA               | Rat          | 11.44.2         | Biotin    | Southern Biotech          |
| Laminin           | Rabbit       | Polyclonal      | None      | Sigma                     |
| Podoplanin (gp38) | Syr. Hamster | 8.1.1           | None      | Home-made                 |
| Streptavidin      |              |                 | APC       | BioLegend                 |
| Rabbit IgG        | Donkey       |                 | Alexa 488 | Molecular probes          |
| Rat IgG           | Donkey       |                 | Cy3       | Jackson<br>ImmunoResearch |
| Goat IgG          | Donkey       |                 | APC       |                           |
| Arm. Hamster IgG  | Goat         |                 | Alexa 594 | BioLegend                 |

---



## 9 References

Agace, W.W., Amara, A., Roberts, A.I., Pablos, J.L., Thelen, S., Uguccioni, M., Li, X.Y., Marsal, J., Arenzana-Seisdedos, F., Delaunay, T., *et al.* (2000). Constitutive expression of stromal derived factor-1 by mucosal epithelia and its role in HIV transmission and propagation. *Curr Biol* *10*, 325-328.

Aghamohammadi, A., Cheraghi, T., Gharagozlou, M., Movahedi, M., Rezaei, N., Yeganeh, M., Parvaneh, N., Abolhassani, H., Pourpak, Z., and Moin, M. (2009). IgA deficiency: correlation between clinical and immunological phenotypes. *J Clin Immunol* *29*, 130-136.

Agren, U.M., Tammi, R.H., and Tammi, M.I. (1997). Reactive oxygen species contribute to epidermal hyaluronan catabolism in human skin organ culture. *Free Radic Biol Med* *23*, 996-1001.

Ahuja, A., Anderson, S.M., Khalil, A., and Shlomchik, M.J. (2008). Maintenance of the plasma cell pool is independent of memory B cells. *Proc Natl Acad Sci U S A* *105*, 4802-4807.

Alon, R., Kassner, P.D., Carr, M.W., Finger, E.B., Hemler, M.E., and Springer, T.A. (1995). The integrin VLA-4 supports tethering and rolling in flow on VCAM-1. *J Cell Biol* *128*, 1243-1253.

Aoki, R., Shoshkes-Carmel, M., Gao, N., Shin, S., May, C.L., Golson, M.L., Zahm, A.M., Ray, M., Wiser, C.L., Wright, C.V., and Kaestner, K.H. (2016). Foxl1-expressing mesenchymal cells constitute the intestinal stem cell niche. *Cell Mol Gastroenterol Hepatol* *2*, 175-188.

Baaten, B.J., Tinoco, R., Chen, A.T., and Bradley, L.M. (2012). Regulation of Antigen-Experienced T Cells: Lessons from the Quintessential Memory Marker CD44. *Front Immunol* *3*, 23.

Bain, C.C., and Mowat, A.M. (2014). The monocyte-macrophage axis in the intestine. *Cell Immunol* *291*, 41-48.

Barone, F., Patel, P., Sanderson, J.D., and Spencer, J. (2009). Gut-associated lymphoid tissue contains the molecular machinery to support T-cell-dependent and T-cell-independent class switch recombination. *Mucosal Immunol* *2*, 495-503.

Belnoue, E., Pihlgren, M., McGaha, T.L., Tougne, C., Rochat, A.F., Bossen, C., Schneider, P., Huard, B., Lambert, P.H., and Siegrist, C.A. (2008). APRIL is critical for plasmablast survival in the bone marrow and poorly expressed by early-life bone marrow stromal cells. *Blood* *111*, 2755-2764.

Belnoue, E., Tougne, C., Rochat, A.F., Lambert, P.H., Pinschewer, D.D., and Siegrist, C.A. (2012). Homing and adhesion patterns determine the cellular composition of the bone marrow plasma cell niche. *J Immunol* *188*, 1283-1291.

Bemark, M., Boysen, P., and Lycke, N.Y. (2012). Induction of gut IgA production through T cell-dependent and T cell-independent pathways. *Ann N Y Acad Sci* *1247*, 97-116.

Bergqvist, P., Gardby, E., Stensson, A., Bemark, M., and Lycke, N.Y. (2006). Gut IgA class switch recombination in the absence of CD40 does not occur in the lamina propria and is independent of germinal centers. *J Immunol* *177*, 7772-7783.

Bergqvist, P., Stensson, A., Lycke, N.Y., and Bemark, M. (2010). T cell-independent IgA class switch recombination is restricted to the GALT and occurs prior to manifest germinal center formation. *J Immunol* *184*, 3545-3553.

## References

---

- Bernasconi, N.L., Onai, N., and Lanzavecchia, A. (2003). A role for Toll-like receptors in acquired immunity: up-regulation of TLR9 by BCR triggering in naive B cells and constitutive expression in memory B cells. *Blood* *101*, 4500-4504.
- Bernasconi, N.L., Traggiai, E., and Lanzavecchia, A. (2002). Maintenance of serological memory by polyclonal activation of human memory B cells. *Science* *298*, 2199-2202.
- Bernier-Latmani, J., Cisarovsky, C., Demir, C.S., Bruand, M., Jaquet, M., Davanture, S., Ragusa, S., Siegert, S., Dormond, O., Benedito, R., *et al.* (2015). DLL4 promotes continuous adult intestinal lacteal regeneration and dietary fat transport. *J Clin Invest* *125*, 4572-4586.
- Bernier-Latmani, J., and Petrova, T.V. (2016). High-resolution 3D analysis of mouse small-intestinal stroma. *Nat Protoc* *11*, 1617-1629.
- Beswick, E.J., Johnson, J.R., Saada, J.I., Humen, M., House, J., Dann, S., Qiu, S., Brasier, A.R., Powell, D.W., Reyes, V.E., and Pinchuk, I.V. (2014). TLR4 activation enhances the PD-L1-mediated tolerogenic capacity of colonic CD90+ stromal cells. *J Immunol* *193*, 2218-2229.
- Bortnick, A., Chernova, I., Quinn, W.J., 3rd, Mugnier, M., Cancro, M.P., and Allman, D. (2012). Long-lived bone marrow plasma cells are induced early in response to T cell-independent or T cell-dependent antigens. *J Immunol* *188*, 5389-5396.
- Bortnick, A., Chernova, I., Spencer, S.P., and Allman, D. (2018). No strict requirement for eosinophils for bone marrow plasma cell survival. *Eur J Immunol* *48*, 815-821.
- Bracke, K.R., Dentener, M.A., Papakonstantinou, E., Vernooy, J.H., Demoor, T., Pauwels, N.S., Cleutjens, J., van Suylen, R.J., Joos, G.F., Brusselle, G.G., and Wouters, E.F. (2010). Enhanced deposition of low-molecular-weight hyaluronan in lungs of cigarette smoke-exposed mice. *Am J Respir Cell Mol Biol* *42*, 753-761.
- Bradley, J.E., Ramirez, G., and Hagood, J.S. (2009). Roles and regulation of Thy-1, a context-dependent modulator of cell phenotype. *Biofactors* *35*, 258-265.
- Brandtzaeg, P. (2009). Mucosal immunity: induction, dissemination, and effector functions. *Scand J Immunol* *70*, 505-515.
- Brandtzaeg, P. (2013). Secretory IgA: Designed for Anti-Microbial Defense. *Front Immunol* *4*, 222.
- Brandtzaeg, P., and Pabst, R. (2004). Let's go mucosal: communication on slippery ground. *Trends Immunol* *25*, 570-577.
- Camp, R.L., Kraus, T.A., and Pure, E. (1991). Variations in the cytoskeletal interaction and posttranslational modification of the CD44 homing receptor in macrophages. *J Cell Biol* *115*, 1283-1292.
- Carlens, J., Wahl, B., Ballmaier, M., Bulfone-Paus, S., Forster, R., and Pabst, O. (2009). Common gamma-chain-dependent signals confer selective survival of eosinophils in the murine small intestine. *J Immunol* *183*, 5600-5607.
- Cassese, G., Arce, S., Hauser, A.E., Lehnert, K., Moewes, B., Mostarac, M., Muehlinghaus, G., Szyska, M., Radbruch, A., and Manz, R.A. (2003). Plasma Cell Survival Is Mediated by Synergistic Effects of Cytokines and Adhesion-Dependent Signals. *The Journal of Immunology* *171*, 1684-1690.
- Castigli, E., Scott, S., Dedeoglu, F., Bryce, P., Jabara, H., Bhan, A.K., Mizoguchi, E., and Geha, R.S. (2004). Impaired IgA class switching in APRIL-deficient mice. *Proc Natl Acad Sci U S A* *101*, 3903-3908.

- 
- Castigli, E., Wilson, S.A., Scott, S., Dedeoglu, F., Xu, S., Lam, K.P., Bram, R.J., Jabara, H., and Geha, R.S. (2005). TACI and BAFF-R mediate isotype switching in B cells. *J Exp Med* *201*, 35-39.
- Cen, S.Y., Moreau, J.M., Furlonger, C., Berger, A., and Paige, C.J. (2018). Differential regulation of IgA(+) B cells in vitro by stromal cells from distinctive anatomical compartments. *J Leukoc Biol*.
- Cerutti, A., Cols, M., Gentile, M., Cassis, L., Barra, C.M., He, B., Puga, I., and Chen, K. (2011). Regulation of mucosal IgA responses: lessons from primary immunodeficiencies. *Ann N Y Acad Sci* *1238*, 132-144.
- Cheng, G., Swaidani, S., Sharma, M., Lauer, M.E., Hascall, V.C., and Aronica, M.A. (2011). Hyaluronan deposition and correlation with inflammation in a murine ovalbumin model of asthma. *Matrix Biol* *30*, 126-134.
- Choe, K., Jang, J.Y., Park, I., Kim, Y., Ahn, S., Park, D.Y., Hong, Y.K., Alitalo, K., Koh, G.Y., and Kim, P. (2015). Intravital imaging of intestinal lacteals unveils lipid drainage through contractility. *J Clin Invest* *125*, 4042-4052.
- Chu, V.T., Beller, A., Nguyen, T.T., Steinhauser, G., and Berek, C. (2011a). The long-term survival of plasma cells. *Scand J Immunol* *73*, 508-511.
- Chu, V.T., Beller, A., Rausch, S., Strandmark, J., Zanker, M., Arbach, O., Kruglov, A., and Berek, C. (2014). Eosinophils promote generation and maintenance of immunoglobulin-A-expressing plasma cells and contribute to gut immune homeostasis. *Immunity* *40*, 582-593.
- Chu, V.T., and Berek, C. (2012). Immunization induces activation of bone marrow eosinophils required for plasma cell survival. *Eur J Immunol* *42*, 130-137.
- Chu, V.T., Frohlich, A., Steinhauser, G., Scheel, T., Roch, T., Fillatreau, S., Lee, J.J., Lohning, M., and Berek, C. (2011b). Eosinophils are required for the maintenance of plasma cells in the bone marrow. *Nat Immunol* *12*, 151-159.
- Cismasiu, V.B., Radu, E., and Popescu, L.M. (2011). miR-193 expression differentiates telocytes from other stromal cells. *J Cell Mol Med* *15*, 1071-1074.
- Cooper, E.H. (1961). Production of lymphocytes and plasma cells in the rat following immunization with human serum albumin. *Immunology* *4*, 219-231.
- Corcoran, L.M., and Nutt, S.L. (2016). Long-Lived Plasma Cells Have a Sweet Tooth. *Immunity* *45*, 3-5.
- Cordeiro Gomes, A., Hara, T., Lim, V.Y., Herndler-Brandstetter, D., Nevius, E., Sugiyama, T., Tani-Ichi, S., Schlenner, S., Richie, E., Rodewald, H.R., *et al.* (2016). Hematopoietic Stem Cell Niches Produce Lineage-Instructive Signals to Control Multipotent Progenitor Differentiation. *Immunity* *45*, 1219-1231.
- Corthesy, B. (2013). Multi-faceted functions of secretory IgA at mucosal surfaces. *Front Immunol* *4*, 185.
- Cremasco, V., Woodruff, M.C., Onder, L., Cupovic, J., Nieves-Bonilla, J.M., Schildberg, F.A., Chang, J., Cremasco, F., Harvey, C.J., Wucherpfennig, K., *et al.* (2014). B cell homeostasis and follicle confines are governed by fibroblastic reticular cells. *Nat Immunol* *15*, 973-981.
- Cretoiu, D., Cretoiu, S.M., Simionescu, A.A., and Popescu, L.M. (2012). Telocytes, a distinct type of cell among the stromal cells present in the lamina propria of jejunum. *Histol Histopathol* *27*, 1067-1078.

## References

---

- Cullender, T.C., Chassaing, B., Janzon, A., Kumar, K., Muller, C.E., Werner, J.J., Angenent, L.T., Bell, M.E., Hay, A.G., Peterson, D.A., *et al.* (2013). Innate and adaptive immunity interact to quench microbiome flagellar motility in the gut. *Cell Host Microbe* *14*, 571-581.
- DiLillo, D.J., Hamaguchi, Y., Ueda, Y., Yang, K., Uchida, J., Haas, K.M., Kelsoe, G., and Tedder, T.F. (2008). Maintenance of long-lived plasma cells and serological memory despite mature and memory B cell depletion during CD20 immunotherapy in mice. *J Immunol* *180*, 361-371.
- Disson, O., Bleriot, C., Jacob, J.M., Serafini, N., Dulauroy, S., Jouvion, G., Fevre, C., Gessain, G., Thouvenot, P., Eberl, G., *et al.* (2018). Peyer's patch myeloid cells infection by *Listeria* signals through gp38(+) stromal cells and locks intestinal villus invasion. *J Exp Med* *215*, 2936-2954.
- Eckburg, P.B., Bik, E.M., Bernstein, C.N., Purdom, E., Dethlefsen, L., Sargent, M., Gill, S.R., Nelson, K.E., and Relman, D.A. (2005). Diversity of the human intestinal microbial flora. *Science* *308*, 1635-1638.
- Edwards, R.A., and Smock, A.Z. (2006). Defective arachidonate release and PGE2 production in Gi alpha2-deficient intestinal and colonic subepithelial myofibroblasts. *Inflamm Bowel Dis* *12*, 153-165.
- el Marjou, F., Janssen, K.P., Chang, B.H., Li, M., Hindie, V., Chan, L., Louvard, D., Chambon, P., Metzger, D., and Robine, S. (2004). Tissue-specific and inducible Cre-mediated recombination in the gut epithelium. *Genesis* *39*, 186-193.
- English, N.M., Lesley, J.F., and Hyman, R. (1998). Site-specific de-N-glycosylation of CD44 can activate hyaluronan binding, and CD44 activation states show distinct threshold densities for hyaluronan binding. *Cancer Res* *58*, 3736-3742.
- Estess, P., DeGrendele, H.C., Pascual, V., and Siegelman, M.H. (1998). Functional activation of lymphocyte CD44 in peripheral blood is a marker of autoimmune disease activity. *J Clin Invest* *102*, 1173-1182.
- Fadlallah, J., El Kafsi, H., Sterlin, D., Juste, C., Parizot, C., Dorgham, K., Autaa, G., Gouas, D., Almeida, M., Lepage, P., *et al.* (2018). Microbial ecology perturbation in human IgA deficiency. *Sci Transl Med* *10*.
- Fagarasan, S., Kawamoto, S., Kanagawa, O., and Suzuki, K. (2010). Adaptive immune regulation in the gut: T cell-dependent and T cell-independent IgA synthesis. *Annu Rev Immunol* *28*, 243-273.
- Fagarasan, S., Kinoshita, K., Muramatsu, M., Ikuta, K., and Honjo, T. (2001). In situ class switching and differentiation to IgA-producing cells in the gut lamina propria. *Nature* *413*, 639-643.
- Fagarasan, S., Muramatsu, M., Suzuki, K., Nagaoka, H., Hiai, H., and Honjo, T. (2002). Critical roles of activation-induced cytidine deaminase in the homeostasis of gut flora. *Science* *298*, 1424-1427.
- Fedorchenko, O., Stiefelhagen, M., Peer-Zada, A.A., Barthel, R., Mayer, P., Ecke, L., Breuer, A., Crispatzu, G., Rosen, N., Landwehr, T., *et al.* (2013). CD44 regulates the apoptotic response and promotes disease development in chronic lymphocytic leukemia. *Blood* *121*, 4126-4136.
- Ferrari, S., Giliani, S., Insalaco, A., Al-Ghonaïm, A., Soresina, A.R., Loubser, M., Avanzini, M.A., Marconi, M., Badolato, R., Ugazio, A.G., *et al.* (2001). Mutations of CD40 gene cause

---

an autosomal recessive form of immunodeficiency with hyper IgM. *Proc Natl Acad Sci U S A* *98*, 12614-12619.

Fletcher, A.L., Acton, S.E., and Knoblich, K. (2015). Lymph node fibroblastic reticular cells in health and disease. *Nat Rev Immunol* *15*, 350-361.

Fooksman, D.R., Nussenzweig, M.C., and Dustin, M.L. (2014). Myeloid cells limit production of antibody-secreting cells after immunization in the lymph node. *J Immunol* *192*, 1004-1012.

Foote, J.B., Mahmoud, T.I., Vale, A.M., and Kearney, J.F. (2012). Long-term maintenance of polysaccharide-specific antibodies by IgM-secreting cells. *J Immunol* *188*, 57-67.

Forman, R., Bramhall, M., Logunova, L., Svensson-Frej, M., Cruickshank, S.M., and Else, K.J. (2016). Eosinophils may play regionally disparate roles in influencing IgA(+) plasma cell numbers during large and small intestinal inflammation. *BMC Immunol* *17*, 12.

Furuya, S., and Furuya, K. (2007). Subepithelial fibroblasts in intestinal villi: roles in intercellular communication. *Int Rev Cytol* *264*, 165-223.

Ganusov, V.V., and De Boer, R.J. (2007). Do most lymphocytes in humans really reside in the gut? *Trends Immunol* *28*, 514-518.

Garrett, W.S., Gordon, J.I., and Glimcher, L.H. (2010). Homeostasis and inflammation in the intestine. *Cell* *140*, 859-870.

Geffroy-Luseau, A., Jego, G., Bataille, R., Campion, L., and Pellat-Deceunynck, C. (2008). Osteoclasts support the survival of human plasma cells in vitro. *Int Immunol* *20*, 775-782.

Glatman Zaretsky, A., Konradt, C., Depis, F., Wing, J.B., Goenka, R., Atria, D.G., Silver, J.S., Cho, S., Wolf, A.I., Quinn, W.J., *et al.* (2017). T Regulatory Cells Support Plasma Cell Populations in the Bone Marrow. *Cell Rep* *18*, 1906-1916.

Gomariz, A., Helbling, P.M., Isringhausen, S., Suessbier, U., Becker, A., Boss, A., Nagasawa, T., Paul, G., Goksel, O., Szekely, G., *et al.* (2018). Quantitative spatial analysis of haematopoiesis-regulating stromal cells in the bone marrow microenvironment by 3D microscopy. *Nat Commun* *9*, 2532.

Goodison, S., Urquidi, V., and Tarin, D. (1999). CD44 cell adhesion molecules. *Mol Pathol* *52*, 189-196.

Greicius, G., Kabiri, Z., Sigmundsson, K., Liang, C., Bunte, R., Singh, M.K., and Virshup, D.M. (2018). PDGFRalpha(+) pericryptal stromal cells are the critical source of Wnts and RSPO3 for murine intestinal stem cells in vivo. *Proc Natl Acad Sci U S A* *115*, E3173-E3181.

Gross, M., Salame, T.M., and Jung, S. (2015). Guardians of the Gut - Murine Intestinal Macrophages and Dendritic Cells. *Front Immunol* *6*, 254.

Gustafson, C.E., Higbee, D., Yeckes, A.R., Wilson, C.C., De Zoeten, E.F., Jedlicka, P., and Janoff, E.N. (2014). Limited expression of APRIL and its receptors prior to intestinal IgA plasma cell development during human infancy. *Mucosal Immunol* *7*, 467-477.

Haase, A.T. (2005). Perils at mucosal front lines for HIV and SIV and their hosts. *Nature Reviews Immunology* *5*, 783-792.

Haberland, K., Ackermann, J.A., Ipseiz, N., Culemann, S., Pracht, K., Englbrecht, M., Jack, H.M., Schett, G., Schuh, W., and Kronke, G. (2018). Eosinophils are not essential for maintenance of murine plasma cells in the bone marrow. *Eur J Immunol* *48*, 822-828.

## References

---

- Hapfelmeier, S., Lawson, M.A., Slack, E., Kirundi, J.K., Stoel, M., Heikenwalder, M., Cahenzli, J., Velykoredko, Y., Balmer, M.L., Endt, K., *et al.* (2010). Reversible microbial colonization of germ-free mice reveals the dynamics of IgA immune responses. *Science* *328*, 1705-1709.
- Harada, H., and Takahashi, M. (2007). CD44-dependent intracellular and extracellular catabolism of hyaluronic acid by hyaluronidase-1 and -2. *J Biol Chem* *282*, 5597-5607.
- Hargreaves, D.C., Hyman, P.L., Lu, T.T., Ngo, V.N., Bidgol, A., Suzuki, G., Zou, Y.R., Littman, D.R., and Cyster, J.G. (2001). A coordinated change in chemokine responsiveness guides plasma cell movements. *J Exp Med* *194*, 45-56.
- Harriman, G.R., Bogue, M., Rogers, P., Finegold, M., Pacheco, S., Bradley, A., Zhang, Y., and Mbawuike, I.N. (1999). Targeted deletion of the IgA constant region in mice leads to IgA deficiency with alterations in expression of other Ig isotypes. *J Immunol* *162*, 2521-2529.
- He, B., Santamaria, R., Xu, W., Cols, M., Chen, K., Puga, I., Shan, M., Xiong, H., Bussel, J.B., Chiu, A., *et al.* (2010). The transmembrane activator TACI triggers immunoglobulin class switching by activating B cells through the adaptor MyD88. *Nat Immunol* *11*, 836-845.
- He, B., Xu, W., Santini, P.A., Polydorides, A.D., Chiu, A., Estrella, J., Shan, M., Chadburn, A., Villanacci, V., Plebani, A., *et al.* (2007). Intestinal bacteria trigger T cell-independent immunoglobulin A(2) class switching by inducing epithelial-cell secretion of the cytokine APRIL. *Immunity* *26*, 812-826.
- Hebel, K., Griewank, K., Inamine, A., Chang, H.D., Muller-Hilke, B., Fillatreau, S., Manz, R.A., Radbruch, A., and Jung, S. (2006). Plasma cell differentiation in T-independent type 2 immune responses is independent of CD11c(high) dendritic cells. *Eur J Immunol* *36*, 2912-2919.
- Holzwarth, K., Kohler, R., Philipsen, L., Tokoyoda, K., Ladyhina, V., Wahlby, C., Niesner, R.A., and Hauser, A.E. (2018). Multiplexed fluorescence microscopy reveals heterogeneity among stromal cells in mouse bone marrow sections. *Cytometry A* *93*, 876-888.
- Hooper, L.V., Littman, D.R., and Macpherson, A.J. (2012). Interactions between the microbiota and the immune system. *Science* *336*, 1268-1273.
- Horneland, R., Paulsen, V., Lindahl, J.P., Grzyb, K., Eide, T.J., Lundin, K., Aabakken, L., Jenssen, T., Aandahl, E.M., Foss, A., and Oyen, O. (2015). Pancreas transplantation with enteroanastomosis to native duodenum poses technical challenges--but offers improved endoscopic access for scheduled biopsies and therapeutic interventions. *Am J Transplant* *15*, 242-250.
- Huang, H.Y., Rivas-Caicedo, A., Renevey, F., Cannelle, H., Peranzoni, E., Scarpellino, L., Hardie, D.L., Pommier, A., Schaeuble, K., Favre, S., *et al.* (2018). Identification of a new subset of lymph node stromal cells involved in regulating plasma cell homeostasis. *Proc Natl Acad Sci U S A* *115*, E6826-E6835.
- Huard, B., McKee, T., Bosshard, C., Durual, S., Matthes, T., Myit, S., Donze, O., Frossard, C., Chizzolini, C., Favre, C., *et al.* (2008). APRIL secreted by neutrophils binds to heparan sulfate proteoglycans to create plasma cell niches in human mucosa. *J Clin Invest* *118*, 2887-2895.
- Ingold, K., Zumsteg, A., Tardivel, A., Huard, B., Steiner, Q.G., Cachero, T.G., Qiang, F., Gorelik, L., Kalled, S.L., Acha-Orbea, H., *et al.* (2005). Identification of proteoglycans as the APRIL-specific binding partners. *J Exp Med* *201*, 1375-1383.
- Ishiwatari-Hayasaka, H., Fujimoto, T., Osawa, T., Hiramata, T., Toyama-Sorimachi, N., and Miyasaka, M. (1999). Requirements for signal delivery through CD44: analysis using CD44-Fas chimeric proteins. *J Immunol* *163*, 1258-1264.

---

Itano, N. (2008). Simple primary structure, complex turnover regulation and multiple roles of hyaluronan. *J Biochem* 144, 131-137.

Itano, N., and Kimata, K. (2008). Altered hyaluronan biosynthesis in cancer progression. *Semin Cancer Biol* 18, 268-274.

Itano, N., Zhuo, L., and Kimata, K. (2008). Impact of the hyaluronan-rich tumor microenvironment on cancer initiation and progression. *Cancer Sci* 99, 1720-1725.

Ivanov, I.I., Atarashi, K., Manel, N., Brodie, E.L., Shima, T., Karaoz, U., Wei, D., Goldfarb, K.C., Santee, C.A., Lynch, S.V., *et al.* (2009). Induction of intestinal Th17 cells by segmented filamentous bacteria. *Cell* 139, 485-498.

Jacobsen, K., Kravitz, J., Kincade, P.W., and Osmond, D.G. (1996). Adhesion receptors on bone marrow stromal cells: in vivo expression of vascular cell adhesion molecule-1 by reticular cells and sinusoidal endothelium in normal and gamma-irradiated mice. *Blood* 87, 73-82.

Johansson, M.E., and Hansson, G.C. (2013). Mucus and the goblet cell. *Dig Dis* 31, 305-309.  
Johansson, M.E., Sjovall, H., and Hansson, G.C. (2013). The gastrointestinal mucus system in health and disease. *Nat Rev Gastroenterol Hepatol* 10, 352-361.

Jorgensen, G.H., Gardulf, A., Sigurdsson, M.I., Sigurdardottir, S.T., Thorsteinsdottir, I., Gudmundsson, S., Hammarstrom, L., and Ludviksson, B.R. (2013). Clinical symptoms in adults with selective IgA deficiency: a case-control study. *J Clin Immunol* 33, 742-747.

Jourdan, M., Cren, M., Robert, N., Bollore, K., Fest, T., Duperray, C., Guilloton, F., Hose, D., Tarte, K., and Klein, B. (2014). IL-6 supports the generation of human long-lived plasma cells in combination with either APRIL or stromal cell-soluble factors. *Leukemia* 28, 1647-1656.

Jung, Y., Wen, T., Mingler, M.K., Caldwell, J.M., Wang, Y.H., Chaplin, D.D., Lee, E.H., Jang, M.H., Woo, S.Y., Seoh, J.Y., *et al.* (2015). IL-1beta in eosinophil-mediated small intestinal homeostasis and IgA production. *Mucosal Immunol* 8, 930-942.

Kamata, T., Nogaki, F., Fagarasan, S., Sakiyama, T., Kobayashi, I., Miyawaki, S., Ikuta, K., Muso, E., Yoshida, H., Sasayama, S., and Honjo, T. (2000). Increased frequency of surface IgA-positive plasma cells in the intestinal lamina propria and decreased IgA excretion in hyper IgA (HIGA) mice, a murine model of IgA nephropathy with hyperserum IgA. *J Immunol* 165, 1387-1394.

Kanamori, Y., Ishimaru, K., Nanno, M., Maki, K., Ikuta, K., Nariuchi, H., and Ishikawa, H. (1996). Identification of novel lymphoid tissues in murine intestinal mucosa where clusters of c-kit+ IL-7R+ Thy1+ lympho-hemopoietic progenitors develop. *J Exp Med* 184, 1449-1459.

Kato, L.M., Kawamoto, S., Maruya, M., and Fagarasan, S. (2014a). Gut TFH and IgA: key players for regulation of bacterial communities and immune homeostasis. *Immunol Cell Biol* 92, 49-56.

Kato, L.M., Kawamoto, S., Maruya, M., and Fagarasan, S. (2014b). The role of the adaptive immune system in regulation of gut microbiota. *Immunol Rev* 260, 67-75.

Katsenelson, N., Kanswal, S., Puig, M., Mostowski, H., Verthelyi, D., and Akkoyunlu, M. (2007). Synthetic CpG oligodeoxynucleotides augment BAFF- and APRIL-mediated immunoglobulin secretion. *Eur J Immunol* 37, 1785-1795.

Keim, C., Kazadi, D., Rothschild, G., and Basu, U. (2013). Regulation of AID, the B-cell genome mutator. *Genes Dev* 27, 1-17.

## References

---

Knoop, K.A., and Newberry, R.D. (2012). Isolated Lymphoid Follicles are Dynamic Reservoirs for the Induction of Intestinal IgA. *Front Immunol* 3, 84.

Kometani, K., and Kurosaki, T. (2015). Differentiation and maintenance of long-lived plasma cells. *Curr Opin Immunol* 33, 64-69.

Komuro, T. (1985). Fenestrations of the basal lamina of intestinal villi of the rat. Scanning and transmission electron microscopy. *Cell Tissue Res* 239, 183-188.

Korn, T., Bettelli, E., Oukka, M., and Kuchroo, V.K. (2009). IL-17 and Th17 Cells. *Annu Rev Immunol* 27, 485-517.

Koskinen, S. (1996). Long-term follow-up of health in blood donors with primary selective IgA deficiency. *J Clin Immunol* 16, 165-170.

Krause, P., Morris, V., Greenbaum, J.A., Park, Y., Bjoerheden, U., Mikulski, Z., Muffley, T., Shui, J.W., Kim, G., Cheroutre, H., *et al.* (2015). IL-10-producing intestinal macrophages prevent excessive antibacterial innate immunity by limiting IL-23 synthesis. *Nat Commun* 6, 7055.

Kucharzik, T., Lugering, N., Rautenberg, K., Lugering, A., Schmidt, M.A., Stoll, R., and Domschke, W. (2000). Role of M cells in intestinal barrier function. *Ann N Y Acad Sci* 915, 171-183.

Kunisawa, J., Gohda, M., Hashimoto, E., Ishikawa, I., Higuchi, M., Suzuki, Y., Goto, Y., Panea, C., Ivanov, I., Sumiya, R., *et al.* (2013). Microbe-dependent CD11b<sup>+</sup> IgA<sup>+</sup> plasma cells mediate robust early-phase intestinal IgA responses in mice. *Nat Commun* 4, 1772.

Landsverk, O.J., Snir, O., Casado, R.B., Richter, L., Mold, J.E., Reu, P., Horneland, R., Paulsen, V., Yaqub, S., Aandahl, E.M., *et al.* (2017). Antibody-secreting plasma cells persist for decades in human intestine. *J Exp Med* 214, 309-317.

Laurent, U.B., Dahl, L.B., and Reed, R.K. (1991). Catabolism of hyaluronan in rabbit skin takes place locally, in lymph nodes and liver. *Exp Physiol* 76, 695-703.

LeBleu, V.S., Taduri, G., O'Connell, J., Teng, Y., Cooke, V.G., Woda, C., Sugimoto, H., and Kalluri, R. (2013). Origin and function of myofibroblasts in kidney fibrosis. *Nat Med* 19, 1047-1053.

Lefebvre, D.C., Lai, J.C., Maeshima, N., Ford, J.L., Wong, A.S., Cross, J.L., and Johnson, P. (2010). CD44 interacts directly with Lck in a zinc-dependent manner. *Mol Immunol* 47, 1882-1889.

Lemke, A., Kraft, M., Roth, K., Riedel, R., Lammerding, D., and Hauser, A.E. (2016). Long-lived plasma cells are generated in mucosal immune responses and contribute to the bone marrow plasma cell pool in mice. *Mucosal Immunol* 9, 83-97.

Lesley, J., Hyman, R., and Kincade, P.W. (1993a). CD44 and its interaction with extracellular matrix. *Adv Immunol* 54, 271-335.

Lesley, J., Kincade, P.W., and Hyman, R. (1993b). Antibody-induced activation of the hyaluronan receptor function of CD44 requires multivalent binding by antibody. *Eur J Immunol* 23, 1902-1909.

Lesley, J., Schulte, R., and Hyman, R. (1990). Binding of hyaluronic acid to lymphoid cell lines is inhibited by monoclonal antibodies against Pgp-1. *Exp Cell Res* 187, 224-233.

---

Ley, K., Laudanna, C., Cybulsky, M.I., and Nourshargh, S. (2007). Getting to the site of inflammation: the leukocyte adhesion cascade updated. *Nat Rev Immunol* 7, 678-689.

Link, A., Vogt, T.K., Favre, S., Britschgi, M.R., Acha-Orbea, H., Hinz, B., Cyster, J.G., and Luther, S.A. (2007). Fibroblastic reticular cells in lymph nodes regulate the homeostasis of naive T cells. *Nat Immunol* 8, 1255-1265.

Litinskiy, M.B., Nardelli, B., Hilbert, D.M., He, B., Schaffer, A., Casali, P., and Cerutti, A. (2002). DCs induce CD40-independent immunoglobulin class switching through BlyS and APRIL. *Nat Immunol* 3, 822-829.

Lorenz, R.G., Chaplin, D.D., McDonald, K.G., McDonough, J.S., and Newberry, R.D. (2003). Isolated lymphoid follicle formation is inducible and dependent upon lymphotoxin-sufficient B lymphocytes, lymphotoxin beta receptor, and TNF receptor I function. *J Immunol* 170, 5475-5482.

Ludvigsson, J.F., Neovius, M., and Hammarstrom, L. (2014a). Association between IgA deficiency & other autoimmune conditions: a population-based matched cohort study. *J Clin Immunol* 34, 444-451.

Ludvigsson, J.F., Neovius, M., Stephansson, O., and Hammarstrom, L. (2014b). IgA deficiency, autoimmunity & pregnancy: a population-based matched cohort study. *J Clin Immunol* 34, 853-863.

Luther, S.A., Tang, H.L., Hyman, P.L., Farr, A.G., and Cyster, J.G. (2000). Coexpression of the chemokines ELC and SLC by T zone stromal cells and deletion of the ELC gene in the *plt/plt* mouse. *Proc Natl Acad Sci U S A* 97, 12694-12699.

Lycke, N., Erlandsson, L., Ekman, L., Schon, K., and Leanderson, T. (1999). Lack of J chain inhibits the transport of gut IgA and abrogates the development of intestinal antitoxic protection. *J Immunol* 163, 913-919.

Lycke, N.Y., and Bemark, M. (2017). The regulation of gut mucosal IgA B-cell responses: recent developments. *Mucosal Immunol* 10, 1361-1374.

Macpherson, A.J., Gatto, D., Sainsbury, E., Harriman, G.R., Hengartner, H., and Zinkernagel, R.M. (2000). A primitive T cell-independent mechanism of intestinal mucosal IgA responses to commensal bacteria. *Science* 288, 2222-2226.

Macpherson, A.J., Lamarre, A., McCoy, K., Harriman, G.R., Odermatt, B., Dougan, G., Hengartner, H., and Zinkernagel, R.M. (2001). IgA production without mu or delta chain expression in developing B cells. *Nat Immunol* 2, 625-631.

Macpherson, A.J., McCoy, K.D., Johansen, F.E., and Brandtzaeg, P. (2008). The immune geography of IgA induction and function. *Mucosal Immunol* 1, 11-22.

Mahapatro, M., Foersch, S., Hefele, M., He, G.W., Giner-Ventura, E., McHedlidze, T., Kindermann, M., Vetrano, S., Danese, S., Gunther, C., *et al.* (2016). Programming of Intestinal Epithelial Differentiation by IL-33 Derived from Pericryptal Fibroblasts in Response to Systemic Infection. *Cell Rep* 15, 1743-1756.

Makela, O., and Nossal, G.J. (1962). Autoradiographic studies on the immune response. II. DNA synthesis amongst single antibody-producing cells. *J Exp Med* 115, 231-244.

Mantis, N.J., Rol, N., and Corthesy, B. (2011). Secretory IgA's complex roles in immunity and mucosal homeostasis in the gut. *Mucosal Immunol* 4, 603-611.

## References

---

- Manz, R.A., Thiel, A., and Radbruch, A. (1997). Lifetime of plasma cells in the bone marrow. *Nature* *388*, 133-134.
- Marhaba, R., Freyschmidt-Paul, P., and Zoller, M. (2006). In vivo CD44-CD49d complex formation in autoimmune disease has consequences on T cell activation and apoptosis resistance. *Eur J Immunol* *36*, 3017-3032.
- Martinez-Gallo, M., Radigan, L., Almejun, M.B., Martinez-Pomar, N., Matamoros, N., and Cunningham-Rundles, C. (2013). TACI mutations and impaired B-cell function in subjects with CVID and healthy heterozygotes. *J Allergy Clin Immunol* *131*, 468-476.
- Mattioli, C.A., and Tomasi, T.B., Jr. (1973). The life span of IgA plasma cells from the mouse intestine. *J Exp Med* *138*, 452-460.
- Maynard, C.L., and Weaver, C.T. (2008). Diversity in the contribution of interleukin-10 to T-cell-mediated immune regulation. *Immunol Rev* *226*, 219-233.
- McKallip, R.J., Do, Y., Fisher, M.T., Robertson, J.L., Nagarkatti, P.S., and Nagarkatti, M. (2002). Role of CD44 in activation-induced cell death: CD44-deficient mice exhibit enhanced T cell response to conventional and superantigens. *Int Immunol* *14*, 1015-1026.
- Mei, H.E., Yoshida, T., Sime, W., Hiepe, F., Thiele, K., Manz, R.A., Radbruch, A., and Dorner, T. (2009). Blood-borne human plasma cells in steady state are derived from mucosal immune responses. *Blood* *113*, 2461-2469.
- Meresse, B., Malamut, G., and Cerf-Bensussan, N. (2012). Celiac disease: an immunological jigsaw. *Immunity* *36*, 907-919.
- Mesin, L., Di Niro, R., Thompson, K.M., Lundin, K.E., and Sollid, L.M. (2011). Long-lived plasma cells from human small intestine biopsies secrete immunoglobulins for many weeks in vitro. *J Immunol* *187*, 2867-2874.
- Michigami, T., Shimizu, N., Williams, P.J., Niewolna, M., Dallas, S.L., Mundy, G.R., and Yoneda, T. (2000). Cell-cell contact between marrow stromal cells and myeloma cells via VCAM-1 and alpha(4)beta(1)-integrin enhances production of osteoclast-stimulating activity. *Blood* *96*, 1953-1960.
- Mifflin, R.C., Pinchuk, I.V., Saada, J.I., and Powell, D.W. (2011). Intestinal myofibroblasts: targets for stem cell therapy. *Am J Physiol Gastrointest Liver Physiol* *300*, G684-696.
- Minges Wols, H.A., Ippolito, J.A., Yu, Z., Palmer, J.L., White, F.A., Le, P.T., and Witte, P.L. (2007). The effects of microenvironment and internal programming on plasma cell survival. *Int Immunol* *19*, 837-846.
- Minges Wols, H.A., Underhill, G.H., Kansas, G.S., and Witte, P.L. (2002). The role of bone marrow-derived stromal cells in the maintenance of plasma cell longevity. *J Immunol* *169*, 4213-4221.
- Mirpuri, J., Raetz, M., Sturge, C.R., Wilhelm, C.L., Benson, A., Savani, R.C., Hooper, L.V., and Yarovinsky, F. (2014). Proteobacteria-specific IgA regulates maturation of the intestinal microbiota. *Gut Microbes* *5*, 28-39.
- Misra, S., Hascall, V.C., Markwald, R.R., and Ghatak, S. (2015). Interactions between Hyaluronan and Its Receptors (CD44, RHAMM) Regulate the Activities of Inflammation and Cancer. *Front Immunol* *6*, 201.
- Miyake, K., Weissman, I.L., Greenberger, J.S., and Kincade, P.W. (1991). Evidence for a role of the integrin VLA-4 in lympho-hemopoiesis. *J Exp Med* *173*, 599-607.

- 
- Mohr, E., Serre, K., Manz, R.A., Cunningham, A.F., Khan, M., Hardie, D.L., Bird, R., and MacLennan, I.C. (2009). Dendritic cells and monocyte/macrophages that create the IL-6/APRIL-rich lymph node microenvironments where plasmablasts mature. *J Immunol* *182*, 2113-2123.
- Moseley, R., Waddington, R.J., and Embery, G. (1997). Degradation of glycosaminoglycans by reactive oxygen species derived from stimulated polymorphonuclear leukocytes. *Biochim Biophys Acta* *1362*, 221-231.
- Motegi, Y., Kita, H., Kato, M., and Morikawa, A. (2000). Role of secretory IgA, secretory component, and eosinophils in mucosal inflammation. *Int Arch Allergy Immunol* *122 Suppl 1*, 25-27.
- Mowat, A.M., and Agace, W.W. (2014). Regional specialization within the intestinal immune system. *Nat Rev Immunol* *14*, 667-685.
- Mummert, M.E., Mohamadzadeh, M., Mummert, D.I., Mizumoto, N., and Takashima, A. (2000). Development of a peptide inhibitor of hyaluronan-mediated leukocyte trafficking. *J Exp Med* *192*, 769-779.
- Nakano, K., Saito, K., Mine, S., Matsushita, S., and Tanaka, Y. (2007). Engagement of CD44 up-regulates Fas ligand expression on T cells leading to activation-induced cell death. *Apoptosis* *12*, 45-54.
- Nandi, A., Estess, P., and Siegelman, M. (2004). Bimolecular complex between rolling and firm adhesion receptors required for cell arrest; CD44 association with VLA-4 in T cell extravasation. *Immunity* *20*, 455-465.
- Naor, D., Nedvetzki, S., Walmsley, M., Yayon, A., Turley, E.A., Golan, I., Caspi, D., Sebban, L.E., Zick, Y., Garin, T., *et al.* (2007). CD44 involvement in autoimmune inflammations: the lesson to be learned from CD44-targeting by antibody or from knockout mice. *Ann N Y Acad Sci* *1110*, 233-247.
- Nguyen, D.C., Garimalla, S., Xiao, H., Kyu, S., Albizua, I., Galipeau, J., Chiang, K.Y., Waller, E.K., Wu, R., Gibson, G., *et al.* (2018). Factors of the bone marrow microniche that support human plasma cell survival and immunoglobulin secretion. *Nat Commun* *9*, 3698.
- Nguyen, T.L., Vieira-Silva, S., Liston, A., and Raes, J. (2015). How informative is the mouse for human gut microbiota research? *Disease models & mechanisms* *8*, 1-16.
- Nibbs, R.J., and Graham, G.J. (2013). Immune regulation by atypical chemokine receptors. *Nat Rev Immunol* *13*, 815-829.
- Njau, M.N., Kim, J.H., Chappell, C.P., Ravindran, R., Thomas, L., Pulendran, B., and Jacob, J. (2012). CD28-B7 interaction modulates short- and long-lived plasma cell function. *J Immunol* *189*, 2758-2767.
- O'Connor, B.P., Raman, V.S., Erickson, L.D., Cook, W.J., Weaver, L.K., Ahonen, C., Lin, L.L., Mantchev, G.T., Bram, R.J., and Noelle, R.J. (2004). BCMA is essential for the survival of long-lived bone marrow plasma cells. *J Exp Med* *199*, 91-98.
- O'Rourke, M., Cullen, C.L., Auderset, L., Pitman, K.A., Achatz, D., Gasperini, R., and Young, K.M. (2016). Evaluating Tissue-Specific Recombination in a Pdgfralpha-CreERT2 Transgenic Mouse Line. *PLoS One* *11*, e0162858.
- Okamoto, I., Kawano, Y., Murakami, D., Sasayama, T., Araki, N., Miki, T., Wong, A.J., and Saya, H. (2001). Proteolytic release of CD44 intracellular domain and its role in the CD44 signaling pathway. *J Cell Biol* *155*, 755-762.

## References

---

- Owens, B.M. (2015). Inflammation, Innate Immunity, and the Intestinal Stromal Cell Niche: Opportunities and Challenges. *Front Immunol* 6, 319.
- Pabst, O. (2012). New concepts in the generation and functions of IgA. *Nat Rev Immunol* 12, 821-832.
- Pabst, O., Herbrand, H., Worbs, T., Friedrichsen, M., Yan, S., Hoffmann, M.W., Korner, H., Bernhardt, G., Pabst, R., and Forster, R. (2005). Cryptopatches and isolated lymphoid follicles: dynamic lymphoid tissues dispensable for the generation of intraepithelial lymphocytes. *Eur J Immunol* 35, 98-107.
- Pabst, O., Ohl, L., Wendland, M., Wurbel, M.A., Kremmer, E., Malissen, B., and Forster, R. (2004). Chemokine receptor CCR9 contributes to the localization of plasma cells to the small intestine. *J Exp Med* 199, 411-416.
- Pabst, R. (2015). Mucosal vaccination by the intranasal route. Nose-associated lymphoid tissue (NALT)-Structure, function and species differences. *Vaccine* 33, 4406-4413.
- Peduto, L., Dulauroy, S., Lochner, M., Spath, G.F., Morales, M.A., Cumano, A., and Eberl, G. (2009). Inflammation recapitulates the ontogeny of lymphoid stromal cells. *J Immunol* 182, 5789-5799.
- Peperzak, V., Vikstrom, I., Walker, J., Glaser, S.P., LePage, M., Coquery, C.M., Erickson, L.D., Fairfax, K., Mackay, F., Strasser, A., *et al.* (2013). Mcl-1 is essential for the survival of plasma cells. *Nat Immunol* 14, 290-297.
- Peterson, D.A., McNulty, N.P., Guruge, J.L., and Gordon, J.I. (2007). IgA response to symbiotic bacteria as a mediator of gut homeostasis. *Cell Host Microbe* 2, 328-339.
- Philippeos, C., Telerman, S.B., Oules, B., Pisco, A.O., Shaw, T.J., Elgueta, R., Lombardi, G., Driskell, R.R., Soldin, M., Lynch, M.D., and Watt, F.M. (2018). Spatial and Single-Cell Transcriptional Profiling Identifies Functionally Distinct Human Dermal Fibroblast Subpopulations. *J Invest Dermatol* 138, 811-825.
- Pinchuk, I.V., Mifflin, R.C., Saada, J.I., and Powell, D.W. (2010). Intestinal mesenchymal cells. *Curr Gastroenterol Rep* 12, 310-318.
- Pinchuk, I.V., Saada, J.I., Beswick, E.J., Boya, G., Qiu, S.M., Mifflin, R.C., Raju, G.S., Reyes, V.E., and Powell, D.W. (2008). PD-1 ligand expression by human colonic myofibroblasts/fibroblasts regulates CD4+ T-cell activity. *Gastroenterology* 135, 1228-1237, 1237 e1221-1222.
- Pinto, D., Montani, E., Bolli, M., Garavaglia, G., Sallusto, F., Lanzavecchia, A., and Jarrossay, D. (2013). A functional BCR in human IgA and IgM plasma cells. *Blood* 121, 4110-4114.
- Ponta, H., Sherman, L., and Herrlich, P.A. (2003). CD44: from adhesion molecules to signalling regulators. *Nat Rev Mol Cell Biol* 4, 33-45.
- Popescu, L.M., and Faussone-Pellegrini, M.S. (2010). Telocytes - a case of serendipity: the winding way from Interstitial Cells of Cajal (ICC), via Interstitial Cajal-Like Cells (ICLC) to Telocytes. *J Cell Mol Med* 14, 729-740.
- Powell, D.W., Pinchuk, I.V., Saada, J.I., Chen, X., and Mifflin, R.C. (2011). Mesenchymal cells of the intestinal lamina propria. *Annu Rev Physiol* 73, 213-237.
- Protin, U., Schweighoffer, T., Jochum, W., and Hilberg, F. (1999). CD44-deficient mice develop normally with changes in subpopulations and recirculation of lymphocyte subsets. *J Immunol* 163, 4917-4923.

- 
- Putignani, L., Del Chierico, F., Petrucca, A., Vernocchi, P., and Dallapiccola, B. (2014). The human gut microbiota: a dynamic interplay with the host from birth to senescence settled during childhood. *Pediatr Res* 76, 2-10.
- Radbruch, A., Muehlinghaus, G., Luger, E.O., Inamine, A., Smith, K.G., Dorner, T., and Hiepe, F. (2006). Competence and competition: the challenge of becoming a long-lived plasma cell. *Nat Rev Immunol* 6, 741-750.
- Radu, B.M., Banciu, A., Banciu, D.D., Radu, M., Cretoiu, D., and Cretoiu, S.M. (2017). Calcium Signaling in Interstitial Cells: Focus on Telocytes. *Int J Mol Sci* 18.
- Ramsay, A.J., Husband, A.J., Ramshaw, I.A., Bao, S., Matthaei, K.I., Koehler, G., and Kopf, M. (1994). The role of interleukin-6 in mucosal IgA antibody responses in vivo. *Science* 264, 561-563.
- Randall, T.D., and Mebius, R.E. (2014). The development and function of mucosal lymphoid tissues: a balancing act with micro-organisms. *Mucosal Immunol* 7, 455-466.
- Reboldi, A., Arnon, T.I., Rodda, L.B., Atakilit, A., Sheppard, D., and Cyster, J.G. (2016). IgA production requires B cell interaction with subepithelial dendritic cells in Peyer's patches. *Science* 352, aaf4822.
- Reikvam, D.H., Derrien, M., Islam, R., Erofeev, A., Grcic, V., Sandvik, A., Gaustad, P., Meza-Zepeda, L.A., Jahnsen, F.L., Smidt, H., and Johansen, F.E. (2012). Epithelial-microbial crosstalk in polymeric Ig receptor deficient mice. *Eur J Immunol* 42, 2959-2970.
- Riehl, T.E., Ee, X., and Stenson, W.F. (2012a). Hyaluronic acid regulates normal intestinal and colonic growth in mice. *Am J Physiol Gastrointest Liver Physiol* 303, G377-388.
- Riehl, T.E., Foster, L., and Stenson, W.F. (2012b). Hyaluronic acid is radioprotective in the intestine through a TLR4 and COX-2-mediated mechanism. *Am J Physiol Gastrointest Liver Physiol* 302, G309-316.
- Riehl, T.E., Santhanam, S., Foster, L., Ciorba, M., and Stenson, W.F. (2015). CD44 and TLR4 mediate hyaluronic acid regulation of Lgr5+ stem cell proliferation, crypt fission, and intestinal growth in postnatal and adult mice. *Am J Physiol Gastrointest Liver Physiol* 309, G874-887.
- Rodda, L.B., Lu, E., Bennett, M.L., Sokol, C.L., Wang, X., Luther, S.A., Barres, B.A., Luster, A.D., Ye, C.J., and Cyster, J.G. (2018). Single-Cell RNA Sequencing of Lymph Node Stromal Cells Reveals Niche-Associated Heterogeneity. *Immunity* 48, 1014-1028 e1016.
- Rodriguez Gomez, M., Talke, Y., Goebel, N., Hermann, F., Reich, B., and Mack, M. (2010). Basophils support the survival of plasma cells in mice. *J Immunol* 185, 7180-7185.
- Roth, K., Oehme, L., Zehentmeier, S., Zhang, Y., Niesner, R., and Hauser, A.E. (2014). Tracking plasma cell differentiation and survival. *Cytometry A* 85, 15-24.
- Rozanski, C.H., Utley, A., Carlson, L.M., Farren, M.R., Murray, M., Russell, L.M., Nair, J.R., Yang, Z., Brady, W., Garrett-Sinha, L.A., *et al.* (2015). CD28 Promotes Plasma Cell Survival, Sustained Antibody Responses, and BLIMP-1 Upregulation through Its Distal PYAP Proline Motif. *J Immunol* 194, 4717-4728.
- Saada, J.I., Pinchuk, I.V., Barrera, C.A., Adegboyega, P.A., Suarez, G., Mifflin, R.C., Di Mari, J.F., Reyes, V.E., and Powell, D.W. (2006). Subepithelial myofibroblasts are novel nonprofessional APCs in the human colonic mucosa. *J Immunol* 177, 5968-5979.
- Schneider, P. (2005). The role of APRIL and BAFF in lymphocyte activation. *Curr Opin Immunol* 17, 282-289.

## References

---

- Sellge, G., Magalhaes, J.G., Konradt, C., Fritz, J.H., Salgado-Pabon, W., Eberl, G., Bandeira, A., Di Santo, J.P., Sansonetti, P.J., and Phalipon, A. (2010). Th17 cells are the dominant T cell subtype primed by *Shigella flexneri* mediating protective immunity. *J Immunol* *184*, 2076-2085.
- Senbanjo, L.T., and Chellaiah, M.A. (2017). CD44: A Multifunctional Cell Surface Adhesion Receptor Is a Regulator of Progression and Metastasis of Cancer Cells. *Front Cell Dev Biol* *5*, 18.
- Shen, L., and Collins, J. (1989). Monocyte superoxide secretion triggered by human IgA. *Immunology* *68*, 491-496.
- Shi, W., Liao, Y., Willis, S.N., Taubenheim, N., Inouye, M., Tarlinton, D.M., Smyth, G.K., Hodgkin, P.D., Nutt, S.L., and Corcoran, L.M. (2015). Transcriptional profiling of mouse B cell terminal differentiation defines a signature for antibody-secreting plasma cells. *Nat Immunol* *16*, 663-673.
- Shlomchik, M.J., and Weisel, F. (2012). Germinal center selection and the development of memory B and plasma cells. *Immunological Reviews* *247*, 52-63.
- Shoshkes-Carmel, M., Wang, Y.J., Wangenstein, K.J., Toth, B., Kondo, A., Massasa, E.E., Itzkovitz, S., and Kaestner, K.H. (2018). Subepithelial telocytes are an important source of Wnts that supports intestinal crypts. *Nature* *557*, 242-246.
- Shreedhar, V.K., Kelsall, B.L., and Neutra, M.R. (2003). Cholera toxin induces migration of dendritic cells from the subepithelial dome region to T- and B-cell areas of Peyer's patches. *Infect Immun* *71*, 504-509.
- Siegelman, M.H., Stanescu, D., and Estess, P. (2000). The CD44-initiated pathway of T-cell extravasation uses VLA-4 but not LFA-1 for firm adhesion. *J Clin Invest* *105*, 683-691.
- Sitnik, K.M., Wendland, K., Weishaupt, H., Uronen-Hansson, H., White, A.J., Anderson, G., Kotarsky, K., and Agace, W.W. (2016). Context-Dependent Development of Lymphoid Stroma from Adult CD34(+) Adventitial Progenitors. *Cell Rep* *14*, 2375-2388.
- Skelton, T.P., Zeng, C., Nocks, A., and Stamenkovic, I. (1998). Glycosylation provides both stimulatory and inhibitory effects on cell surface and soluble CD44 binding to hyaluronan. *J Cell Biol* *140*, 431-446.
- Slifka, M.K., and Ahmed, R. (1998). Long-lived plasma cells: a mechanism for maintaining persistent antibody production. *Curr Opin Immunol* *10*, 252-258.
- Slifka, M.K., Antia, R., Whitmire, J.K., and Ahmed, R. (1998). Humoral immunity due to long-lived plasma cells. *Immunity* *8*, 363-372.
- Stern, R. (2004). Hyaluronan catabolism: a new metabolic pathway. *Eur J Cell Biol* *83*, 317-325.
- Stern, R., Kogan, G., Jedrzejewski, M.J., and Soltes, L. (2007). The many ways to cleave hyaluronan. *Biotechnol Adv* *25*, 537-557.
- Stzpourginski, I., Eberl, G., and Peduto, L. (2015). An optimized protocol for isolating lymphoid stromal cells from the intestinal lamina propria. *J Immunol Methods* *421*, 14-19.
- Stzpourginski, I., Nigro, G., Jacob, J.M., Dulauroy, S., Sansonetti, P.J., Eberl, G., and Peduto, L. (2017). CD34+ mesenchymal cells are a major component of the intestinal stem cells niche at homeostasis and after injury. *Proc Natl Acad Sci U S A* *114*, E506-E513.

---

Suzuki, K., and Fagarasan, S. (2008). How host-bacterial interactions lead to IgA synthesis in the gut. *Trends Immunol* *29*, 523-531.

Suzuki, K., and Fagarasan, S. (2009). Diverse regulatory pathways for IgA synthesis in the gut. *Mucosal Immunol* *2*, 468-471.

Suzuki, K., Meek, B., Doi, Y., Muramatsu, M., Chiba, T., Honjo, T., and Fagarasan, S. (2004). Aberrant expansion of segmented filamentous bacteria in IgA-deficient gut. *Proc Natl Acad Sci U S A* *101*, 1981-1986.

Taillardet, M., Haffar, G., Mondiere, P., Asensio, M.J., Gheit, H., Burdin, N., Defrance, T., and Genestier, L. (2009). The thymus-independent immunity conferred by a pneumococcal polysaccharide is mediated by long-lived plasma cells. *Blood* *114*, 4432-4440.

Takeuchi, A., Ozawa, M., Kanda, Y., Kozai, M., Ohigashi, I., Kurosawa, Y., Rahman, M.A., Kawamura, T., Shichida, Y., Umemoto, E., *et al.* (2018). A Distinct Subset of Fibroblastic Stromal Cells Constitutes the Cortex-Medulla Boundary Subcompartment of the Lymph Node. *Front Immunol* *9*, 2196.

Tangye, S.G. (2011). Staying alive: regulation of plasma cell survival. *Trends Immunol* *32*, 595-602.

Thomson, C.A., van de Pavert, S.A., Stakenborg, M., Labeeuw, E., Matteoli, G., Mowat, A.M., and Nibbs, R.J.B. (2018). Expression of the Atypical Chemokine Receptor ACKR4 Identifies a Novel Population of Intestinal Submucosal Fibroblasts That Preferentially Expresses Endothelial Cell Regulators. *J Immunol* *201*, 215-229.

Thorne, R.F., Legg, J.W., and Isacke, C.M. (2004). The role of the CD44 transmembrane and cytoplasmic domains in co-ordinating adhesive and signalling events. *J Cell Sci* *117*, 373-380.

Tokoyoda, K., Egawa, T., Sugiyama, T., Choi, B.I., and Nagasawa, T. (2004). Cellular niches controlling B lymphocyte behavior within bone marrow during development. *Immunity* *20*, 707-718.

Toyoda, H., Ina, K., Kitamura, H., Tsuda, T., and Shimada, T. (1997). Organization of the lamina propria mucosae of rat intestinal mucosa, with special reference to the subepithelial connective tissue. *Acta Anat (Basel)* *158*, 172-184.

Tsuji, M., Suzuki, K., Kinoshita, K., and Fagarasan, S. (2008). Dynamic interactions between bacteria and immune cells leading to intestinal IgA synthesis. *Semin Immunol* *20*, 59-66.

Tsuneki, M., and Madri, J.A. (2016). CD44 Influences Fibroblast Behaviors Via Modulation of Cell-Cell and Cell-Matrix Interactions, Affecting Survivin and Hippo Pathways. *J Cell Physiol* *231*, 731-743.

Utey, S., James, D., Mavila, N., Nguyen, M.V., Vendryes, C., Salisbury, S.M., Phan, J., and Wang, K.S. (2014). Fibroblast growth factor signaling regulates the expansion of A6-expressing hepatocytes in association with AKT-dependent beta-catenin activation. *J Hepatol* *60*, 1002-1009.

Vaishnav, S., Yamamoto, M., Severson, K.M., Ruhn, K.A., Yu, X., Koren, O., Ley, R., Wakeland, E.K., and Hooper, L.V. (2011). The antibacterial lectin RegIIIgamma promotes the spatial segregation of microbiota and host in the intestine. *Science* *334*, 255-258.

Van Driel, M., Gunthert, U., van Kessel, A.C., Joling, P., Stauder, R., Lokhorst, H.M., and Bloem, A.C. (2002). CD44 variant isoforms are involved in plasma cell adhesion to bone marrow stromal cells. *Leukemia* *16*, 135-143.

## References

---

- Vannucchi, M.G., Traini, C., Manetti, M., Ibba-Manneschi, L., and Fausone-Pellegrini, M.S. (2013). Telocytes express PDGFRalpha in the human gastrointestinal tract. *J Cell Mol Med* *17*, 1099-1108.
- Vicente-Suarez, I., Larange, A., Reardon, C., Matho, M., Feau, S., Chodaczek, G., Park, Y., Obata, Y., Gold, R., Wang-Zhu, Y., *et al.* (2015). Unique lamina propria stromal cells imprint the functional phenotype of mucosal dendritic cells. *Mucosal Immunol* *8*, 141-151.
- von Bulow, G.U., van Deursen, J.M., and Bram, R.J. (2001). Regulation of the T-independent humoral response by TACI. *Immunity* *14*, 573-582.
- Wang, L.L., Guo, H.H., Huang, S., Feng, C.L., Han, Y.X., and Jiang, J.D. (2017a). Comprehensive evaluation of SCFA production in the intestinal bacteria regulated by berberine using gas-chromatography combined with polymerase chain reaction. *J Chromatogr B Analyt Technol Biomed Life Sci* *1057*, 70-80.
- Wang, N., and Hammarstrom, L. (2012). IgA deficiency: what is new? *Curr Opin Allergy Clin Immunol* *12*, 602-608.
- Wang, Y., Liu, L., Moore, D.J., Shen, X., Peek, R.M., Acra, S.A., Li, H., Ren, X., Polk, D.B., and Yan, F. (2017b). An LGG-derived protein promotes IgA production through upregulation of APRIL expression in intestinal epithelial cells. *Mucosal Immunol* *10*, 373-384.
- Weissmann, B., Meyer, K., Sampson, P., and Linker, A. (1954). Isolation of oligosaccharides enzymatically produced from hyaluronic acid. *J Biol Chem* *208*, 417-429.
- West, N.R., Hegazy, A.N., Owens, B.M.J., Bullers, S.J., Linggi, B., Buonocore, S., Coccia, M., Gortz, D., This, S., Stockenhuber, K., *et al.* (2017). Oncostatin M drives intestinal inflammation and predicts response to tumor necrosis factor-neutralizing therapy in patients with inflammatory bowel disease. *Nat Med* *23*, 579-589.
- Wijburg, O.L., and Strugnell, R.A. (2006). Mucosal Immune Responses to Escherichia coli and Salmonella Infections. *EcoSal Plus* *2*.
- Wijburg, O.L., Uren, T.K., Simpfendorfer, K., Johansen, F.E., Brandtzaeg, P., and Strugnell, R.A. (2006). Innate secretory antibodies protect against natural Salmonella typhimurium infection. *J Exp Med* *203*, 21-26.
- Wilmore, J.R., and Allman, D. (2017). Here, There, and Anywhere? Arguments for and against the Physical Plasma Cell Survival Niche. *J Immunol* *199*, 839-845.
- Winter, O., Moser, K., Mohr, E., Zotos, D., Kaminski, H., Szyska, M., Roth, K., Wong, D.M., Dame, C., Tarlinton, D.M., *et al.* (2010). Megakaryocytes constitute a functional component of a plasma cell niche in the bone marrow. *Blood* *116*, 1867-1875.
- Wittig, B.M., Johansson, B., Zoller, M., Schwarzler, C., and Gunthert, U. (2000). Abrogation of experimental colitis correlates with increased apoptosis in mice deficient for CD44 variant exon 7 (CD44v7). *J Exp Med* *191*, 2053-2064.
- Wolfs, T.G., Derikx, J.P., Hodin, C.M., Vanderlocht, J., Driessen, A., de Bruine, A.P., Bevins, C.L., Lasitschka, F., Gassler, N., van Gemert, W.G., and Buurman, W.A. (2010). Localization of the lipopolysaccharide recognition complex in the human healthy and inflamed premature and adult gut. *Inflamm Bowel Dis* *16*, 68-75.
- Xavier, R.J., and Podolsky, D.K. (2007). Unravelling the pathogenesis of inflammatory bowel disease. *Nature* *448*, 427-434.

---

Xie, T., Wang, Y., Deng, N., Huang, G., Taghavifar, F., Geng, Y., Liu, N., Kulur, V., Yao, C., Chen, P., *et al.* (2018). Single-Cell Deconvolution of Fibroblast Heterogeneity in Mouse Pulmonary Fibrosis. *Cell Rep* **22**, 3625-3640.

Yel, L. (2010). Selective IgA deficiency. *J Clin Immunol* **30**, 10-16.

Youngman, K.R., Franco, M.A., Kuklin, N.A., Rott, L.S., Butcher, E.C., and Greenberg, H.B. (2002). Correlation of tissue distribution, developmental phenotype, and intestinal homing receptor expression of antigen-specific B cells during the murine anti-rotavirus immune response. *J Immunol* **168**, 2173-2181.

Zehentmeier, S., Roth, K., Cseresnyes, Z., Sercan, O., Horn, K., Niesner, R.A., Chang, H.D., Radbruch, A., and Hauser, A.E. (2014). Static and dynamic components synergize to form a stable survival niche for bone marrow plasma cells. *Eur J Immunol* **44**, 2306-2317.

Zhang, Y., Tech, L., George, L.A., Acs, A., Durrett, R.E., Hess, H., Walker, L.S.K., Tarlinton, D.M., Fletcher, A.L., Hauser, A.E., and Toellner, K.M. (2018). Plasma cell output from germinal centers is regulated by signals from Tfh and stromal cells. *J Exp Med* **215**, 1227-1243.

Zheng, L., Riehl, T.E., and Stenson, W.F. (2009). Regulation of colonic epithelial repair in mice by Toll-like receptors and hyaluronic acid. *Gastroenterology* **137**, 2041-2051.

Zheng, Y., Zhang, M., Qian, M., Wang, L., Cismasiu, V.B., Bai, C., Popescu, L.M., and Wang, X. (2013). Genetic comparison of mouse lung telocytes with mesenchymal stem cells and fibroblasts. *J Cell Mol Med* **17**, 567-577.

Zheng, Z., Katoh, S., He, Q., Oritani, K., Miyake, K., Lesley, J., Hyman, R., Hamik, A., Parkhouse, R.M., Farr, A.G., and Kincade, P.W. (1995). Monoclonal antibodies to CD44 and their influence on hyaluronan recognition. *J Cell Biol* **130**, 485-495.